VALENTIN ELIAS JANN

Phosphorous Loads in the Heilsau Catchment
Spatial Distribution and Temporal Variation

2024

VALENTIN ELIAS JANN

Phosphorous Loads in the Heilsau Catchment
Spatial Distribution and Temporal Variation

Supervisors:
Prof. Dr. Luis CHÍCHARO
Dr. Kai WELLBROCK

Master's thesis submitted to obtain the degree of
MSc. in Applied Ecohydrology

2024

Declaration of Authorship

I, Valentin Elias Jann, declare I am the author of this work titled "Phosphorous Loads in the Heilsau Catchment - Spatial Distribution and Temporal Variation", which is original and unpublished. The sources consulted have been duly cited in the text and included in the list of references.

Signed:

Date:

To my friends and loved ones. And to those who I have lost.
You are always with me.

Abstract

Eutrophication of aquatic ecosystems is a global environmental issue. Mostly caused by excessive inputs of nutrients such as phosphorous and nitrogen, a catchment-wide understanding of nutrient and sediment pathways and their drivers is necessary. This thesis focuses on the assessment of phosphorus (P) inputs in the Heilsau Catchment, aiming to better understand its impact on eutrophication. Utilising both historical data and own field measurements, this study examines various sources of phosphorus and their contributions to the total phosphorus load in the catchment. The study area was characterised by its hydrological, topographical, and land use features, with an assessment of soil, watercourses, and anthropogenic modifications. Discharge and precipitation data were integrated with instream water quality measurements to track the temporal variation and potential drivers of phosphorus loads. Furthermore, the concentration-discharge (C-Q) relationship was analysed, and a model was built for estimating P concentrations through baseflow and direct runoff contribution. Sampling of tributaries, sewage effluents, and drainage systems provided additional data on the spatial distribution of phosphorus from point and diffuse sources. Results indicate that the majority of phosphorous reaches the waterbodies through erosion, sewage effluents, and drainage. The analysis on a subcatchment level enabled to identify hotspot areas and hence interpret consequences for an improved catchment management. Measures should include the retention of sediments and dissolved phosphorous from erosion-prone areas, and the enhancement of P-removal in sewage treatment. This study contributes to the ongoing efforts of improving the water quality and secure ecosystem services in the Heilsau catchment, offering actionable insights for environmental management.

Keywords: phosphorous, mass balance, source apportionment, C-Q relationship, eutrophication, catchment analysis

Sumário

A eutrofização dos ecossistemas aquáticos é um problema ambiental global, causada sobretudo por uma quantidade excessivade nutrientes como o fósforo e o azoto. Portanto, é necessário compreender os caminhos de escoamento dos nutrientes e dos sedimentos e os seus factores determinantes. Esta tese centra-se na avaliação das entradas de fósforo (P) na bacia hidrográfica de Heilsau, na Alemanha, com o objetivo de melhor compreender o seu impacto na eutrofização. Utilizando dados históricos e medições no terreno, este estudo examina várias fontes de fósforo e as suas contribuições para a carga total de fósforo na bacia hidrográfica. A área de estudo foi caracterizada por seus aspectos hidrológicos, topográficos e de utilização da terra, com uma avaliação do solo, dos cursos de água e das modificações antropogênicas. Os dados de descarga e precipitação foram integrados com medições da qualidade da água nos cursos de água para acompanhar a variação temporal e os potenciais fatores de carga de fósforo. Além disso, foi analisada a relação concentração-descarga (C-Q) e foi construído um modelo para estimar as concentrações de P através do escoamento de base e da contribuição direta do escoamento superficial. A amostragem de afluentes, efluentes de esgotos e sistemas de drenagem forneceu dados adicionais sobre a distribuição espacial do fósforo proveniente de fontes pontuais e difusas. Os resultados indicam que a maior parte do fósforo chega aos corpos de água através da erosão, dos efluentes de esgotos e da drenagem. A análise a nível da sub-bacia permitiu identificar zonas de risco einterpretar as consequências para a bacia, melhorando seu gerenciamento.As medidas de gerenciamento devem incluir a retenção de sedimentos e de fósforo dissolvido em zonas propensas à erosão e a melhoria da remoção de P no tratamento de águas residuais. Este estudo soma-se aos esforços de melhorar a qualidade da água e assegurar os serviços ecossistémicos na bacia hidrográfica de Heilsau, oferecendo perspectivas acionáveis para a gestão ambiental.

Palavras-chave: Fósforo, balanço de massa, identificação de fontes, relação C-Q, eutrofização, análise de bacia

Contents

List of Figures

List of Tables

1 Introduction

Eutrophication of aquatic ecosystems is a global environmental issue. Mostly caused by excessive inputs of nutrients such as phosphorous and nitrogen, it can lead to harmful algal blooms (HAB), fish kills, loss of biodiversity and generally decreased water quality (Chakrabarti, 2018; Chislock et al., 2013; Schindler, 2012). The process of eutrophication can happen naturally over centuries, as sediments and nutrients accumulate in lentic systems (Addy & Green, 1996; Carpenter (1981) as cited in Chislock et al., 2013). Human activities, however, accelerate this process, as key nutrients are entering the water cycle through agricultural runoff, sewage discharge, industrial waste, and other pathways, coining the term "cultural eutrophication" (Schindler, 2012).

To control eutrophication, a catchment-wide understanding of nutrient and sediment pathways and their drivers is necessary, as well as information on the internal nutrient cycling and ecological state of the affected waterbodies. This is even more important when looking at highly modified waters, where natural processes such as nutrient cycles are impacted (Baldwin & Mitchell, 2000; Wang et al., 2018).

The study area for this thesis is a prime example of such a highly modified catchment on a small spatial scale. Located in the German state of Schleswig-Holstein, the city of Reinfeld is known for its ponds in and around the city. These ponds, however, did not form naturally but were constructed for aquaculture by Cistercian monks in the 12th century. The biggest pond, the Herrenteich, resulted from damming the river Heilsau (Stresius, 2006; *www.reinfeld.de*). Aquaculture is still active at present, with the cultivation of fish giving the city its nickname Karpfenstadt, "carp town". The cultural and historic relevance of the carp can even be seen on the city's coat of arms (see *Karpfenstadt Reinfeld*).

Problem Statement and Research Question

The ponds of Reinfeld, however, are increasingly affected by nutrient inputs, which led to seasonal eutrophication and siltation in the past, among other problems. As not only the water quality but also other ecosystem services such as the recreational value, flood retention and food production are affected by this development, the city is cooperating with the Technical University of Applied Sciences Lübeck (TH Lübeck) and the Hamburg University of Applied Sciences (HAW Hamburg). Their shared project "VerTe" has the task to identify causes of eutrophication and siltation, aiming to find sustainable management practices for both the

catchment and its ponds, ultimately strengthening the ecosystem services of the area (*BFN*, n.d.).

In previous studies by Hackemann (1994) and Stresius (2006), the ponds have already been analysed regarding their water quality and ecological status (Hackemann, 1994; Stresius, 2006). These studies, however, focussed on the immediate inflows and the ponds themselves, whereas sources and processes from the main tributary of the Herrenteich, the Heilsau, have not been investigated further upstream. As a starting point, Hackemann (1994) calculated the phosphorous and nitrogen loads reaching the Herrenteich for the year 1993 and concluded that the Heilsau is the dominant contributor of nutrients among all tributaries including urban runoff from the surrounding area (Hackemann, 1994). Later, Stresius (2006) found that the phosphorous concentrations in the Herrenteich were constantly exceeding the threshold for growth limitation of primary production, making this nutrient the dominant driver for eutrophication (Stresius, 2006).

Until now, it has only been possible to speculate about where and in what quantities these nutrients come from and how the load can vary between years and seasons. However, addressing this knowledge gap is important: With a better understanding of nutrient pathways (especially phosphorous) in the catchment of the Heilsau, measures to reduce the loads could be targeted more efficiently, potentially saving time and costs spent on restoration. Furthermore, uncertainty about the common causes for excess nutrient input – namely sewage water, aquaculture, and agriculture – can cause conflicts between sectors regarding their contribution and thus their responsibility.

Therefore, the aim of this thesis is to carry out a phosphorous mass balance for the Heilsau catchment, with a particular focus on the area upstream of the Herrenteich. Of key interest are the yearly and seasonal variations of phosphorous loads reaching the Herrenteich through the Heilsau river. Furthermore, this study tries to determine the origin of the key nutrient within the catchment, in particular whether the loads are dominated by point sources or diffuse sources. With the results of this study, stakeholders such as the city of Reinfeld and upstream municipalities should be able to make informed decisions on how to effectively and efficiently address the issue of eutrophication in the ponds of Reinfeld.

To systematically approach the research questions, I will start with a detailed review of past research and projects on the topic. This includes the general role of phosphorous in aquatic ecosystems as well as introducing studies relevant to the catchment of the Heilsau river. After

the review, I will present the methodology used to derive the phosphorous mass balance, its temporal variation, and its spatial distribution. Finally, the results are presented and discussed regarding their quality as well as limitations, before concluding with the key outcomes.

2 Review of Past Research and Projects

2.1 Eutrophication and the Role of Phosphorous

2.1.1 Forms of Phosphorous and their Bioavailability

The availability of phosphorous (or briefly: P) to aquatic organisms, i.e. bioavailability, depends on its chemical speciation. The most readily available form is soluble reactive P, which comprises orthophosphates (hereafter ortho-P) in solution as well as colloidal bound P. Less bioavailable are inorganic forms of particulate P such as ferric-bound P or apatite-P, which are found in sediments for example. The availability of the latter two, however, can change with the redox potential and pH of the environment (Reynolds and Davies 2001, Schwoerbel 2022). Another fraction of P found in aquatic systems are organic forms such as nucleic acids, inositol phosphates, and phospholipids (Baldwin 2013), found in organisms and detritus.

In general, all forms of P can be grouped into dissolved organic P (DOP), dissolved inorganic P (DIP), particulate organic P (POP) and particulate inorganic P (PIP), and all of them combined make up the total phosphorous (TP) content in the environment (Worsfold 2008, Schwoerbel 2022). When it comes to measuring P in water samples, various methods have been developed. In this study, molybdate-based tests from Hach © are used, in particular the orthophosphate and total phosphorous tests. This allows to analyse the most important fraction regarding bioavailability, namely ortho-P, and the overall P content, which – as mentioned above – could potentially become bioavailable through microbial activity or a change of chemical conditions.

2.1.2 Phosphorous and its Role in Eutrophication

In natural waterbodies without anthropogenic influence, the background concentration of dissolved inorganic P only amounts to a few µg per litre, which makes P often the limiting substrate for primary producers (Schwoerbel 2022). This underlines the impact which additional P reaching waterbodies through human activities can have. When phosphorous is no longer the limiting factor for growth, nitrogen can become the new limitation, which can shift the composition of primary producers: Smith (1983) reported for example that cyanobacteria capable of fixing atmospheric nitrogen became dominant where phosphorous was abundant (Smith, 1983). When both nitrogen and phosphorous are enriched, the response of primary producers to eutrophication is even stronger (Elser et al., 2007). Therefore, to improve eutrophic aquatic systems it is necessary to identify the key limiting substrates before planning potential measures for nutrient reduction (Elser et al., 2007). Furthermore, phosphorous entering lentic

waterbodies can accumulate in sediments and biomass, which leads to the phenomenon that even after external P inputs were reduced, the stored phosphorous can be released slowly, therefore prolonging eutrophic conditions (Carpenter, 2005).

2.2 Summary of Past Research Related to the Heilsau Catchment

Recently, there have been various studies conducted which are relevant for the Heilsau catchment. Some of them specifically focused on the water quality of the Heilsau itself or the pond system in Reinfeld, others took place on a regional to country scale. This section will present these studies to show the current understanding of the area. Detailed results from these studies are shown in a separate section of the methodology, as they will be used for this thesis.

2.2.1 Schleswig-Holstein: Nutrient Model from 2010-2017 and 2019-2023

The Forschungszentrum Jülich (hereafter **FZ Jülich**), a research institute based in North Rhine-Westphalia, Germany, integrated multiple modelling tools to estimate nitrogen and phosphorous pathways into groundwater and surface water. These tools included the regionalised agricultural and environmental information system RAUMIS, the large-scale water balance model GROWA, reactive N transport models DENUZ (for the unsaturated zone) and WEKU (for groundwater residence times and reactive N transport), and the P transport model MEPhos. With ten different input pathways considered and an emphasis on diffuse agricultural sources, their comprehensive and spatially differentiated multi-model framework can be used by the federal states of Germany to identify hotspot regions, determine nutrient reduction needs, or predict the impact of measures, among others (Tetzlaff et al., 2017).

In the case of Schleswig-Holstein, the FZJ had been commissioned by a ministry of the state (*Ministerium für Energiewende, Landwirtschaft, Umwelt und ländliche Räume Schleswig-Holstein*) to produce a nutrient report. This report from 2017 (hereafter referred to as **FZ Jülich report**) was available for this thesis and was consulted for its methodology and findings. Additionally, thanks to the coordinator and leading author of this project, Dr. Tetzlaff, and in agreement with Dr. Trepel from the *Ministerium für Energiewende, Klimaschutz, Umwelt und Natur des Landes Schleswig-Holstein* (hereafter **MEKUN**), even more recent data from 2019 to 2023 was provided. This dataset will be referred to as **FZ Jülich Model**.

The results of the report show the apportionment of different nutrient sources with a spatial resolution down to municipalities and a temporal reference of multi-year mean values (Tetzlaff et al., 2017, p.45). For phosphorous sources in the Heilsau catchment, nine different nutrient pathways were identified and were given English translations with their definitions in Table

2.1. It should be noted that the atmospheric deposition was only modelled and calculated for the direct deposition on water surfaces, as all other areas such as arable land, forests, and urban areas already included the atmospheric input indirectly (Tetzlaff et al., 2017). The report's data will be presented later, as it is used in the methodology.

Table 2.1: Definition of phosphorous pathways according to Tetzlaff et al. (2017), with English translation and their short IDs.

Pathway GER – original	**Pathway EN – own translation**	**Short ID**	**Description**
Atmosphärische Deposition auf Gewässerflächen	Atmospheric Deposition	AtmDepos	Direct atmospheric deposition of P on water surfaces only.
Dränageabfluss	Drainage Water	Drain	P in effluent of agricultural drainage pipes.
Grundwassergebürtiger Abluss	Contribution from Groundwater	GW	P from groundwater which reaches surface waters as e.g. baseflow.
Natürlicher Zwischenabfluss	Natural Interflow	Interflow	Seepage water on non-drained sites which reaches surface waters as interflow (lateral sub-surface flow).
Abschwemmung	Nutrient Washout	Washout	Input of dissolved phosphorus which is washed-out from agricultural land. The runoff process is closely linked to erosion processes, but in contrast to erosion, washout also takes place on grassland in relevant quantities.
Erosion	Erosion	Erosion	Particulate P entering waterbodies through surface erosion, particularly from cropland.
Trennkanalisation	Separated Rainwater Canalisation	RainCanal	P inputs through surface runoff from sealed areas within settlement areas, which do not enter the sewage treatment.
Kommunale Kläranlagen	Municipal Sewage Treatment Plants	Mun-STPs	P from centralised, municipal sewage treatment effluent.
Kleinkläranlagen	Private Sewage Treatment Plants	Priv-STPs	P from decentralised, private sewage treatment effluent at the household level.

2.2.2 Governmental Measurements for the Water Framework Directive

In line with the Water Framework Directive (WFD) of the European Union, the government of Schleswig-Holstein is coordinating monitoring programmes for surface waterbodies and groundwater through its responsible ministry, MEKUN (ministry for energy transition, climate mitigation, environment, and nature). This includes the monitoring of nutrient concentrations, where the measurements are made available to the public (see Themenportale SH, schleswig-holstein.de). In case of the Heilsau catchment, measurements from four sampling locations along the river Heilsau are available, all sampled monthly but not continuous throughout the years. The analysed parameters include TP, ortho-P from filtrated samples, several nitrogen

compounds, and dissolved oxygen. Again, the results from these measuring campaigns and sampling locations are shown later.

2.2.3 Studies in the Heilsau Catchment

With several studies specifically focussing on the ponds of Reinfeld and their catchment, the scientific and local interest in the water quality and ecosystem services is obvious. Two studies have been mentioned in the introduction and will now be presented in more detail. Additionally, more recent theses and projects from the TH Lübeck are introduced in their chronological order.

2.2.3.1 Hackemann (1994): Nutrients and water quality of the Herrenteich

Hackemann was commissioned by the city of Reinfeld to analyse the state of the Herrenteich regarding its physical, chemical, and bacteriological parameters. Their sampling took place from March 1993 to March 1994 and included water and sediment samples from the pond itself, as well as water samples from the tributaries reaching the pond and some inputs from separated rain canalisations.

They found that the Herrenteich can be categorised as hypertrophic due to its high primary production and elevated nutrient concentrations, both N and P. Furthermore, a load calculation with discharges from an upstream gauge suggested the Heilsau to be the main external contributor of nutrients to the system, with a share of 80-90% of total external nutrient loads. Hackemann therefore concluded that the nutrient sources reaching the Heilsau upstream of the Herrenteich should be the main target of management strategies to improve the trophic state of the pond (Hackemann, 1994).

2.2.3.2 Hansen and Greuner-Pönicke (2002): Strategies towards a more natural development of watercourses in the Heilsau catchment

The “Gewässerpflegeverband Heilsau”, which is the association responsible for the management of watercourses in a large part of the catchment, commissioned a team of engineers and biologists to develop a strategy towards a more natural management of the catchment. The study area covered most part of the Heilsau and a few tributaries. Their report based on field surveys from the 1990s and included the analysis of the current state of the study area regarding aspects like river morphology, flow-dynamics, biodiversity, and sediment dynamics. In the process, so called “Leitbilder” (guiding principles) were formulated, describing the state which the rivers and their immediate surroundings should develop towards. Among these ideal states, the team first developed a scenario without any human influence (the best case for natural development), before considering the limitations by anthropogenic interference (such as

agricultural land use claims and infrastructure) in a second scenario. With these limitations in mind, potential measures for improving the river morphology and quality were presented and ranked by their feasibility and impact (Hansen & Greuner-Pönicke, 2002).

Their report, especially the suggested measures, could be used by the authorities as guidelines when tackling the problems of nutrients and sediments reaching the Herrenteich. The results from this thesis can contribute as a validation of some of the observations that Hansen and Greuner-Pönicke (2002) made regarding flow and nutrient dynamics.

2.2.3.3 Stresius (2006): The ponds of Reinfeld and their potential for an ecological aquaculture

Stresius aimed to assess whether converting the ponds of Reinfeld to an ecological system is feasible and advisable. The study involved a literature review to understand ecological pond management guidelines, comparing these to current practices, and assessing the water quality of the ponds. This assessment included the analysis of water and sediment samples of the ponds as well as water samples from in- and outflows of the pond system during the year 2005. The findings revealed that the ponds are heavily nutrient-loaded and do not currently meet ecological standards. Furthermore, as mentioned before, phosphorous was found to be constantly exceeding the threshold for growth limitation of primary production, making this nutrient the dominant driver for eutrophication (Stresius, 2006).

2.2.3.4 Osterhoff (2020): Total suspended solids from rainwater canalisation

In the context of a planned legislative change regarding the allowed load of total suspended solids (TSS) from urban runoff, especially rainwater canalisations, Osterhoff analysed the levels of TSS reaching the Heilsau and its tributaries through rainwater outlets. For this study in particular, the fine section of TSS between diameters of 0.45 µm and 63 µm was relevant, therefore looking at the fraction smaller than sand. The study did not include their own measurements but instead calculated the expected TSS loads from urban runoff depending on area-specific categories of pollution provided by public data. Although the focus was on TSS and how to manage rain outlets which did not meet effluent standards (Osterhoff, 2020), the results might be useful for this thesis when looking at the pollution level from rain canalisations in the catchment.

2.2.3.5 VerTe (2022 - 2025): Research project on improving the ecosystem services of the ponds of Reinfeld

As mentioned in the introduction, “Verbesserung der Ökosystemleistungen in den Reinfelder Teichen” (VerTe) is a project of the city of Reinfeld in cooperation with HAW Hamburg and TH Lübeck. It is supported by the *Bundesamt für Naturschutz* (BfN), the federal environmental protection agency of Germany, which secured funds for this project from the *Bundesministerium für Umwelt, Naturschutz, nukleare Sicherheit und Verbraucherschutz* (BMUV) – the federal ministry of Environment, Nature Conservation, Nuclear Safety, and Consumer Protection (*BFN*, n.d.).

This shared project has the task to identify causes of eutrophication and siltation, aiming to find sustainable management practices for both the catchment and its ponds, ultimately strengthening the ecosystem services of the area (*BFN*, n.d.). To achieve this task, there are several work packages defined, for example Monitoring and Assessment, Identifying Causes of Sludge Load, or Developing Sustainable Measures, to name a few.

As the present thesis is done in cooperation with the TH Lübeck as part of VerTe, the materials used in this study are funded by VerTe and all results will be made available for further project-related use. In turn, the data already collected by VerTe is available for this work and includes measurements in and around the ponds of Reinfeld from an ongoing campaign which started in 2023. It should be mentioned that this thesis is not the first within the project, as the following paragraph shows.

2.2.3.6 Baroto (2023): Master’s thesis within VerTe

Contributing to VerTe with their master’s thesis, Baroto investigated the impact of the tributaries’ water quality on the Herrenteich. Therefore, they analysed water samples from March 2023 to June 2023 at the in- and outflows of the Herrenteich, similar to Stresius (2006). Besides physico-chemical parameters and a load calculation with discharge measurements, the focus of this thesis were foremost the ecosystem services which the Herrenteich provided and how they could be affected by its tributaries (Baroto, 2023). The results from this measuring campaign are part of the continuously growing dataset from VerTe and are hereafter included as data from VerTe.

3 Methodology

The methodology chapter will start with a description of the study area, followed by the identification of potential phosphorous sources. Furthermore, the existing data on water quality and quantity is presented, after which a monitoring strategy for additional (missing) data from own measurements is developed. Subsequently, the methods of laboratory analysis will be shown as well as tools used for data processing. This is followed by methods of estimating TP concentrations and loads. Finally, the steps to analyse the spatial and temporal distribution of phosphorous in the catchment are presented.

3.1 Description of Study Area

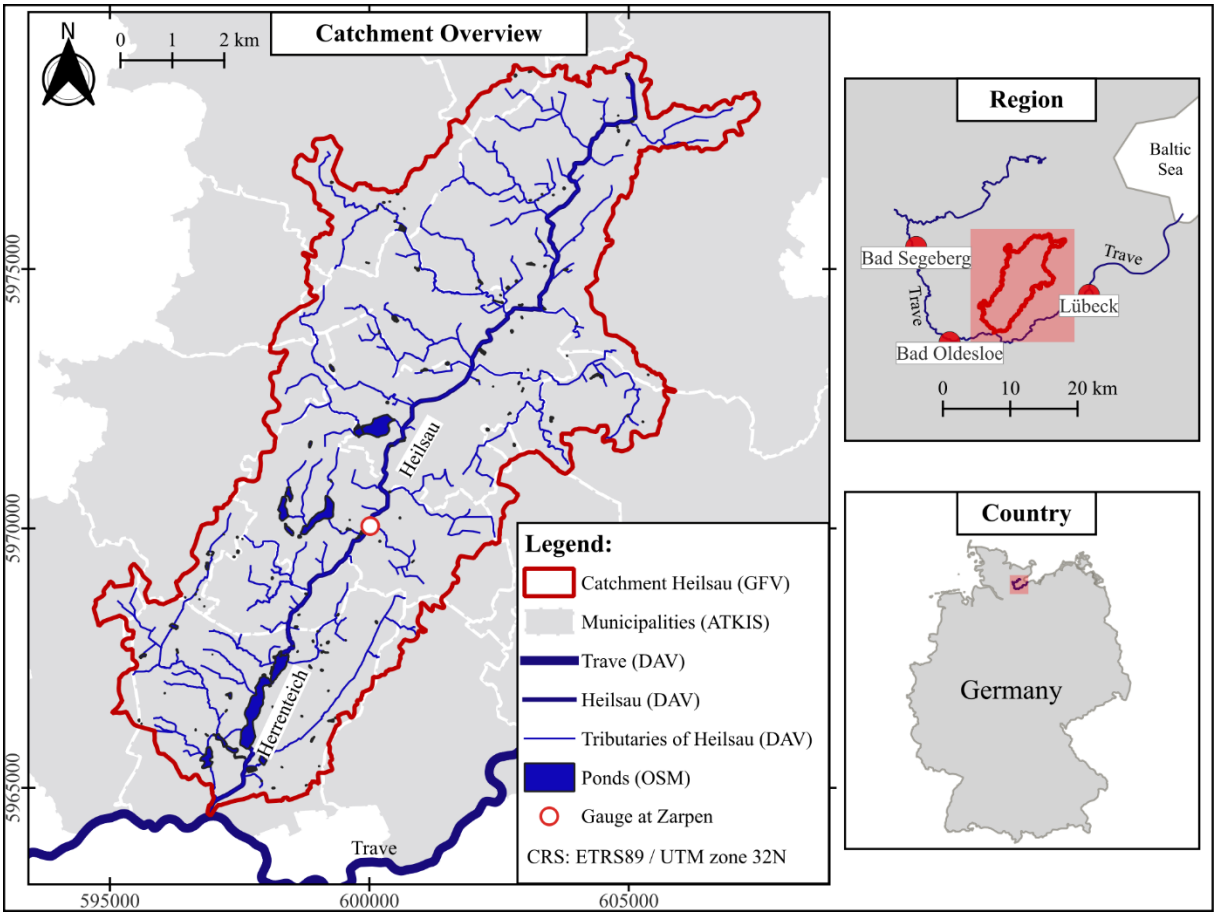

Figure 3.1: Overview of the Heilsau catchment.

3.1.1 Location

As seen in Figure 3.1, the 20 km long Heilsau is a tributary of the river Trave, which drains into the Baltic Sea to the north of Germany. The topographic catchment of the Heilsau drains an area of 74.5 km^2 and overlaps with 14 municipalities, where the main channel starts in the

municipality of Stockelsdorf to the north and flows through Mönkhagen, Heilshoop, Zarpen, Heidekamp and finally Reinfeld to the south.

3.1.2 Topography

With the highest point in the catchment being at 76.6 m NN[1] and the lowest at around 2.3 m NN, the Heilsau has an average slope of 3.7 m/km, or 0.37%. As seen in the two maps at the bottom of Figure 3.2**Error! Reference source not found.**, the Heilsau is running through the catchment diagonally from north-east (upstream) to south-west (downstream). The western half of the catchment has generally more hills and includes narrow steep valleys with slopes up to 100% and more (black areas in slope map); the eastern half, however, is mostly flat.

3.1.3 Soil and Hydrogeology

Regarding the distribution of soils, information about the soil coverage was taken from the BUEK250 data and processed in QuantumGIS 3.34.4 (hereafter QGIS). The translation and classification into English terms is shown in the Appendix, Figure 8.1. The result is shown in the top left map of Figure 3.2: The largest share of the catchment is covered by loam or sandy loam, with 85.9 % of the total area. In the low-lying areas around the Heilsau stream the soil textures range from loamy sand to peat, covering a total of 7.3 % and 4.3 % respectively. The few remaining areas are covered by silty clay loam (~ 1.1 %), silty loam (~ 0.3 %), and the biggest ponds, which were not classified regarding their "soil".

Regarding the hydrogeology of the catchment, the top right map of Figure 3.2 shows the thickness of layers covering the aquifer beneath, according to data from the LfU. As seen, the data is rather coarse, but a comparison with core drilling data from the groundwater sampling stations[2] shows a good overlap regarding the thickness of less permeable layers on the top, such as clay, silty loam, or silt.

3.1.4 Hydrology

As shown in Figure 3.1, with 74.5 km^2 the Heilsau catchment counts to the group of small catchments below 200 km^2 and has correspondingly low flow rates: The gauge at Zarpen, which drains about 66 % (≈ 49.468 km^2) of the total catchment, informs about a mean annual discharge MQ of 0.440 m^3/s (= 440 l/s), a mean lowest discharge MNQ of 0.020 m^3/s, and a mean highest discharge MHQ of 4.100 m^3/s, referring to the period of 1990 to 2018. The highest discharge

[1] NN stands for the German elevation reference „Normalnull", with the reference sea level being the gauge in Amsterdam, „Normaal Amsterdams Peil (NAP)" (*Amtlicher Höhenbezug*, 2021).
[2] available through the Web Feature Service "WFS Fachthemen Umwelt", operated by LfU-SH

ever recorded in this period was 6.580 m^3/s, on the 10th of January 1998 (*Pegel - Zarpen - Hauptwerte*, 2024). By dividing the discharge over its draining area, the so-called specific discharge q [$l/(s*km^2)$] can be calculated. For Zarpen, these specific discharges amount to Mq = 8.895, MNq = 0.404, and MHq = 82.882 $l/(s*km^2)$.

Regarding precipitation, the catchment lies in an area between three weather stations operated by the German Meteorological Service (DWD): Söhren to the west, Groß Parin to the north-east, and Lübeck-Blankensee to the south-east (also shown later in Figure 3.5). In the order of their respective appearance, their annual average precipitation amounts to 767.6 mm, 699.9 mm, and 676 mm, referring to the period from 1991 to 2020 (according to open data from DWD, *CDC Open Data*, n.d.).

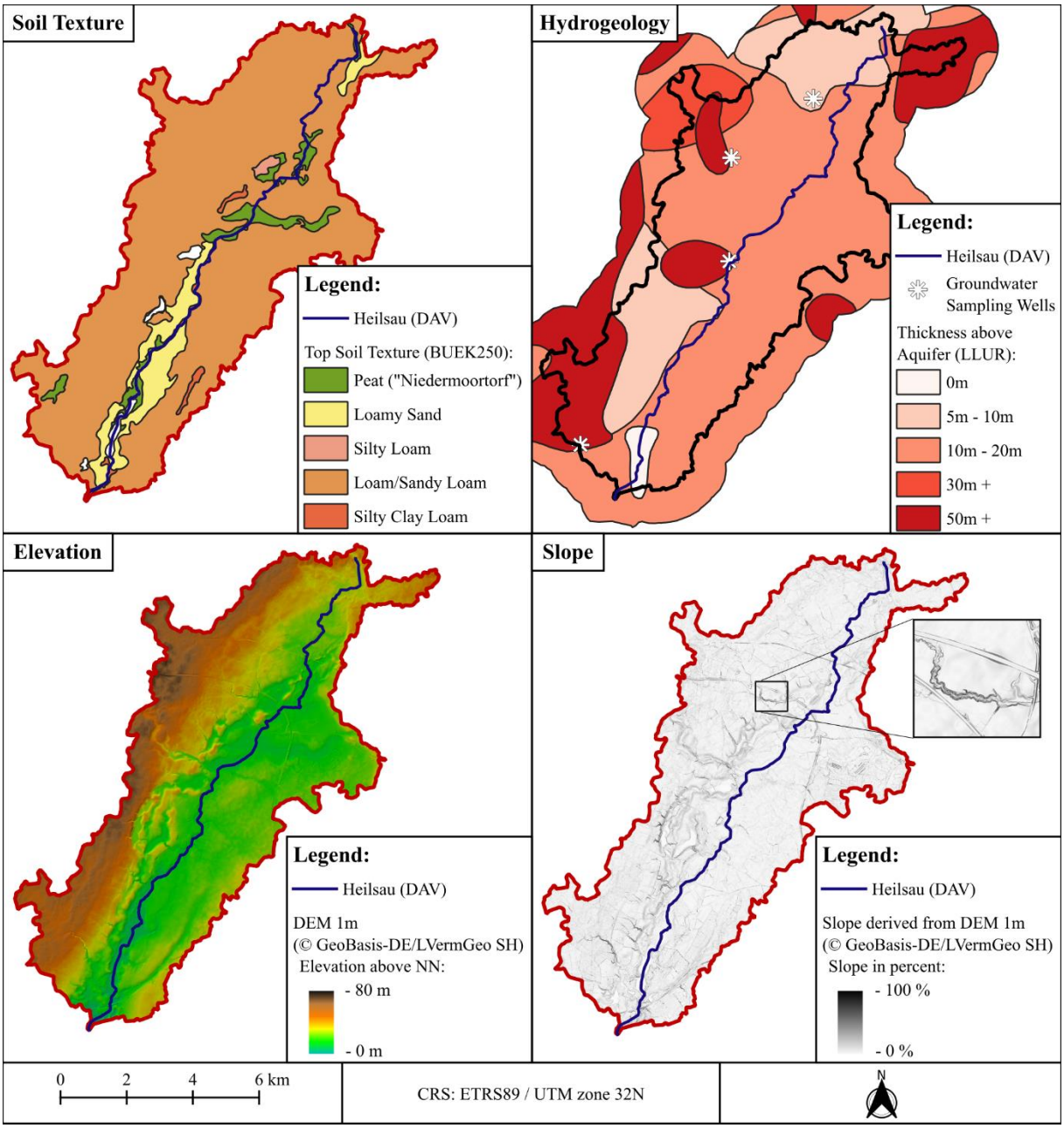

Figure 3.2: Maps containing data about soil texture, hydrogeology, elevation, and slope in the Heilsau catchment.

3.1.5 Land Use

As seen in Figure 3.3, which shows the distribution of land use classes and the location of towns or villages, the majority of the catchment is used for agriculture: Croplands make up 57.6 % of the total area, grasslands 12.5 %. The second biggest land use class is forestry, with 13.2 % coverage. Urban areas account to 7.1 %, most of that occupied by Reinfeld in the south. Industrial areas are only found at the border of the catchment in Reinfeld, close to the outlet, and make up less than one percent. Traffic areas, on the other hand, account to 4.1 %, a significant part of that being the highway A20, which passes Mönkhagen and Langniendorf. The land use shown is based on recent data from 2023, derived from the “Amtliches

Topographisches Kartographisches Informationssystem" (ATKIS), available on the geoportal of Schleswig-Holstein (*Schleswig-Holstein Downloadportal*, 2024).

Regarding the agriculture in the catchment, it should be noted that according to local farmers, nearly all of the agricultural land use is drained through tile-drainage and ditches, which could be confirmed during field surveys. Furthermore, the report by Hansen and Greuner-Pönicke (2002) reported that particularly the floodplains along the Heilsau were heavily drained for agricultural use (Hansen & Greuner-Pönicke, 2002). Detailed information about the location and extend of drainage pipes, however, were not available.

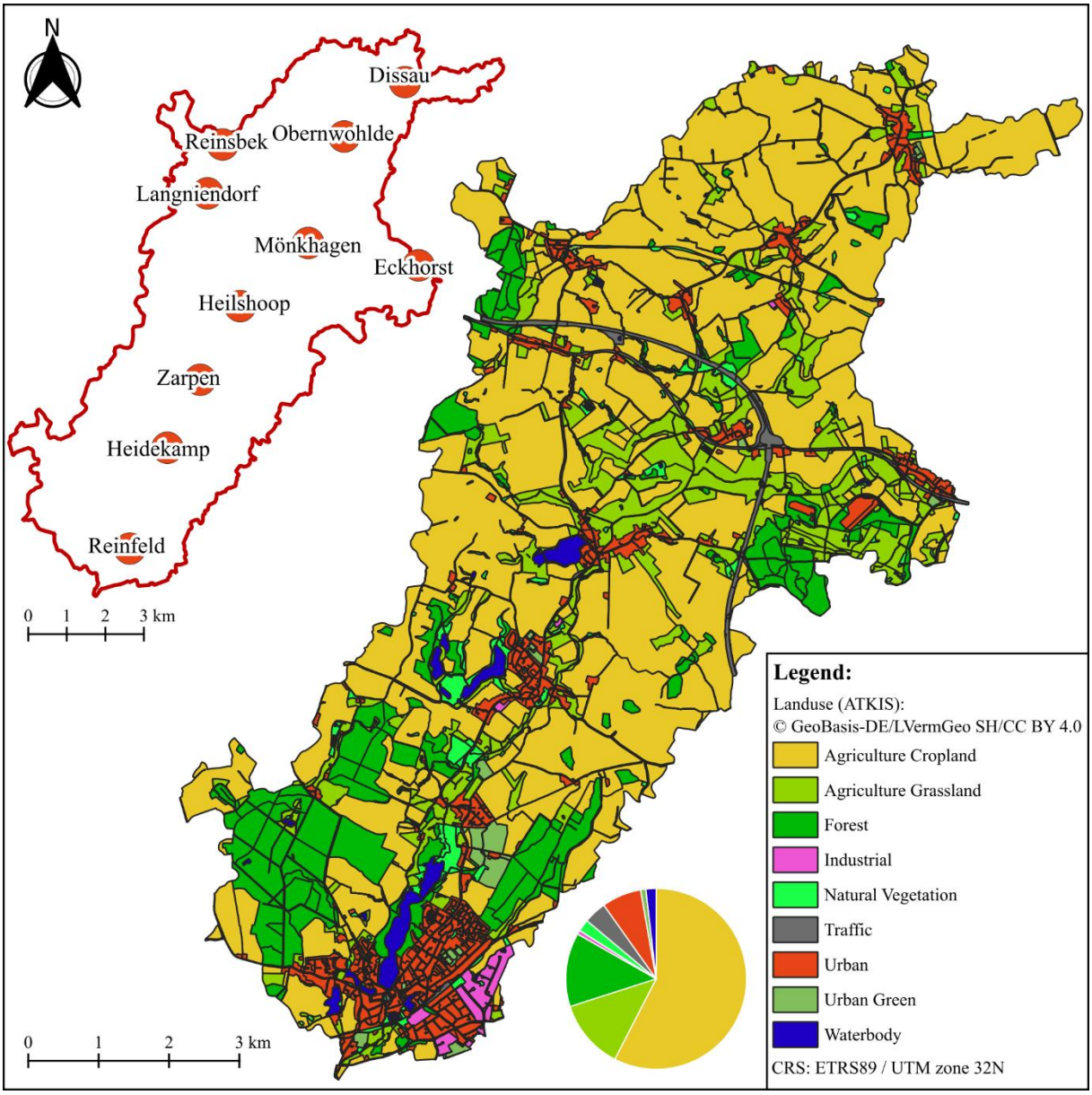

Figure 3.3: Distribution and share of land use classes. On the top left, the location of towns or villages is indicated.

3.1.6 Watercourse Modifications

Although land use can already be seen as a modification of the catchment, this section specifically presents the alterations done to the watercourses: As mentioned in the introduction, the Heilsau is highly modified due to the ponds which were constructed by monks around Reinfeld. The biggest pond, the Herrenteich, is dammed at the city of Reinfeld and has an area of 30 to 68 ha depending on the water level (Hansen & Greuner-Pönicke, 2002). In the map of Figure 3.1 for example, the Herrenteich is shown with an area of around 39 ha, to the south of the catchment.

The ponds, however, are not the only modification impacting the Heilsau, as the report from Hansen and Greuner-Pönicke (2002) summarised: Starting in the 1950s, parts of the river were straightened between Heilshoop and Reinfeld, in order to better drain the lands and make the grasslands more arable. The river's cross-sections were changed towards trapezoidal shapes. Moreover, substantial parts of the river network (both tributaries and main channel) were piped and urban settlements including their infrastructure (bridges, culverts) further affected the natural morphology of the Heilsau. Lastly, the Herrenteich itself has an additional impact besides the damming, as every year the pond is emptied for fishery; the time to refill the pond then takes around one to two weeks (Hansen & Greuner-Pönicke, 2002).

On a positive remark regarding its impact on the watercourse, it should be mentioned that the northern part of the Herrenteich and its surroundings were declared a nature conservation area in 1999, called "NSG Oberer Herrenteich" (*NSG Oberer Herrenteich*, n.d.). This supports the protection of biodiversity in the area (Hansen & Greuner-Pönicke, 2002), and the natural zone with its riparian vegetation might have a positive impact on nutrient retention and cycling.

3.2 Potential Phosphorous Inputs and Procedure for their Quantification

After having described the catchment properties, this section will investigate the potential phosphorous sources that could reach the Heilsau and therefore the Herrenteich. First, typical sources identified in research are presented, followed by defining the relevant sources for the Heilsau catchment upstream of the Herrenteich. Finally, an overview of the procedure to quantify those sources and the spatial and temporal distribution of P loads will be given.

3.2.1 Common Phosphorous Sources

Besides a relatively small natural background concentration of P from rock weathering and acidic leaching (Borbor-Cordova et al., 2006; Reynolds & Davies, 2001), numerous sources introduced or amplified by human activity have been identified. In general, sources are often divided into point sources and diffuse sources (European Environment Agency, 2005). Regarding point sources, the major contributors have been sewage effluents and discharges from industry (Contreras et al., 2024; Mockler et al., 2017). Diffuse sources on the other hand include a range of pathways, such as atmospheric deposition (which can be increased by industry), fertilizers and manure from agriculture, erosion from bare soils, forestry, or losses from paved areas (Carpenter et al., 1998; Contreras et al., 2024; European Environment Agency, 2005; Mockler et al., 2017; Tetzlaff et al., 2017; White & Hammond, 2006).

3.2.2 Potential Sources in the Heilsau Catchment

As presented in the review of past research related to the Heilsau catchment, this thesis will divide the sources of P into nine pathways, following the classifications from the FZ Jülich report shown in Table 2.1. As the study focusses on the part of the catchment upstream of the Herrenteich, no industrial sources are present (see land use map). Overall, the sources can be grouped into point and diffuse origins, as shown in Figure 3.4.

3.2.3 General Procedure to Quantify Phosphorous Inputs

To quantify the P inputs reaching the Heilsau upstream of the Herrenteich, as it is the aim of this thesis, both existing data from previous studies, literature as well as own measurements will be used. Relevant for a mass balance of P within a river are both concentration and discharge data, as their multiplication yields the load, defined as mass transported over time. A good approximation of loads requires qualified measurements, yet these are not always available at the needed temporal resolution or spatial scale. Therefore, the first step towards a P mass balance will be to investigate existing data for the Heilsau catchment. Where measurements are not sufficient, own samplings will be included. However, not all pathways are possible to sample separately or for the required period within the constraints of this thesis, therefore models will be used to estimate those knowledge gaps. Once the data is processed and compiled, the spatial and temporal distribution of loads can be derived and ideally the contribution from different pathways is separable.

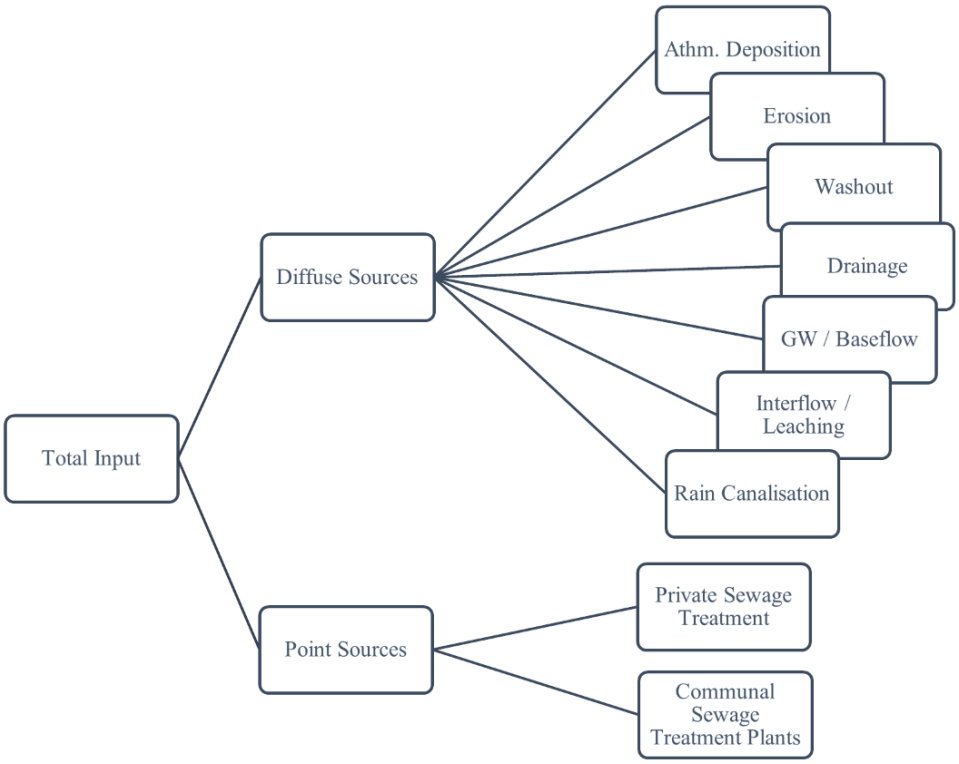

Figure 3.4: Potential Sources of Phosphorous in the Study Area. For definitions see Table 2.1.

3.3 Overview of Available Data

3.3.1 Sources and Spatial Context of Available Data

This section presents the available data from previous studies and public institutions and functions as an overview for the following sections of the methodology, where this data was used. Figure 3.5 indicates the distribution of water sampling stations, weather stations, and locations of point sources such as communal sewage treatment plants. Table 3.1 and Table 3.2 show the relevant data which was used from each source, as well as details regarding the number and frequency of observations.

Furthermore, data from the FZ Jülich report as well as from a rainwater measuring campaign by the TH Lübeck will be presented in more detail. Particularly the FZ Jülich model results required further processing to allow its application in the catchment analysis.

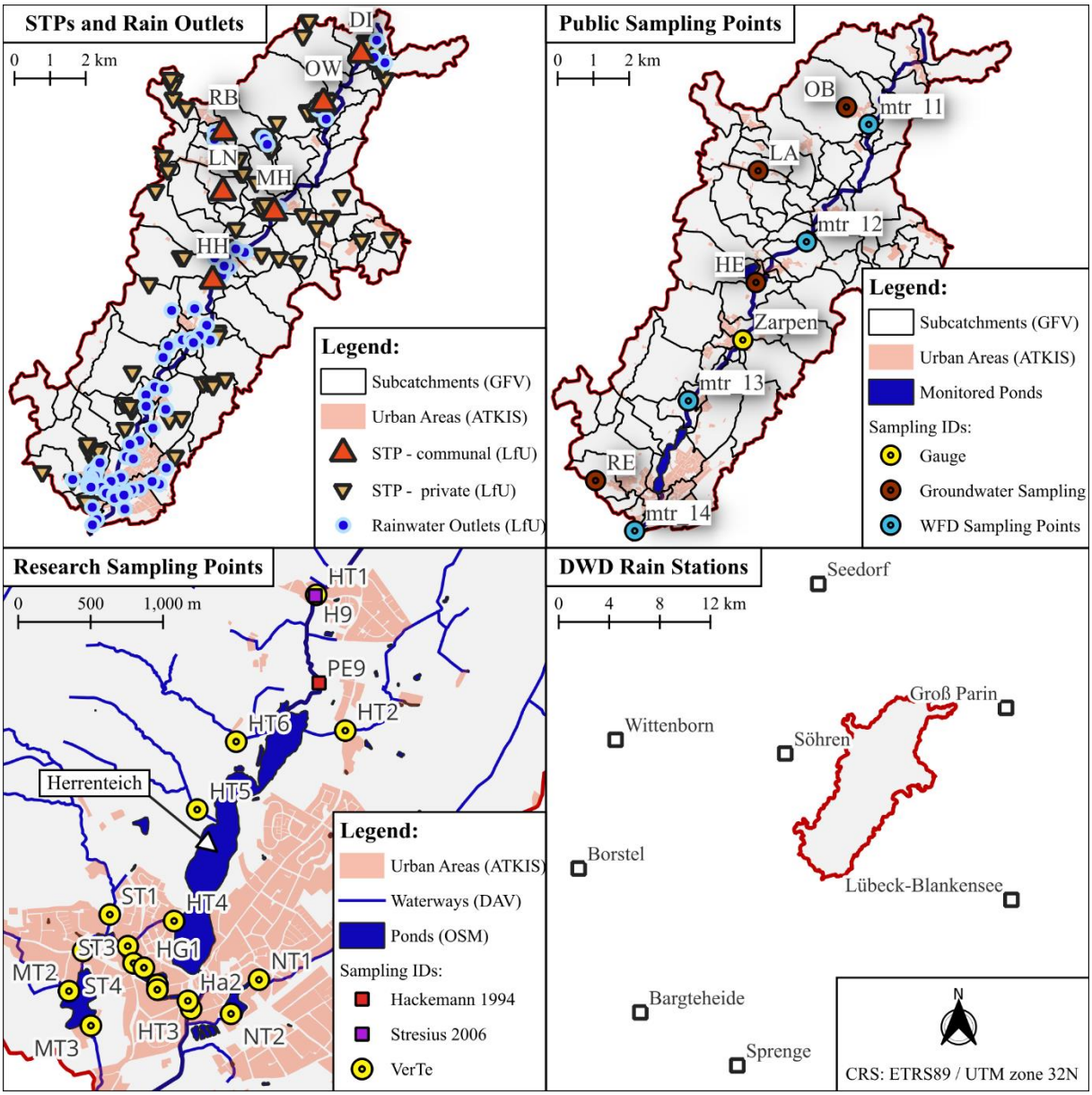

Figure 3.5: Overview of publicly available and georeferenced data. ***Top left:*** *private and communal sewage treatment plants (STPs), as well as positions of rainwater outlets.* ***Top right:*** *Sampling locations of public measurement campaigns regarding water levels, groundwater chemistry, and water quality in the Heilsau.* ***Bottom left:*** *Sampling locations of research activities by the TH Lübeck. Note that for Hackemann and Stresius, only the points from the Heilsau inlet into the Herrenteich are shown.* ***Bottom right:*** *Locations of nearby weather stations operated by DWD.*

Table 3.1: Available Data from Observations and Databases

Source/Provider	Data	Frequency of Data	Observation Period	Total of Observations
MEKUN, monitoring for the Water Framework Directive	Concentrations of: TP, ortho-P, Nitrogen compounds	Monthly	1991 - 2023 (not continuously for every location)	222 (for TP) 224 (for ortho-P)
D. Wolf from LKN*	W (observation), Q (calculated through rating curve and seasonal coefficient)	Daily (public), Hourly (on request)	November 1984 - 2024	> 14,000 (daily)
DWD** (CDC Open Data)	Precipitation data	Daily, hourly	Variable for each station	> 25,000 (daily)

C. Lüring from LfU***, Data accessed by VerTe from LfU	Type and location of private STPs Location and design capacity of municipal/communal STPs	-	-	-
Amt Trave-Land	Sewage effluent quality data of STP Reinsbek	Monthly	2021 - May 2024	Up to 54 per parameter
Data accessed by L. Osterhoff from LfU (available to VerTe)	Location of rainwater outlets	-	-	-
LVermGeo-SH ****	ATKIS Land use DEM 1m DOP 20m BUEK250	-	-	-
Gesundheitsamt Kreis Stormarn (Public Health Office)	Information on presence of cyanobacteria in the Herrenteich and Moorteich	Monthly from May to September	2018 - 2023	25 (Herrenteich) 25 (Moorteich)

** LKN: Landesbetrieb für Küstenschutz, Nationalpark und Meeresschutz*
*** DWD: Deutscher Wetterdienst*
**** LfU: Landesamt für Umwelt, Schleswig-Holstein*
***** Landesamt für Vermessung und Geoinformation Schleswig-Holstein*

Table 3.2: Available Data from Models

Source/Provider	**Name in this Study**	**Data**
H. Hund from LfU (© dl-de/by-2-0)	"GFV" or "GFV Statistics"	GFV subcatchment delineation, Regionalised values of flow (MNQ, MQ, MHQ, HQs of various return periods)
B. Tetzlaff from FZ Jülich, M. Trepel from MEKUN	"FZ Jülich Model"	Modelled TP Loads [kg/a, unless stated otherwise] of: AtmDepos (Vector, polygons of open water surfaces) Drain (Raster, 25m resolution) GW (Raster, 25m resolution) Interflow (Raster, 25m resolution) Washout (Raster, 5m resolution) Erosion (Raster, 5m resolution) RainCanal (Raster, 25m resolution) Mun-STPs (Vector, point geometry) Priv-STPs (Vector, polygons at municipality level) [kg/(a*ha)]

3.3.2 FZ Jülich Model Results

3.3.2.1 Data Provided by FZ Jülich and MEKUN

As mentioned before, the FZ Jülich wrote a report on the modelling of nutrient flows for Schleswig-Holstein in 2017. The updated dataset of model results based on more recent data from 2019 to 2023 was kindly provided for the Heilsau catchment. As seen in Table 3.2, the provided data comprised georeferenced vector and raster files containing the modelled TP loads as annual averages in kg/a.

The resolutions of the raster files were mostly 25 m. Only the Erosion and Washout raster data had a finer resolution of 5 m, as their modelling relied on the spatially sensitive parameters of slope and length of slope and was therefore calculated at a higher resolution (Tetzlaff et al., 2017, p.56).

The shape files had varying vector geometries: Municipal sewage treatment plants were included as points with an attributed annual TP load. Private sewage treatment on the other hand was represented as polygons, which had the extend of the municipalities. Moreover, the load for this pathway was given as kg/(a*ha). This could be explained as these loads were estimated based on the number of people who were not connected to municipal sewage treatment and an average per capita TP load from such private treatment facilities (Tetzlaff et al., 2017). Since there were no more details on the location of private STPs or their household size, the researchers could only estimate the total load per municipality, which they then divided over the municipalities' area, hence the unit change (Tetzlaff et al., 2017).

Data on atmospheric deposition (AtmDepos) on water surfaces was expressed as kg/a, referring to all surface water bodies which were connected to the stream network. The load was calculated by the area of those water surfaces which met this connectivity criteria, multiplied by a value of 0.5 kg/(ha*a) (Tetzlaff et al., 2017). In the model results from 2023, a deposition rate of 0.7 kg/(ha*a) was used, an updated value obtained from other measurement campaigns (statement by Dr. Tetzlaff).

3.3.2.2 Use of FZ Jülich Model Results

All these georeferenced loads were processed in QGIS to derive the estimated annual loads coming from each GFV subcatchment (the subcatchments were provided by the LfU, as seen in Table 3.2). The following paragraphs explain the relevant processing steps.

The provided atmospheric deposition vector file had some inaccuracies, e.g. the Moorteich at Heilshoop was not included as a water surface for deposition, those areas were updated. Following the method of the FZ Jülich report, the DAV stream network from the AWGV-SH Web Feature Service (WFS) was used to derive the geometry of the water surfaces (Tetzlaff et al., 2017). To derive the surface of the streams, the channel width from WFS dataset was used for a variable buffer width along the stream network. Note that those parts of the stream network which were piped were not included, as no atmospheric deposition occurs there. To include lentic waterbodies, the pond polygons from a QuickOSM query (searched for natural=water), were used. However, since the waterbodies need to be connected to the stream network to be

counted as contributors, the ponds were filtered for those intersecting with a 10m buffer of the stream network. Some waterbodies which fell out of that buffer but were clearly connected were added manually, e.g. the ponds around Zarpen. Finally, the resulting polygons of stream and pond surfaces were intersected with the GFV subcatchments and then multiplied by the mentioned deposition rate of 0.7 kg/(ha*a). This yielded the subcatchment-specific TP load from AtmDepos in kg/a.

For the raster files, subcatchment-specific loads were derived as follows: For a true mean load per subcatchment, the empty values of the rater files needed to be converted to zero. These modified raster files could then be used for a zonal statistics analysis with the GFV subcatchments as the mask layer (boundary for zones). The resulting mean load of TP in kg/(ha*a) could then be multiplied with the respective subcatchment area to derive the load in kg/a which comes from that specific subcatchment, for the respective raster file (i.e. pathway).

For the case of private STPs, the polygons in the shape of the municipalities were intersected with the GFV subcatchments. The resulting fragments were then used by multiplying their area with the municipality-specific areal loading [kg/(ha*a)] to derive the load in kg/a. These loads were then summed up for each subcatchment if more than one municipality overlapped in one GFV.

The combination of the above, with addition of the point source load of municipal STPs, resulted in a catchment-specific annual TP load as modelled by FZ Jülich, separated by each pathway such as Interflow, Erosion, GW, AtmDepos, Mun-STPs, or Drain. The summation of those pathways yielded the total annual load of TP per subcatchment. It should be noted that these loads are results of model simulations at a bigger scale, therefore they were used as indicators for potential hotspots of phosphorous sources, as well as a likely apportionment between the nine pathways. The validation of those simulation results would need additional measurements in the subcatchments, which will be discussed later in the section of the field campaign.

3.4 Discharge and Precipitation

3.4.1 Discharge Data

Within the catchment there is one gauge, positioned in the Heilsau at Zarpen (see Figure 3.5, top right). It is operated by the LKN, as shown in Table 3.1, which provides daily and on request even hourly readings of the water level W as well as the respective discharge Q. Q is calculated

through a rating curve and a seasonal coefficient, which is calibrated through monthly measurements (as explained by D. Wolf, LKN). Secondly, there are regionalised values for low flow, mean flow, and flood discharges available for each GFV subcatchment, provided by the LfU. These statistics of discharge have been regionalised based on numerous explaining variables such as land use, geology, soil, topography, and precipitation (Willems & Stricker, 2017). Finally, there is data from discharge measurements carried out by VerTe for most of the project's sampling points shown in Figure 3.5, bottom left.

To estimate discharges for more parts of the catchment than the gauge in Zarpen alone, the above-mentioned data was used as follows: It is proposed to use the discharge from Zarpen and multiply it with a subcatchment-specific coefficient α, derived from the GFV regionalisation data. This coefficient was calculated by the ratio of MQs between the subcatchment of interest and the subcatchment of the gauge in Zarpen, based on the hypothesis that the flows within the catchment are positively correlated to each other. The equations used to derive the discharge of interest and α were the following:

$$Q_{GFV_x} = \alpha \cdot Q_{GFV_{Zarpen}}$$

$$\alpha = \frac{MQ_{GFV_x}}{MQ_{GFV_{Zarpen}}}$$

Where GFV_x is the subcatchment of interest and MQ the mean discharge from the regionalised LfU dataset. The discharge of interest could therefore be estimated for every day which had a gauge observation in Zarpen.

To test the quality of this method, the measured discharges from VerTe were plotted against calculated discharges as a visual analysis. As a numerical goodness of fit criteria, the root mean square error (RMSE) was calculated between observed and estimated values (see equation below). Furthermore, the normalised RMSE (nRMSE) was derived by dividing the RMSE over the range of observed discharges at the sampling location. This was done for comparability among different sites, as their discharges varied in orders of magnitude to each other.

$$RMSE = \sqrt{\frac{\sum_{i=1}^{N} \left(Q_{Calc,i} - Q_{Obs,i}\right)^2}{N}}$$

$$nRMSE = \frac{RMSE}{max(Q) - min(Q)}$$

Where N is the number of observations, Q_{Calc} the calculated or estimated discharge, and Q_{Obs} the observed or measured discharge. For the *nRMSE*, the maximum and minimum of discharges were used as the respective range.

3.4.2 Precipitation

As no weather station from the DWD was found within the Heilsau catchment, precipitation recordings from surrounding stations needed to be used for reference. A common way to spatially interpolate precipitation data in hydrology is the Inverse Distance Weighted (IDW) method (Kurtzman et al., 2009; Li & Heap, 2014), which was used in this thesis. The method calculates an unknown variable (here: precipitation) based on observations in the surrounding area, where each observation is weighted based on the distance to the location of interest. Mathematically, this calculation follows the equation below:

$$P(x_0) = \frac{\sum_{i=1}^{n} P(x_i) \cdot w_i}{\sum_{i=1}^{n} w_i}$$

Where:

- $P(x_0)$ is the interpolated precipitation at the location of interest x_0.
- $P(x_i)$ is the observed precipitation value at station i.
- w_i is the weight assigned to station i, with $w_i = \frac{1}{d(x_0,x_i)^p}$.
- $d(x_0, x_i)$ is the distance between x_0 and x_i.
- p is the power parameter.

A location of interest for interpolating the precipitation data needed to be chosen. For simplicity, the centre of mass (centroid) of the catchment upstream of the Herrenteich was seen as representative for the catchment and chosen as the location for interpolation. For the known observations of daily precipitation, the three weather stations Lübeck-Blankensee, Söhren, and Groß Parin were chosen (see bottom right map of Figure 3.5) and their missing values were removed. Their distances to the centroid were 14.973 km, 8.026 km, and 10.227 km respectively (measured in QGIS). The power parameter for the distance weighting was chosen as p=2, a medium value according to literature (Kurtzman et al., 2009). All interpolation calculations were done in Python. The resulting IDW precipitation was used as a reference precipitation for all following analyses and is hereafter simply referred to as precipitation or IDW precipitation.

3.5 Instream Water Quality

3.5.1 Available Measurements for Main Channel

As mentioned before, several studies within the catchment had been conducted in the past, and their water quality data was used for analysis. Firstly, monthly measurements from MEKUN, which were taken for monitoring reasons regarding the WFD, included four sampling stations along the main channel of the Heilsau (see Figure 3.5, top right). As seen in Table 3.1, the TP and ortho-P measurements were used from this database. Secondly, the studies conducted by Hackemann (1994) and Stresius (2006) provided additional data points, and their TP and ortho-P concentrations upstream of the Herrenteich were included. Lastly, measurements from VerTe, including those of Baroto (2023), were added for analysis.

The data was checked for consistency and plausibility. In particular for data from VerTe, if concentrations were below the measuring range of the used laboratory tests, the values were halved – a common method to consider such low readings (Tetzlaff et al., 2017). After preprocessing, the concentration data from the Heilsau upstream of the Herrenteich was plotted over time for a trend analysis, along with precipitation data. Furthermore, to identify the annual distribution, boxplots of TP concentrations were generated, grouped by their respective month.

3.5.2 Field Campaign in Upper Catchment

As there was little data available for the subcatchments upstream of the Herrenteich, I organised and carried out additional field measurements. Of particular interest was the water quality in the tributaries along the Heilsau. However, apart from point sources like the sewage treatment plants shown in Figure 3.5 (top left), there was little known about potential hotspots of phosphorous sources, and more information was needed to select qualitative sampling locations. Therefore, land use and slope information (as shown in the description of the study area) was used to identify potential areas of high diffuse P inputs. However, the data from the FZ Jülich Model proved most suitable, as their relatively fine spatial scale allowed a good estimation of potential P sources and their magnitude.

Figure 3.6 shows the total annual load of TP per subcatchment from the Jülich model results, processed as described in 3.3.2.2. Furthermore, the map shows the sampling locations at selected GFV outlets: Firstly, the highest polluting subcatchments indicated in dark shades were chosen. Additionally, the total load was divided by the MQ from the respective regionalised GFV statistics, to derive an initial approximation of mean concentrations which could be expected. From those subcatchments above the detection limit of 0.05 mg/l TP, some were

chosen for sampling to obtain a better spatial distribution. It should be mentioned that not all locations were accessible, e.g. a catchment to the west of GFV_20, where the outlet of the piped waterway could not be found in the field. Moreover, some points were specifically chosen along the main course of the Heilsau (e.g. GFV_45). This would allow a section-wise mass balance in the post-processing.

In total, 16 locations were selected for the field campaign, 13 of them located in the catchment upstream of the Herrenteich. The remaining three in the south were only added for future research of VerTe, as these overlap with previous sampling locations and could be useful for a mass balance around the ponds of Reinfeld.

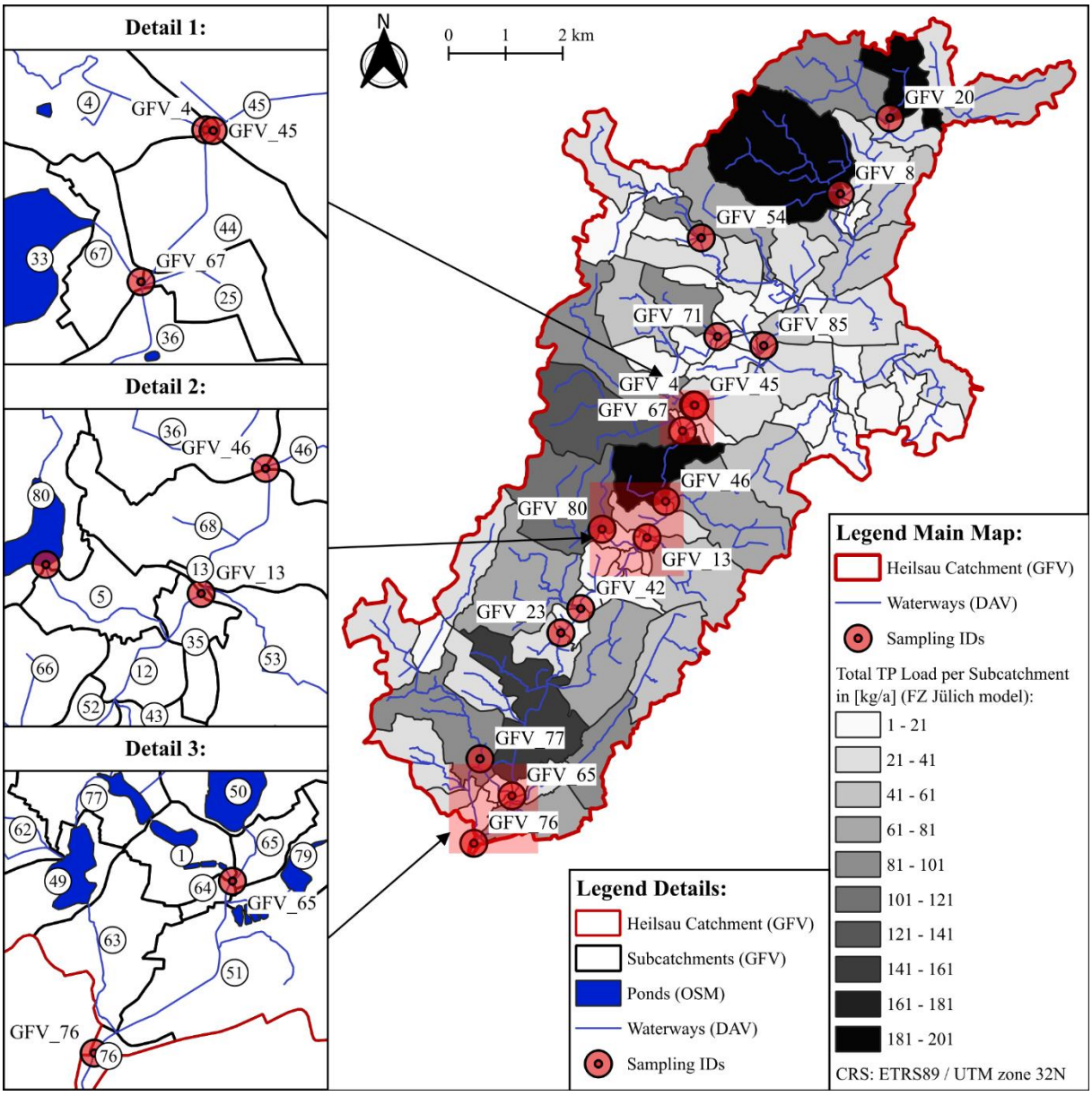

Figure 3.6: Map of sampling locations from field campaign, based on total TP loads from FZ Jülich model results. Note that the subcatchment IDs, shown in white circles on the left, were randomly generated and then used consistently.

3.5.2.1 Weekly Sampling

The selected 16 locations from above were sampled on a weekly basis, with the campaign for the upper catchment starting on April 30th, 2024. Every Tuesday the selected streams were sampled following to the sampling procedure described in the Appendix, 8.2, including live instream measurements of the parameters pH, temperature, dissolved oxygen (DO), and electric conductivity (EC). The refrigerated grab samples were analysed the following day in a laboratory of TH Lübeck in Reinfeld, again the detailed procedure is described in the Appendix, 8.3. It should be noted that the lab analysis was not only done for phosphorous compounds but extended to nitrogen compounds for future research. The weekly campaign finished on June 18th, 2024, therefore comprising eight consecutive weeks of data. The resulting measurements were processed in MS Excel, QGIS, and Python.

3.5.2.2 Event Measurement: Reaction of Catchment to Intense Rainfall

Besides the weekly sampling, there was an interest in measuring the catchment's behaviour towards extreme events of rainfall. Therefore, weather forecasts were regularly consulted, with warnings set up for thunderstorms. This way, an extreme rainfall event in May 2024 with more than 40 mm/d could be included in the measurement campaign. The event followed a dry period of nearly three weeks with no rain.

In order to analyse the catchment's reaction to such an event, the sampling station GFV_13 at the gauge in Zarpen was selected for high frequency sampling. This location had the advantage of simultaneous hourly discharge data available on request from the LKN, which would allow a concentration-discharge relationship (C-Q relationship) analysis. Such C-Q relationships have been studied to identify patterns like enrichment or dilution on different timescales (like seasons or events) and can help identify the responsible drivers for those patterns (Evans & Davies, 1998; Godsey et al., 2019; Speir et al., 2024).

To receive high frequency water quality data, an autosampler provided by the TH Lübeck could be used (©MAXX, model PB-M-L). The sampling frequency was dynamically adjusted, so that periods of high interest, such as the rising limb of the discharge following the start of the rain event, could be sampled at a high frequency of every 30 minutes to one hour, and periods of lower interest, such as the slowly declining falling limb one day after the event, could be sampled at lower frequencies of three to six hours. This ensured to not exceed the capacity of the lab and the available sampling containers. The following Table 3.3 shows the frequency of sampling from May 22nd to May 26th. In summary, 68 samples were taken for this event. These

were analysed in the lab for TP, ortho-P, total nitrogen (TN), nitrate (NO3), ammonium (NH4), and some for their pH.

Table 3.3: Sampling frequencies during extreme rain event in May 2024, at GFV_13.

From	To	Frequency
22/05/2024 09:00	22/05/2024 11:00	1 h
22/05/2024 12:00	23/05/2024 05:30	30 min
23/05/2024 06:00	23/05/2024 20:00	1 h
23/05/2024 21:00	24/05/2024 21:00	3 h
25/05/2024 00:00	26/05/2024 00:00	6 h

The resulting parameters were plotted over time, along with hourly discharge values from the gauge in Zarpen. Furthermore, higher frequency precipitation data was needed, for which the same inverse distance method as described before was used. However, the station in Söhren only registers daily precipitation, whereas Lübeck-Blankensee and Groß Parin register hourly data. To impose an hourly curve onto the precipitation data from Söhren, hourly data from the latter two stations were used along with hourly data from Wittenborn, a station 13.47 km further to the west of Söhren, as seen in the overview of Figure 3.5, bottom right. A detailed explanation of the interpolation method is shown in the Appendix, with Table 8.1. The resulting hourly precipitation for the Zarpen catchment was plotted alongside the concentrations and discharge.

In addition to the time series, concentrations of TP were plotted against their respective discharges in a log-log scale, for a C-Q hysteresis analysis as discussed in literature (Evans & Davies, 1998; House & Warwick, 1998; Speir et al., 2024). All plots were made in Python, using the Plotly library (© 2016-2018 Plotly, Inc).

3.5.3 C-Q Analysis for GFV_23 (Heidekamp)

As mentioned above, the relationship between solute concentrations and discharge, called C-Q relationships, have been the focus of numerous studies (Godsey et al., 2019; House & Warwick, 1998; Musolff et al., 2015; Yang et al., 2020). Their analysis can help identify patterns of dilution or enrichment, and more importantly potential causes for these patterns, such as biological, meteorological, or geological drivers (Moatar et al., 2017; Speir et al., 2024). Moreover, if sufficient data is available, C-Q relationships can be used to predict concentrations through discharge data (Minaudo et al., 2019). This section will present the methodology used for a C-Q relationship analysis of TP. Furthermore, the steps towards building a C-Q model will be explained, which was used for the interpolation of missing TP concentration data and later for load estimation.

3.5.3.1 C-Q Relationship Analysis

A common way to visualise a C-Q relationship is the hydro-chemograph, which shows the concentration of the parameter of interest along with the discharge over time. Additionally, several metrics exist to further describe the link between discharge and concentrations, for example the C-Q-slope, where concentrations are plotted against discharges in a log-log space. A positive slope can be interpreted as enrichment of C with Q and a negative slope as dilution, whereas a slope close to zero usually indicates chemostatic behaviour of the solute towards discharge (Minaudo et al., 2019; Speir et al., 2024).

For this thesis, the C-Q relationship was investigated for the sampling station GFV_23 at Heidekamp. This station was chosen for two reasons: Firstly, it drains the part of the Heilsau catchment upstream of the Herrenteich, just before entering its nature reserve area. Secondly, this station had the most TP concentration measurements in the upper catchment, thanks to sampling campaigns from MEKUN for the WFD and research from the TH Lübeck. However, a disadvantage towards the station at Zarpen was the lack of its own gauge, therefore the discharge at GFV_23 needed to be estimated with the method described in 3.4.1.

For the analysis, the calculated discharge Q_{calc} was plotted along with TP measurements in a hydro-chemograph. The data included not only publicly available data, but also the measurements from this thesis' field campaign. Furthermore, the C-Q relationship was analysed for chemodynamic or chemostatic behaviour through a log-log space plot of observations. This would allow an interpretation of the C-Q slope.

3.5.3.2 C-$Q_{quick\text{-}slow}$ Model

Minaudo et al. (2019) developed a model to incorporate catchment reactions to both short-term and long-term variations of Q, meaning storm events and seasonal discharge variation. The two processes were named "quick" and "slow" and can be compared with direct runoff from rain events and baseflow (Minaudo et al., 2019). The researchers' C-$Q_{quick\text{-}slow}$ model showed to improve nutrient load estimations when compared to a standard discharge-weighted method and allowed to interpolate monthly concentration data to a high-frequency timestep like days (Minaudo et al., 2019). Following the methodology of Minaudo et al. (2019), a model to estimate concentrations at GFV_23 for days without measurements has been implemented. This involved several steps:

Firstly, the daily discharge data Q_{calc} needed to be separated into storm events and seasonal flow, i.e. Q_{quick} and Q_{slow}. These partitions were estimated with the "baseflow recursive filter

method" with 3 passes and a filter parameter of 0.925, using MS Excel (Lyne & Hollick, 1979; Minaudo et al., 2019; Nathan & McMahon, 1990). The recursive filter method was inspired by digital signals' analysis and separates an input (e.g. discharge) into high and low frequency contributions, i.e. Q_{quick} and Q_{slow} (Lyne & Hollick, 1979). As Minaudo et al. verified the seasonality of Q_{slow} through autocorrelation curves, such a curve was generated and verified for the resulting Q_{slow} from the GFV_23 discharge, using the *NumPy* library in Python (© 2005-2024, NumPy Developers).

Once the flow had been separated, it could be used for linear regression of the following model equation as presented in Minaudo et al. (2019):

$$C(t) = \beta_0 + \beta_1 \cdot log\big(Q_{slow}(t)\big) + \beta_2 \cdot log\left(Q_{quick}(t)\right) + \varepsilon$$

where $C(t)$ is the concentration at time t, β_i the coefficients to be determined by linear regression, $Q_x(t)$ the respective parts of the discharge at time t as explaining variables, and ε the residuals (Minaudo et al., 2019).

To determine the coefficients β_i, the model was fitted through an ordinary least squares (OLS) linear regression in Python, using the *statsmodels* library (© 2024, statsmodels). For $C(t)$ the concentration of TP was of interest. Additionally, if the $Q_x(t)$ entries were zero (for example no stormflow), it would cause negative infinite values when log-transformed, therefore their logarithmic values were set to zero to allow the regression model to converge. The resulting coefficients of the model were seen as statistically significant if their p-value was below 0.05 (Minaudo et al., 2019). In case the coefficients were significant, the model results were used to calculate the estimated TP concentrations for each day, following the equation from above (excluding ε).

The resulting estimated TP concentrations were plotted against measured concentrations, along with the discharge and the separated baseflow (Q_{slow}) from the recursive filter method. Additionally, the observed and modelled TP concentrations were plotted against discharge in a log-log space for a C-Q slope analysis in combination with the ratio of stormflow to baseflow.

3.6 Effluents from Point and Diffuse Sources

In addition to the analysis of instream water quality, the aim was to collect more detailed information about phosphorous coming from specific sources. Both point and diffuse pathways were considered, although a discrete measurement of diffuse sources proves difficult by their

nature. Nevertheless, the following sections describe the methodology to gather data for said sources.

3.6.1 Drainage Sampling

Besides the sampling of the Heilsau and its tributaries, the field campaign included the survey for drainage pipe outlets within the catchment. This involved contacting farmers for insights regarding drainage areas and outlet locations, as well as personal investigations in search for outlets in the catchment. Where a drainage outlet was found and accessible, water samples were taken following the same procedure as for the GFV subcatchment sampling, described in the Appendix, 8.2. Additionally, for discharge values, measuring jugs of 500 ml to 1 l were used and the time for filling a certain volume was taken. This was repeated at least three times to derive an average discharge in volume over time. The drainage samples were then stored and further processed in the lab, as described in the general sampling protocol (Appendix, 8.2). The tested parameters were the same as for instream water quality (i.e. TP, ortho-P, TN, NO3, NH4). However, the pH, temperature, and EC were measured in the lab, as the drainage discharges were too low to fully immerse the multiparameter probes in field.

3.6.2 Rain Canalisation

A detailed sampling campaign for rainwater outlets was not possible in the scope of this thesis. However, since the TH Lübeck was running a project specifically on rainwater systems in two towns close to Hamburg (MaReT-SH), some of their data was used alongside with model results from FZ Jülich to estimate phosphorous coming from rain canalisation separated from sewage. The FZ Jülich report combined land use classes with literature values for their respective percentage of sealed surfaces to model the runoff from those areas which were connected to separate sewers. These discharges were then multiplied with land-use-specific TP concentrations from literature.

3.6.3 Sewage Data

3.6.3.1 Municipal STPs

Regarding sewage effluents, six municipal treatment plants were found in the catchment area, as shown before in Figure 3.5: From north to south there were STPs in Dissau, Obernwohlde, Reinsbek, Langniendorf, Mönkhagen, and Heilshoop. Their individual location and design capacity in population equivalents (PEs) was provided from a dataset available to VerTe, received from the LfU.

To receive information on the effluent quality or get permission to sample the STPs for this thesis, the responsible offices (in German: Amt) were contacted. Although only two were reached, these two covered four of the six STPs. From email exchange with the Amt Nordstormarn, the actual PEs connected to the STPs within their jurisdiction was provided, as well as the permission to sample their treatment plants. From an exchange with the Amt Trave-Land the respective PE and even monthly measurement data were provided for their STP in Reinsbek. These sources combined yielded the data summarised in Table 3.4.

Table 3.4: Available data for municipal sewage treatment plants (various sources).

Municipal STP	**ID**	**Capacity [PE]**	**Utilisation [PE] (Date)**	**Provided Measurements**	**Source**
Dissau	DI	650	-	-	VerTe dataset
Obernwohlde	OW	104	-	-	VerTe dataset
Reinsbek	RB	525	418 (in 2023)	Monthly (from 2021 to May 2024): T, pH, TOC, COD, BOD5, TN, NH4, NO3, NO2, TP, occurrence of waterweed	Amt Trave-Land
Langniendorf	LN	300	284 (in 2023)	-	Amt Nordstormarn
Mönkhagen	MH	335	322 (in 2023)	-	
Heilshoop	HH	600	538 (in 2023)	-	

Unfortunately, none of the sources included discharge values which would allow a load estimation. Therefore, the authorisation by the Amt Nordstormarn to sample the STPs of Langniendorf, Mönkhagen, and Heilshoop was used to both derive discharge measurements as well as additional water quality data. The sampling was done in May and June 2024, with both dry and wet conditions. The dry conditions were of high interest, as these would be used to estimate an overall per capita load from the effluents. The wet conditions could be used for analysing the change in effluent concentrations under higher inflow, i.e. the performance under varying conditions.

The sampling procedure involved the installation of two autosamplers (©MAXX, models TP5 C and PB-M-L) per STP, one sampling the inflow, one the effluent. Their programme was set to take samples every 15 minutes, with four samplings mixed into one bottle. This allowed a 24-hour sampling with one sampling container for each hour. These containers were kept cool using ice packs within the autosampler, to reduce microbial activity during the sampling period. The samples were then collected the next day when the sampler's programme finished and transferred immediately to the lab for analysis.

In addition to the water quality samples, the discharge of the effluent was measured where possible. This was done using a 5-litre measuring jug in combination with a stopwatch. Each

discharge was sampled six times in series to derive an average. For Heilshoop and Mönkhagen this could be achieved for dry conditions, where no rain was recorded over two days before sampling. The Q measurement for Langniendorf co-occurred with 6 mm precipitation within the 48 hours before (according to IDW precipitation data from the Zarpen catchment).

Moreover, during the field survey and visits on the treatment plants, the treatment type was determined. The STP at Obernwohlde could not be categorised nor found, but the other five STPs were categorised as waste stabilisation pond systems (WSPs) of two to three ponds in series, following general descriptions by Biswas et al. and Rousseau (Biswas et al., 2022; Rousseau, 2023). Three out of the five treatment plants were systems without any active aeration, therefore suggesting a system of the type anaerobic or a combination of anaerobic and facultative (Rousseau, 2023). Only Heilshoop and Dissau had an additional aeration system, where Heilshoop alternated aeration between the first two of its three ponds.

3.6.3.2 Private STPs

Although the location and even types of private treatment plants at the household level were provided in the dataset from the LfU, as seen before in the top left map of Figure 3.5, the actual household size remained unknown. Therefore, it was not possible to accurately estimate potential TP loads at the same spatial detail as the private STP positions. However, the data from the FZ Jülich model could again be used as an alternative. The research team used an average per capita loading rate of 0.7 g TP per person and day, a value provided by the LfU, and multiplied this with the total number of people without a connection to municipal STPs (Tetzlaff et al., 2017). Additionally, an assumption the researchers had regarding the share of private STPs discharging into groundwater could be supported: The model assumed a low share of such discharges into groundwater (Tetzlaff et al., 2017), and an analysis of the dataset provided by the LfU in QGIS confirmed that, as only one out of 124 STPs (=0.8 %) in the whole catchment area discharges into groundwater.

3.7 TP Load: Temporal Variation

With the collected data from above the loads of total phosphorous were determined where possible. In general, the TP load was calculated by multiplication of discharge and concentration, and these loads were then analysed for temporal and spatial variation. The following section discusses the methodology for temporal patterns of instream phosphorous transport as well as sewage and drainage effluents where possible.

3.7.1 Instream Phosphorous Loads

For the most significant outlet GFV_23, at Heidekamp, the C-$Q_{quick\text{-}slow}$ model allowed to calculate the loads of TP for each day where discharge data was available. These loads were summed up to monthly and then yearly loads for the years 1991 to 2024, to analyse the seasonal and annual variation of TP inputs from the Heilsau towards the Herrenteich.

To compare these loads from the simulation with another load estimation approach, the Q-weighted method as shown in Minaudo et al. (2019) was used additionally, a method similar to the one used by Hackemann (1994). Where concentration measurements were available, the monthly and yearly loads were calculated with the following equation:

$$L_T = \frac{\sum C_i \cdot Q_i}{\sum Q_i} \cdot \bar{Q}_T$$

With L_T the load for the period T (year or month), C_i and Q_i the concentrations and discharges within the period T, and $\bar{Q}_T$ the average discharge during the period T (adapted from Minaudo et al., 2019).

Discharges were estimated for GFV_23 as presented before in Section 3.4.1 (Q_{calc}). Additionally, the yearly Q-weighted loads were calculated with the discharges from the gauge at Zarpen. On the one hand, this would remove the uncertainty of the discharge estimation method. On the other hand, this underestimates the discharge, as additional water coming from subcatchments between Zarpen and Heidekamp is ignored. The use of this additional step, however, was the determination of a lower boundary for the TP load estimations, a minimum.

Furthermore, the results from the FZ Jülich Model were used to derive the annual *modelled* load reaching the Herrenteich from the upstream catchment. This would serve as another comparison between load estimations. To derive said load, all nine pathways were summed up in QGIS for the area of the upper catchment reaching the outlet of GFV_23.

Lastly, the event measurement done in May 2024 could be used to analyse the hourly load reaching the gauge at Zarpen. This was restricted to the duration of the high frequency sampling only, yet it would allow to compare the loads transported in short periods during a rain event versus the loads estimated without such high frequency data.

3.7.2 Loads from Source-Specific Measurements

For drainage effluents, loads could be calculated for some samples where discharges were measurable, yet the determination of the draining area proved difficult. A representative land-

use-specific drainage load could therefore not be calculated with the available data, only a speculative estimation would be possible.

For STP measurements, the 24-hour mixed samples from the field campaign could be used along with effluent discharge measurements to determine the respective loads of TP. The data was examined for weather conditions, i.e. dry or wet conditions, and where discharge and concentration measurements took place under dry conditions, a “dry load” could be derived. These loads were then compared with the number of people connected to the respective STP and a daily load of TP per capita was determined. Regarding temporal fluctuations of effluent quality, the 24-hour samples were analysed at an interval of 4 hours. This allowed an insight into potential variations within a day.

3.8 TP Load: Spatial Distribution

3.8.1 Apportionment according to FZ Jülich

The provided results from the FZ Jülich Model were used to analyse the spatial distribution of the annual TP load at the level of the GFV subcatchments. As described before in Section 3.3.2.2 and shown in Figure 3.6, this was done by processing the available raster and vector data in QGIS and sum up each path within each subcatchment. For a differentiation between point and diffuse sources, the loads from municipal STPs were handled separately, whereas all the other pathways were combined to one load per subcatchment. It should be mentioned that the private STPs were treated as diffuse sources at that stage, as their large number and spatial spread in this relatively small catchment could be compared to that of drainage pipe outlets. Besides, the determination of their loads could only be done at the level of municipalities, as mentioned before in Section 3.3.2.2.

Furthermore, for a source apportionment of the loads reaching the Herrenteich through the Heilsau river, the data from FZ Jülich was investigated regarding the total share of each pathway at the outlet of GFV_23 at Heidekamp. For this, each of the nine pathways was summed up separately and the percentage of the total was calculated.

3.8.2 Load Apportionment from Field Campaign

Besides the TP load separation by source and subcatchment based on modelled data, the field campaign allowed an additional investigation regarding the spatial distribution of TP and ortho-P transport. To derive each subcatchment’s load, the discharge for each sampling point was again estimated using the method described in Section 3.4.1 (apart from station GFV_13,

positioned at the gauge in Zarpen itself). Furthermore, the subcatchments were combined to larger ones where necessary, and the loads needed to be updated in certain cases: If a sampling point had no further sampling point upstream, it was representing the whole area upstream of that point and the calculated load would originate from that area. However, if there was a sampling point A and another sampling point B located upstream of A, the area of A and its load originating from that area was reduced by the area and load of B. This avoided double-counting of loads. Furthermore, this mass balance between upstream and downstream sampling points allowed further insights into how much phosphorous was reaching the stream along the way, and it could even indicate sinks along the way: Where a load downstream was lower than upstream, the mass balance would suggest a sink or loss on the way from the upstream sampling point to downstream. The resulting "produced" (or lost) loads were mapped for each catchment and each sampling week in QGIS.

4 Results

4.1 Discharge Data

As mentioned in the methodology, the discharge from the gauge in Zarpen was used to estimate discharges for other locations within the catchment, based on regionalised flow data from the LfU. To validate the method of using the coefficient α, the discharge measurements from VerTe were plotted against the calculated Q. From the 17 sampling locations of VerTe, eight overlapped well with the outlets of the GFV subcatchments. These eight locations were used for validation plots. An overview with all eight plots and their sampling location can be seen in the Appendix, Figure 8.2.

4.1.1 Visual Analysis for GFV_23

As a detail, Figure 4.1 shows the validation plot for GFV_23, the sampling location at Heidekamp, just upstream of the Herrenteich. There was a good fit for discharges ranging from MNQ (0.029 m^3/s) up to four times the mean discharge (with MQ = 0.457 m^3/s). Above 2 m^3/s, however, the calculated discharge exceeded the measured one significantly. This threshold of approximately 4*MQ was a trend observed for all validation locations. It should be mentioned, however, that the measurements by VerTe could have been underestimations for those higher discharges, as the case of GFV_23 showed: Situated about 2.4 km downstream of the gauge in Zarpen, the discharges should be equal or higher than in Zarpen. However, for the two "outliers" seen in Figure 4.1, the measured Q was significantly below the discharge in Zarpen. On the 14.12.2023, the Q measured by VerTe in Heidekamp amounted to 3.69 m^3/s, versus 5.22 m^3/s at the gauge in Zarpen. On the 21.12.2023, the VerTe measurement read 2.54 m^3/s versus 3.56 m^3/s in Zarpen. This discrepancy could be due to an underestimation of the measurement, or the discharge of the Heilsau on these high flow dates was highly non-stationary, where a point measurement might vary greatly from the average flow of the day.

4.1.2 RMSE and nRMSE Analysis

Table 4.1 shows the goodness of fit expressed as RMSE and nRMSE for the eight sampling stations which were used for the validation of the discharge estimation method. Unfortunately, half of the locations had only five or less observations, which impaired the significance of their analysis. Furthermore, the effect of high discharges on the overall quality is shown with the adjusted values, which are marked with an asterisk (*): Their performance increased

significantly, for example the RMSE of GFV_23 decreased from 0.519 to an RMSE* of 0.109 m^3/s. The same trend was observed for the nRMSE, where the error has halved.

Overall, the estimated discharges should be taken with care and there are more validation measurements needed, especially for high flows. In lack of a better approximation, however, the calculated discharges were used for the GFV sampling points throughout the catchment.

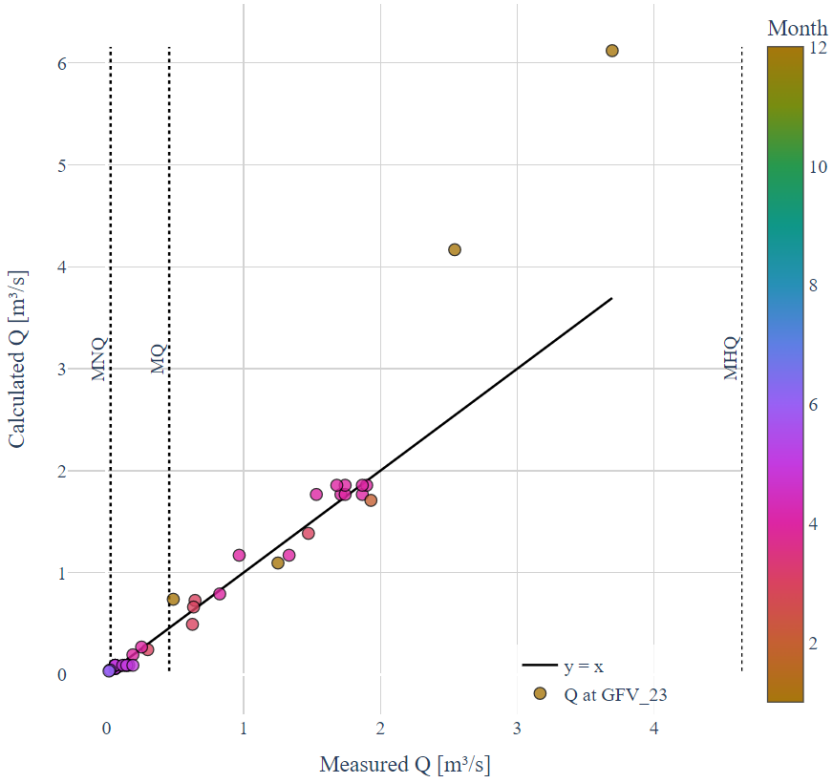

Figure 4.1: Measured against calculated discharges for GFV_23 , with α=1.171466. The vertical dotted lines indicate the regionalised flows from LfU. Note that there were only two measurements above 2 m^3/s available, reducing the significance of the estimation method for higher flow rates.

*Table 4.1: Goodness of fit for Q estimation, with N being the number of observations. Values marked with * are excluding observations above 4*MQ, to underline the role of a mismatch at higher flow rates.*

Station ID	N	RMSE	nRMSE	N*	RMSE*	nRMSE*
GFV_23	33	0.519403	0.141284	27	0.108518	0.062899
GFV_31	13	0.008303	0.403821	13		0.403821
GFV_49	5	0.068974	1.544413	5		1.544413
GFV_62	3	0.029447	0.855513	2	0.016408	7.292528
GFV_65	17	1.083836	0.240838	14	0.377814	0.186971
GFV_77	5	0.020440	0.215455	5		0.215455
GFV_78	12	0.002307	0.192626	12		0.192626
GFV_79	4	0.011816	0.102745	3	0.010342	0.337782

4.2 Instream Water Quality

4.2.1 Available Measurements for Main Channel

4.2.1.1 Monthly Distribution of TP Concentrations

Figure 4.2 shows the monthly distribution of TP concentrations as measured by MEKUN, Hackemann (1994), and Stresius (2006). From top to bottom, the plots refer to the stations from upstream to downstream, and the data from Hackemann and Stresius was included in station mtr_13, at Heidekamp. Additionally, the monthly distribution of discharges at the gauge in Zarpen is shown as violin plots, including boxplots marking the first, second, and third quartiles (reference period: Jan 1991- May 2024). The upstream stations mtr_11 and mtr_12 were only sampled for one and two years respectively, but more data was available for the downstream stations mtr_13 and mtr_14, as the scatter plots (overlaying the boxplots) show.

Regarding the TP concentrations, Figure 4.2 indicates that all four stations showed a trend of lower concentrations during winter and spring and higher concentrations during summer and autumn. Station mtr_11 recorded the largest range and highest absolute concentration, with 0.11 mg/l TP in February (minimum) and 4.7 mg/l TP in August (maximum). Station mtr_12 further downstream ranged from 0.11 mg/l TP in January and February to 0.74 mg/l TP in August. Station mtr_13, which is the most relevant regarding the flow into the Herrenteich, ranged from 0.077 mg/l TP in March and April to 0.98 mg/l TP in September. Station mtr_14, which is located at the outlet of the whole catchment and therefore downstream of the Herrenteich, ranged from 0.063 mg/l TP in April to 1.00 mg/l TP in August; there was one outlier observed in October, with 1.4 mg/l TP (not displayed in plot).

Regarding discharges recorded at Zarpen, Figure 4.2 shows a general trend of higher peak flows during winter and spring and lower peak flows during summer, with one exception in July, where peak flows reached discharges of 6 m^3/s and more, similar to winter. Besides the peak flows, however, every month revealed median flows below 0.6 m^3/s, with the highest median flow in January at 0.5378 m^3/s, and the lowest median flow observed in July (0.0498 m^3/s). The highest mean flow of 0.930 m^3/s was ascribed to February, and the lowest mean flow to June, with 0.091 m^3/s. For both median and mean flows, the range therefore covered an order of magnitude between low flow and high flow months.

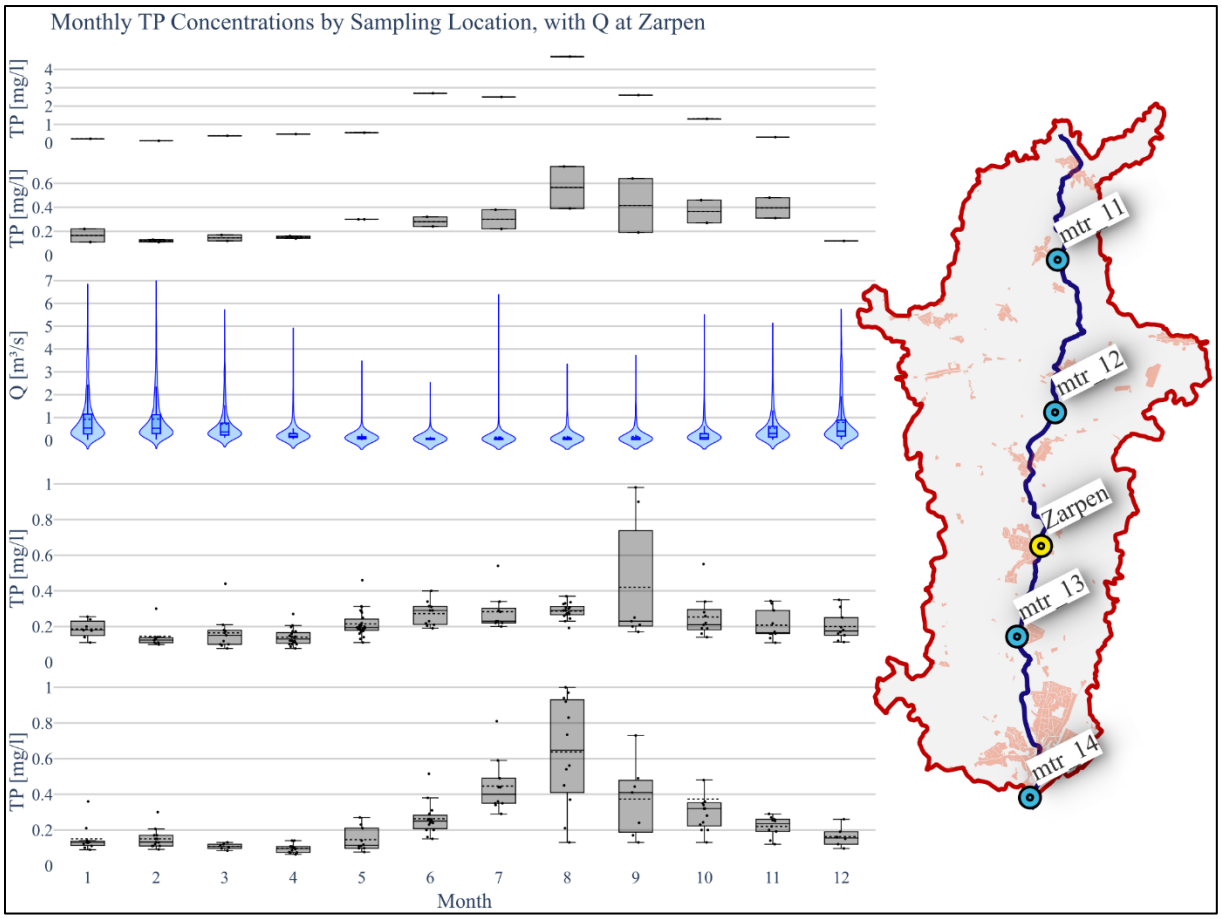

Figure 4.2: Monthly boxplots of TP concentrations available before own field campaign. ***From top to bottom,*** *the plots follow the map on the right, where the station names of the WFD monitoring programme by MEKUN are shown from upstream to downstream. Dotted lines in boxplots indicate average values, straight lines within boxes indicate median values. The additional* ***violin plot in the middle*** *shows the density of discharge observations for each month at the gauge in Zarpen, with a reference period of 1991 to May 2024 (LKN).*

4.2.1.2 Time Series of TP Measurements at Heidekamp

As station GFV_23 (at Heidekamp, equal to "mtr_13" from above) is the most relevant for the analysis of phosphorous reaching the Herrenteich via the Heilsau river, the concentrations of TP were plotted over time along with the discharge from the gauge at Zarpen, seen in Figure 4.3. It shows that overall, there were six years sampled by MEKUN and three years sampled by research works within the TH Lübeck, some of them overlapping with those of MEKUN. Furthermore, the seasonality of both the discharges and TP concentrations can be observed in the figure, as already indicated by the monthly distribution above. As the first year with observations was 1993 (Hackemann, 1994), the discharges and precipitation values were plotted two years further into the past, to indicate the previous hydrologic conditions before said sampling year.

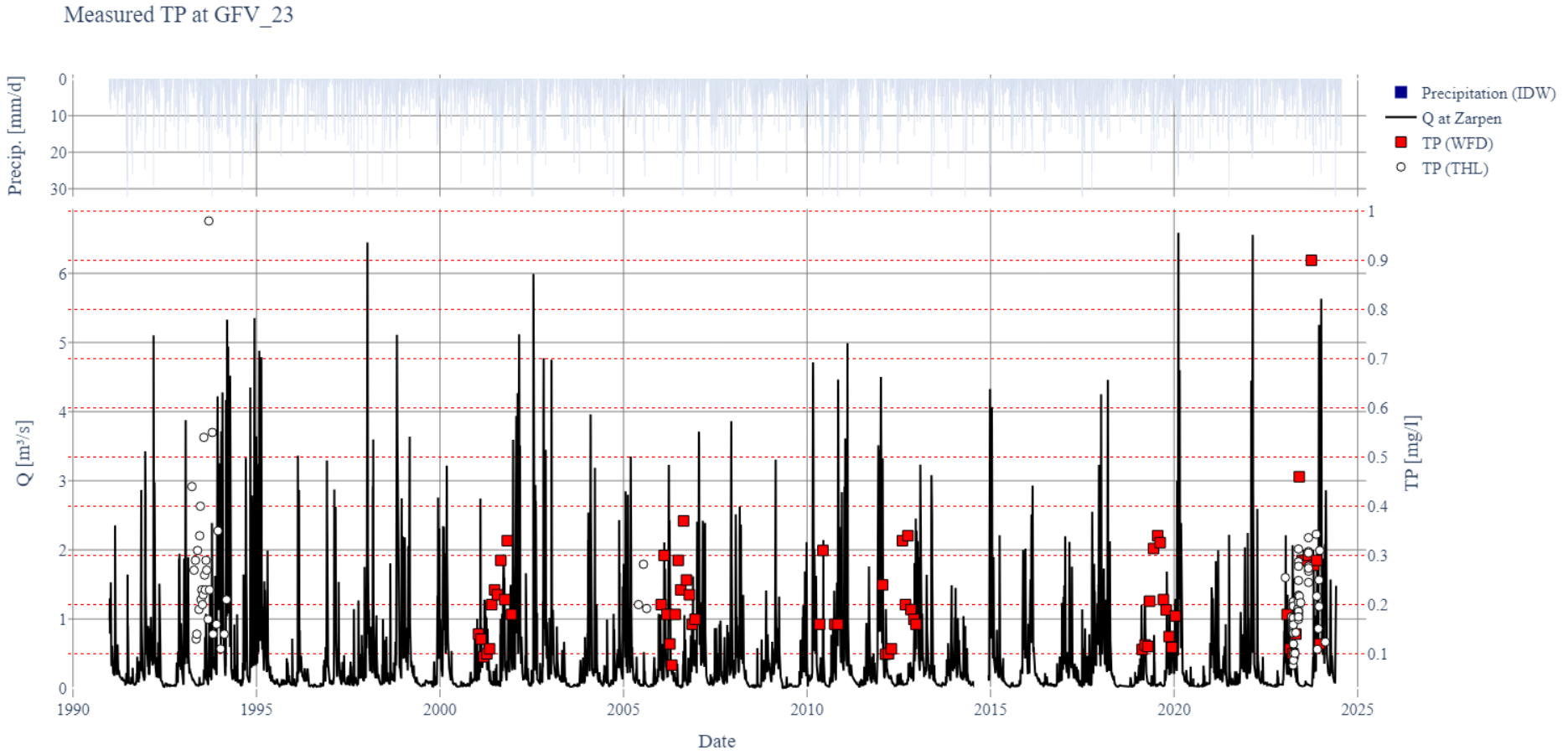

Figure 4.3: TP concentrations at GFV_23 (Heidekamp), from previous research and monitoring campaigns. ***Top:*** *Daily precipitation as interpolated for the upper catchment via IDW method (values above 30 mm/d are cropped for readability).* ***Bottom:*** *Daily discharge from gauge at Zarpen (in black), TP measurements for WFD monitoring by MEKUN (red squares), and TP measurements done by TH Lübeck ("THL", white circles), which included data from VerTe, Hackemann (1994), Stresius (2006), and Baroto (2023).*

4.2.2 Field Campaign in Upper Catchment

As mentioned in the methodology, the data which was available at the beginning of the thesis was complemented by own measurements in the field, to gather information about the catchment upstream of the Herrenteich. The results of the sampling campaign will be shown in the following subsections.

4.2.2.1 Weekly Sampling

Figure 4.4 shows the TP concentrations measured during the weekly field campaign, along with daily precipitation sums and hourly discharges where available. The TP concentrations at GFV_13 (Zarpen) from high frequency sampling were included for completeness but will be discussed in detail in the next subsection.

Regarding the precipitation and discharge during these seven to eight weeks, the end of April and the first three weeks of May received little rain, as only six days recorded precipitation, ranging between 1.56 and 3.15 mm/d. The discharge therefore shows a declining hydrograph. This changed with an intense rain event of over 47 mm/d on May 22nd, followed by a generally more wet period the consecutive weeks. The discharge therefore increased significantly from 0.08 m^3/s before the rain event to over 1.5 m^3/s at the beginning of June.

Regarding the weekly TP measurements, a general increase of concentrations could be observed during the first four sampling weeks for all sampling locations, both in the main channel and the tributaries. Four stations showed a particularly strong trend of concentration: GFV_20 along the main channel, and GFV_71, GFV_54, and GFV_8 located at tributaries respectively. Within the first four sampling weeks, these four stations showed an increase of TP concentrations of up to 4 times the initial concentration on April 30th. During that period, the discharge at Zarpen decreased from 0.186 m^3/s to 0.08 m^3/s, a decrease by almost 57%. This shows a literal "concentration" of phosphorous with decreasing discharges within the catchment. Moreover, when considering the position of these four sampling stations, all of them were located downstream of municipal STPs (Dissau, Obernwohlde, Reinsbek, and Langniendorf) and at relatively small stream sizes, as even the main channel station GFV_20 is located at the headwater area of the Heilsau river, receiving relatively low flows compared to further downstream.

During the second half of the sampling campaign, the concentrations of the four mentioned stations generally went down with increasing discharge and precipitation, as Figure 4.4 shows. Some other stations, however, experienced a significant increase of TP concentrations, such as

GFV_42, GFV_4, and GFV_46. These stations had no municipal STP located in their drainage area, which suggests the increase of phosphorous concentrations to be linked with diffuse sources and mobilisation during rainfall. Furthermore, the high frequency data from station GFV_13 (Zarpen) showed a steep temporary increase of TP from around 0.2 to 1.0 mg/l, along with the intense rainfall in May, despite the increase of discharge. This shows a discrepancy between high frequency data and weekly data, especially for the main channel, when comparing station GFV_13 with other stations of the Heilsau channel.

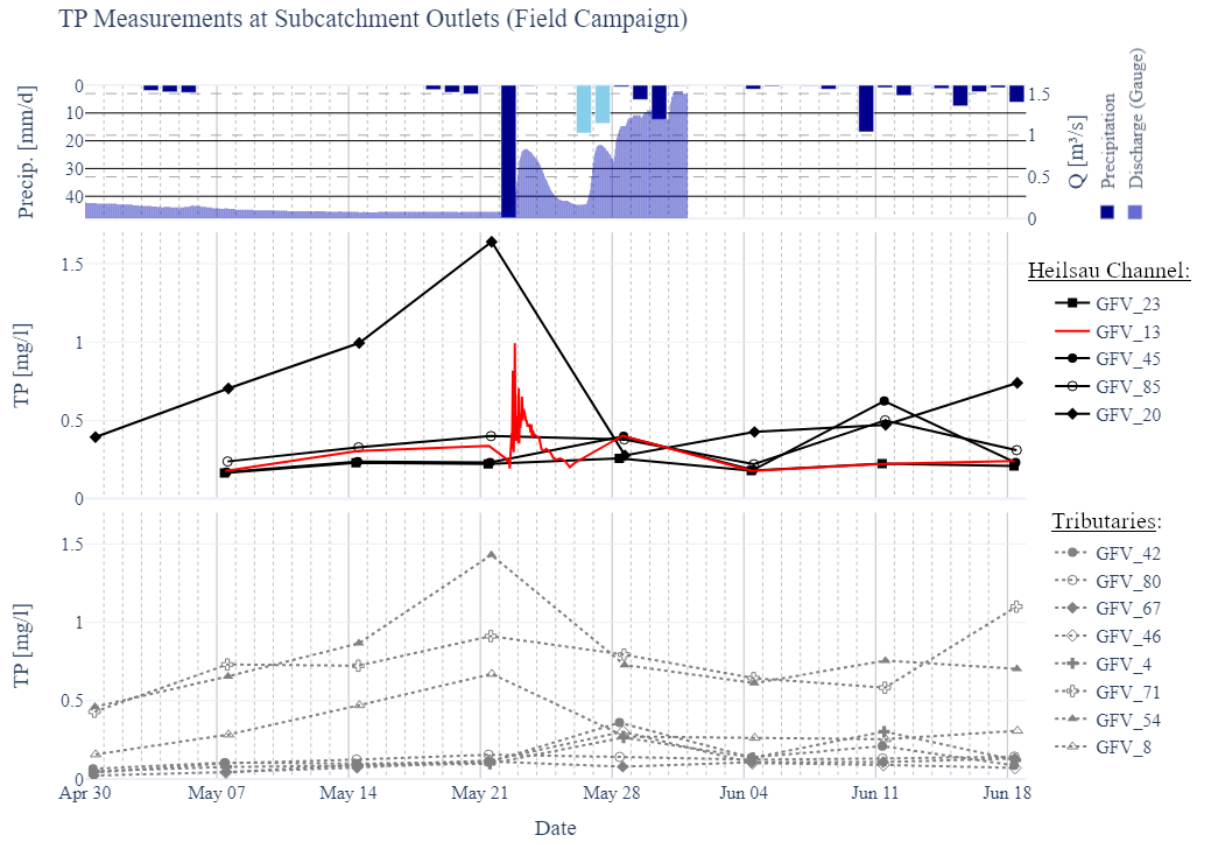

Figure 4.4: TP measurements taken at GFV subcatchment outlets during the field campaign in 2024. ***Top:*** *Interpolated precipitation data, where the shade of blue indicates the number of stations with available data for interpolation (dark blue: all three stations; light blue: only two stations); Additionally, the hourly discharge at Zarpen was plotted as a hydrograph where available.* ***Middle:*** *TP concentrations measured along the main channel of the Heilsau. The red curve includes not only the weekly sampling, but also the high frequency measurements done in May 2024 at Zarpen.* ***Bottom:*** *TP concentrations measured at tributaries of the Heilsau.*

4.2.2.2 Event Measurement: Reaction of Catchment to Intense Rainfall

As indicated above, the high frequency sampling revealed different trends of phosphorous concentrations compared to the weekly intervalls. As Figure 4.5 and Figure 4.6 show, the TP concentrations measured at GFV_13 (Zarpen) increased during the rising limb of the discharge and decreased during the falling limb. Figure 4.5 shows peak concentrations of TP occuring almost instantly with the rise of discharge. This rise of concentrations and discharge happened simultaneaously with the start of the rain event at 3 pm on May 22nd. The peak discharge of

0.834 m^3/s was reached at 8 am the next day, on May 23rd. Within that period of the rain event, the total precipitation amounted to 47.86 mm for the catchment upstream (interpolated with the IDW method). From the moment of peak discharge onwards, both Q and TP (and ortho-P) decreased over time. These trends led to a clockwise hysteresis between TP and Q, as shown in Figure 4.6.

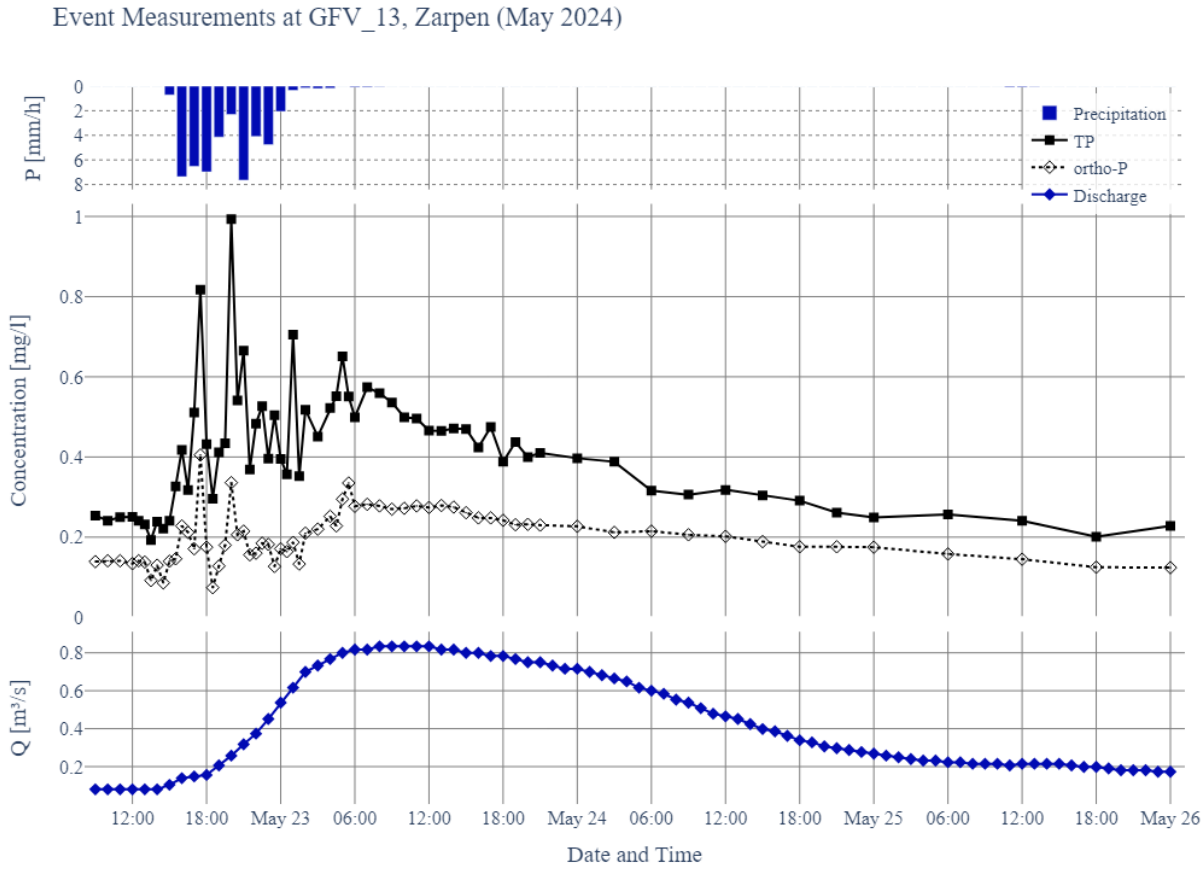

Figure 4.5: Detail of high frequency data including interpolated precipitation, phosphorous compounds, and discharge during event measurements at Zarpen (May 2024). Note that TP and ortho-P concentrations are shown as PO4-P, for comparability.

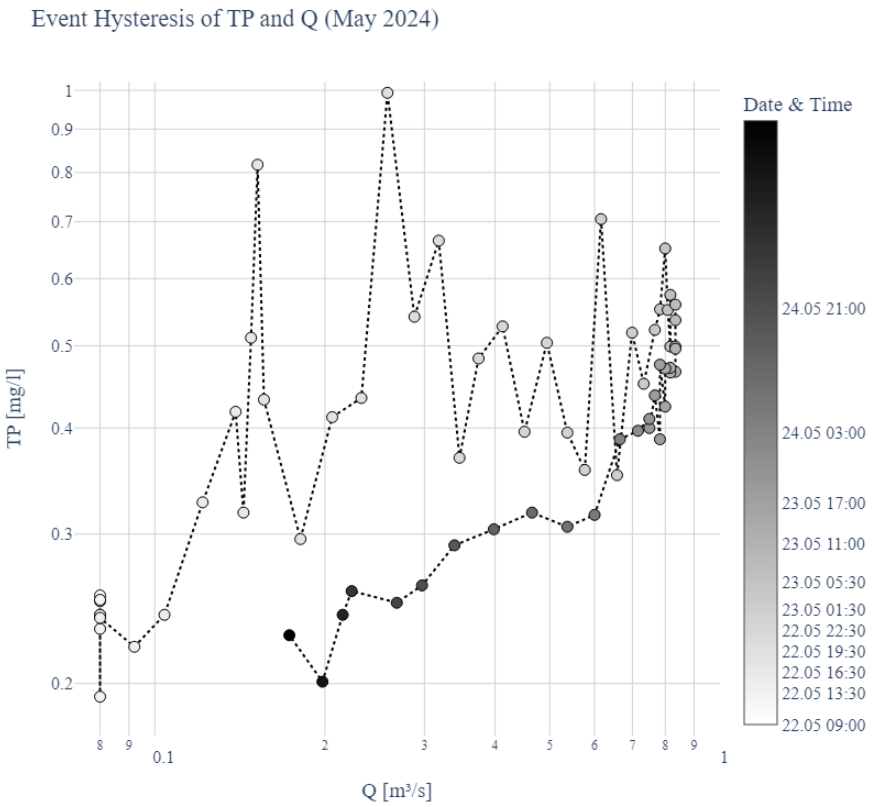

Figure 4.6: Event hysteresis of TP concentrations versus discharge in a log-log scale (sampling station GFV_13, Zarpen). The greyscale bar on the right indicates the time of sampling for each datapoint.

4.2.3 C-Q Analysis for GFV_23 (Heidekamp)

4.2.3.1 C-$Q_{quick\text{-}slow}$ Model

As described in the methodology, the discharge for station GFV_23 (Heidekamp) needed to be separated for their "quick" and "slow" parts, to use it for the C-$Q_{quick\text{-}slow}$ Model. The result of the recursive filter method for separation is shown in Figure 4.7, exemplary for 2023. The autocorrelation of the baseflow is shown in the Appendix, Figure 8.3, and shows a clear seasonal correlation as expected.

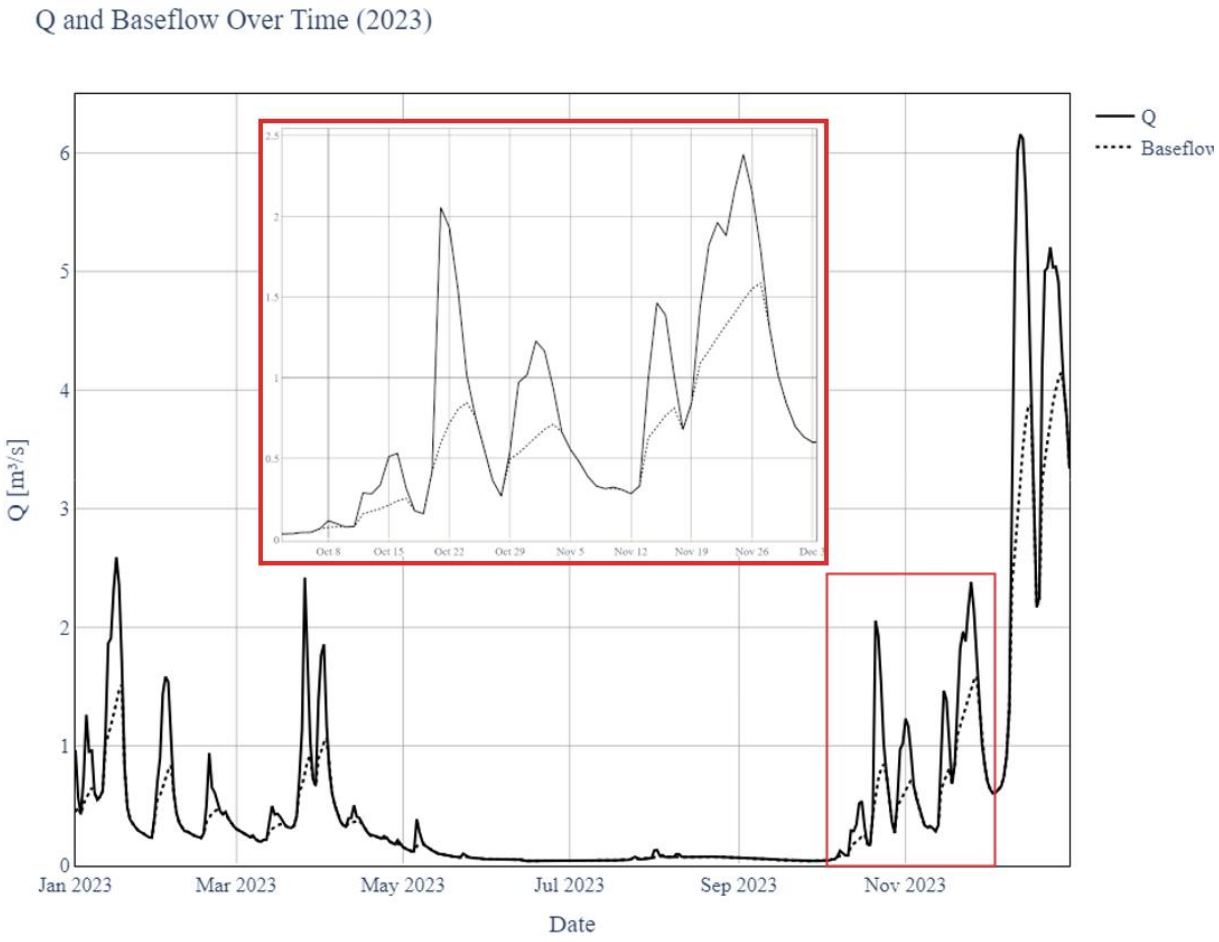

Figure 4.7: Result of baseflow separation for discharges at GFV_23 (Heidekamp) , for the year 2023. In red box: Detail for October and November.

As mentioned, the model was then built with these separated flows and the observed TP concentrations from MEKUN, TH Lübeck, and the field campaign of this thesis. The results of the linear regression can be seen in Table 4.2. The coefficients for calculating the TP concentrations were therefore $\beta_0 = 0.1869$, $\beta_1 = -0.0155$, and $\beta_2 = -0.0090$, with p-values of 0.0, 0.044, and 0.038 respectively. Hence the ability of the explaining variables $logQ_{slow}$ and $logQ_{quick}$ to predict the TP concentration was statistically significant. Overall, the adjusted R-squared value for the model was 0.062, a low yet not unrealistic performance for these type of models (Minaudo et al., 2019). The negative values of β_1 and β_2 suggest a dillution of TP with both higher baseflows and flood discharges, a trend which will be investigated with a C-Q realtionship analysis in a later section.

With the coefficients derived from the linear regression, the TP concentrations were calculated for all days with available discharge. A hydro-chemograph with modelled versus measured concentrations is shown for the years 2019 to 2024 in Figure 4.8, the full plot for the years 1991 to 2024 can be seen in the Appendix, Figure 8.4. The seasonal trend of modelled concentrations

had the same seasonality as the observed concentrations, i.e. higher during summer months and lower during winter months. However, the discrepancy between modelled and observed values as indicated by the adjusted R-squared value from above could also be seen in the visual analysis. When looking at the observed concentrations in 2023, however, a high variability could be observed even within the same days where multiple measurements were taken, which implies the need for a more detailed model capturing subdaily fluctuations.

Table 4.2: Results and performance of C-$Q_{quick\text{-}slow}$ Model.

Regression Equation	$C(t) = \beta_0 + \beta_1 \cdot log\left(Q_{slow}(t)\right) + \beta_2 \cdot log\left(Q_{quick}(t)\right) + \varepsilon$
Linear Regression Method	*statsmodels* (python package), ordinary least squares (OLS)
Number of Observations	149
Adj. R-squared	0.062
β_0	0.1869 (p-value = 0.0)
β_1	-0.0155 (p-value = 0.044)
β_2	-0.0090 (p-value = 0.038)

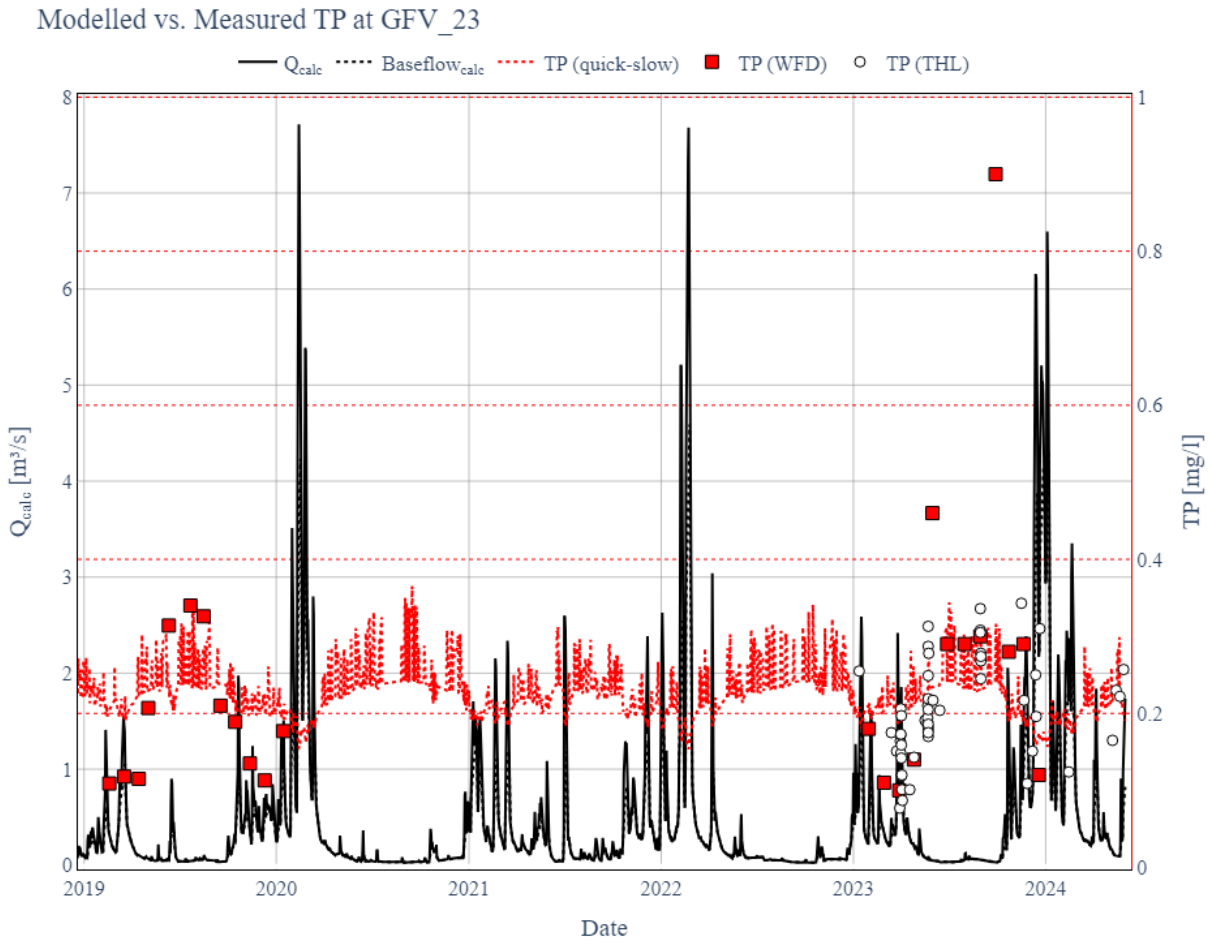

Figure 4.8: Modelled versus measured TP concentrations for GFV_23 at Heidekamp, 2019 to 2024.

4.2.3.2 C-Q Relationship Analysis

As mentioned before, to investigate the C-Q relationship for total phosphorous, the concentrations at GFV_23 were plotted against their discharges in a log-log space. The result for both measured and modelled TP concentrations can be seen in Figure 4.9. Regarding the measured concentrations (square markers), a negative slope could be observed, although scattered. The colouring according to the quick to slow ratio of Q revealed that most measurements were taken at times where baseflow was clearly dominant compared to direct runoff (dark blue shading), with only a few points sampled with slight dominance of direct runoff (red shades).

Regarding the modelled concentrations, a more pronounced negative slope is visible in Figure 4.9 (small circle markers). However, the point clouds are divided sharply, as TP values with no Q_{quick} component (discharge ratio = 0, full blue) followed a slope which is only impacted by the Q_{slow} coefficient β_1, and not a combined impact of both discharge components (see regression equation in Table 4.2). Both measured and modelled concentrations showed a clear chemodynamical C-Q relationship, with a negative slope, thus experiencing overall dilution with higher discharges. This stands in contrast with the findings from the high frequency event measurements shown above.

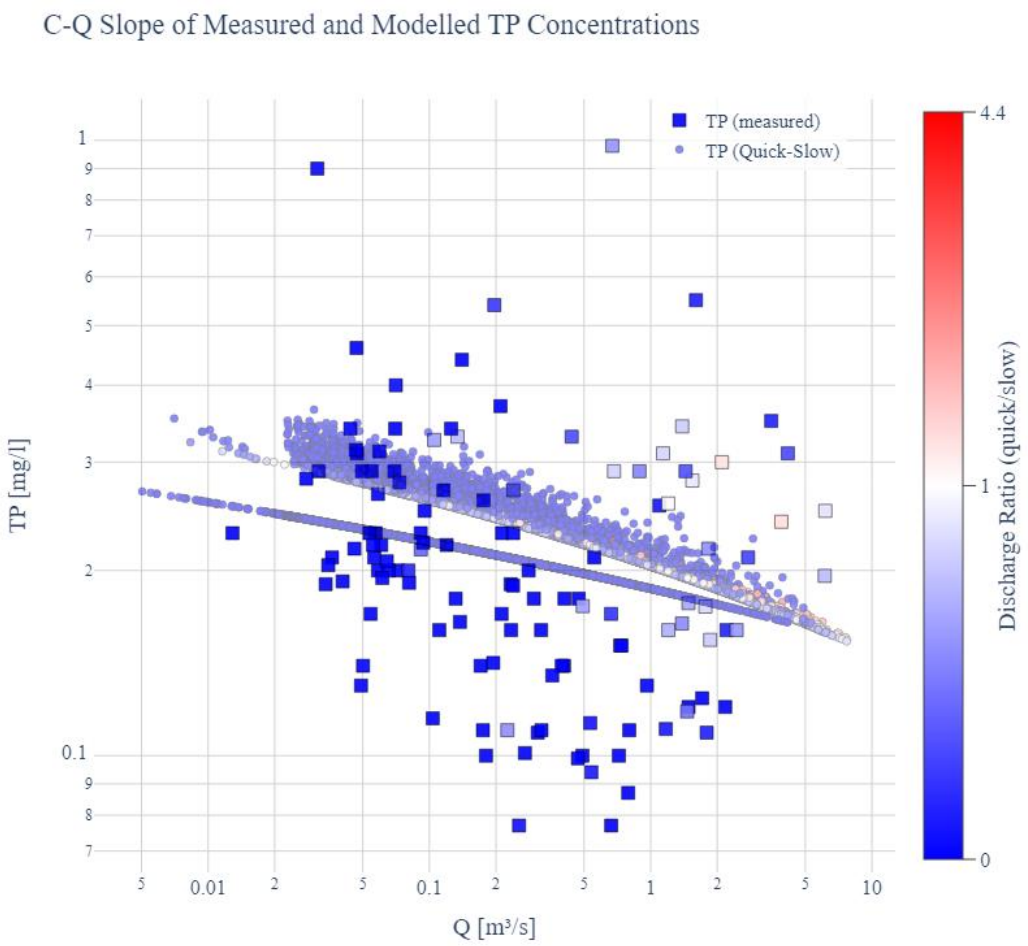

Figure 4.9: C-Q slope of TP concentrations in a log-log space. The colour of the markers refers to the scale on the right, which indicates the ratio of Q_{quick} to Q_{slow} on the day of the observation and therefore the dominant hydrologic part.

4.3 Effluents from Point and Diffuse Sources

4.3.1 Drainage Sampling

Only a few drainage outlets were found and sampled during the field campaign: From the 13 locations which were found during the field survey, a total of 20 samples could be taken (i.e. on average less than two samples per location), and only 12 of these samples could be taken in combination with a discharge measurement. This was due to limitations of measuring the discharge with a jug and stopwatch, as not all drainage outlets were pipes which allowed this method, and in one case there was a manhole to access the drainage system, but the pipe was partly under water and therefore not free of backflow. The total of 12 discharge measurements ranged from a minimum of ca. 18 l/d to a maximum of 42 m^3/d, with most of them around 1 to 3 m^3/d (sampling period: April – June 2024; 1 m^3/d = 0.01157 l/s). Others were dry or not measurable.

Furthermore, five drainage outlets could be linked to their approximate draining area, thanks to descriptions from local farmers. However, only three of them could be sampled. In response to this lack of representative data, only the measured concentrations were analysed further. Figure 4.10 shows the distribution of these concentrations for several parameters. It was observed as expected that nitrogen compounds were found at significantly higher concentrations (up to 13.6 mg/l TNb) compared to phosphorous (maximum at 1.11 mg/l TP). Furthermore, it should be mentioned that the three outliers of TP and ortho-P were from samples of nearly dry drainage pipes or standing water and should therefore be treated with care, as the samples visibly included fine sediments. The remaining TP concentrations ranged from 0 to 0.38 mg/l TP, with more than half of the readings below the detection limit of 0.05 mg/l. Overall, the lack of data led to a preference of the FZ Jülich model results to be used for further analysis of phosphorous from drainage systems.

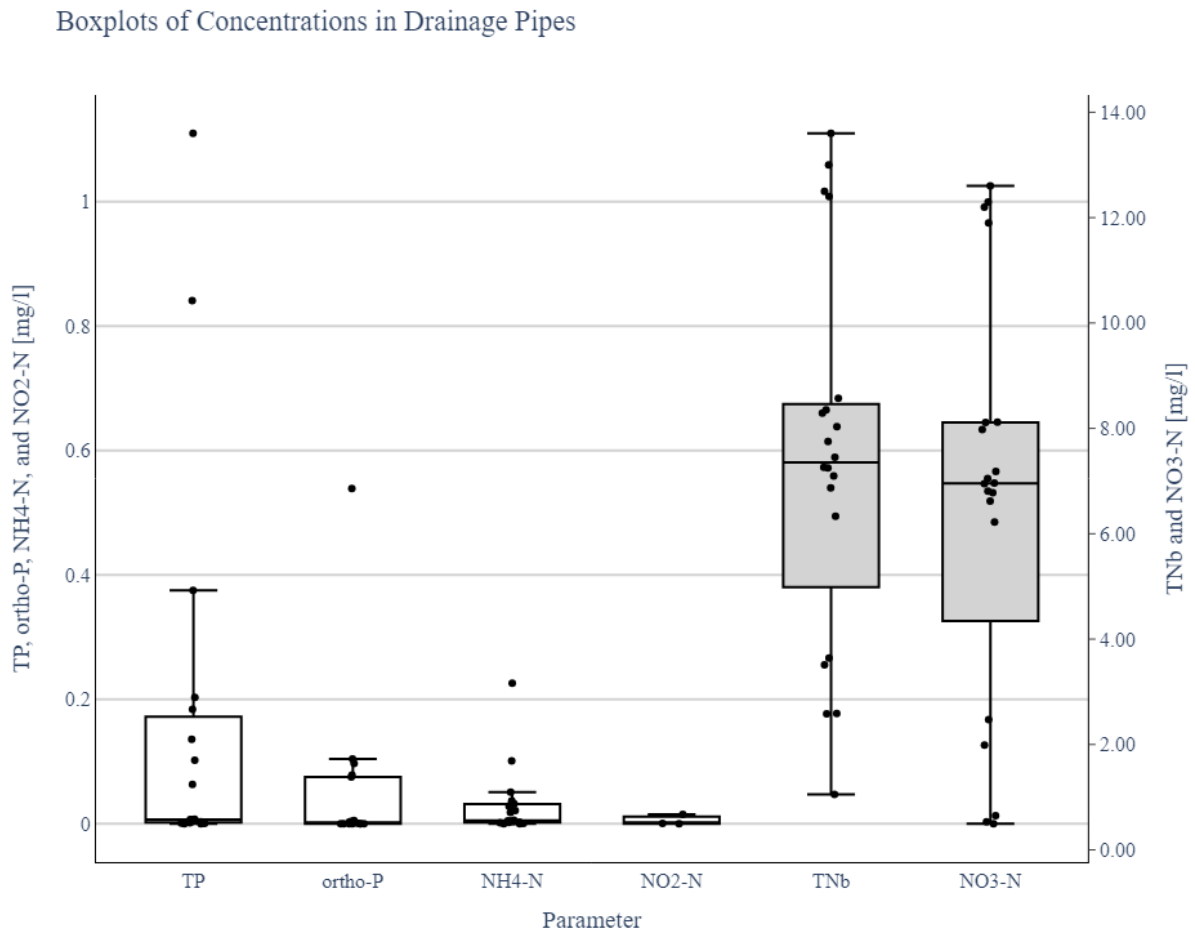

Figure 4.10: Chemical analysis of drainage effluents from field campaign 2024.

4.3.2 Rain Canalisation

As mentioned in the methodology, the analysis of rainwater canal systems (separate sewers) was limited within the scope of this thesis. Using the calculated yearly TSS loads from the work

of Osterhoff (2020) as a proxy for TP loads was considered (Osterhoff, 2020), but an analysis of TSS versus TP concentrations with available data from MaReT-SH did not show a promising predictive power of this proxy. Therefore, values from literature were preferred for further investigations: The FZ Jülich report for example used their modelled land-use-specific runoffs in combination with TP concentrations of for example 0.25 mg/l TP for runoff from suburban areas, or 0.50 mg/l TP from traffic areas (Tetzlaff et al., 2017). These concentrations were in the same order of magnitude as measurements from MaReT-SH, were the mean TP concentration amounted to 0.2 mg/l for the inlets of rain retention basins in the period from September 2022 to January 2024 (*Leistungsfähigkeit von Maßnahmen zur Regenwasserbewirtschaftung im Trennsystem in Schleswig-Holstein (MaReT-SH)*, 2024). With this support from other data, the FZ Jülich model results were used for further analysis of phosphorous loads from rain canalisation (see later in Section 4.5).

4.3.3 Municipal STPs

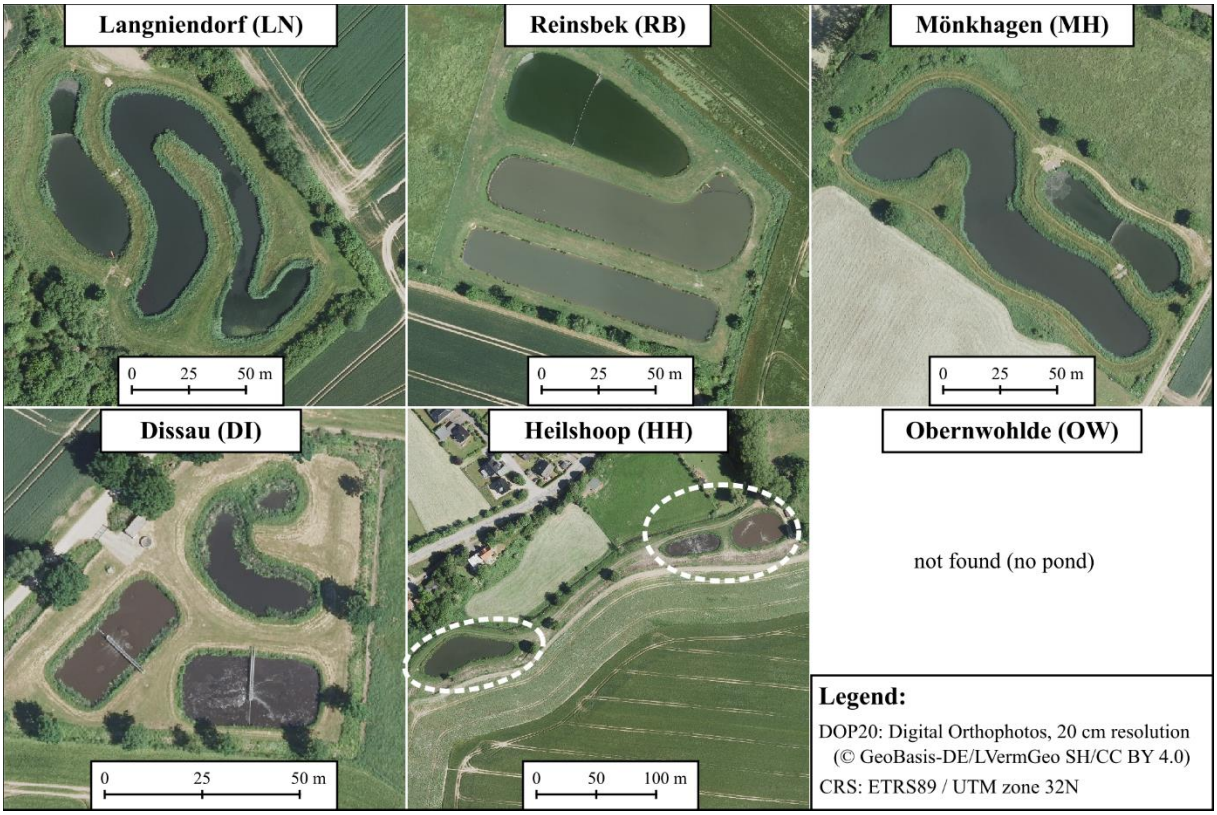

Figure 4.11: Orthophotos of municipal sewage treatment plants in the Heilsau catchment. For Dissau and Heilshoop the aeration ponds can be identified as the stirred water surfaces of the ponds. The STP of Obernwohlde could not be found.

Figure 4.11 shows orthophotos of the municipal STPs within the catchment, although the plant of Obernwohlde could not be identified in field nor QGIS. The remaining five plants, however, showed typical designs for waste stabilisation ponds. The STPs pf Langniendorf, Reinsbek, and Mönkhagen had no aeration system and therefore probably work solely with anaerobic and

facultative ponds. Dissau and Heilshoop had two aerated ponds each (see Figure 4.11, bottom), with an anaerobic or facultative pond downstream, before their outlets.

As mentioned in the methodology, the provided data did not include updated discharge values, which were thus derived during the field campaign where possible. Table 4.3 shows the resulting measurements for the STPs which were possible to sample. The average discharge from six consecutive jug measurements were therefore 22.54 m^3/d for Langniendorf, 94.19 m^3/d for Heilshoop, and 48.72 m^3/d for Mönkhagen. Regarding the effluent quality, the lab results from the field campaign are summarised in the Appendix, Table 8.2. Additionally, the provided data for STP Reinsbek is shown in a chemograph in the Appendix, Figure 8.5.

Table 4.3: Discharge measurements for municipal STPs.

LN effluent: 19/06/2024 15:00						
V (l)	5	4	4.1	4.3	4.3	4.25
dt (s)	19.33	15.49	15.31	16.43	16.45	16.49
Q (l/s)	0.258665	0.258231	0.267799	0.261716	0.261398	0.257732
Average:	in l/s:	0.260924	in m^3/d:	22.5438		
HH effluent: 24/06/2024 14:20						
V (l)	4.1	4.4	4.4	3.8	3.8	3.6
dt (s)	3.75	4.01	4.27	3.42	3.42	3.28
Q (l/s)	1.093333	1.097257	1.030445	1.111111	1.111111	1.097561
Average:	in l/s:	1.090136	in m^3/d:	94.18778		
MH effluent: 24/06/2024 16:00						
V (l)	3	3.7	3.1	3.2	3.2	3
dt (s)	4.93	6.94	5.65	5.7	5.65	5.31
Q (l/s)	0.608519	0.533141	0.548673	0.561404	0.566372	0.564972
Average:	in l/s:	0.563847	in m^3/d:	48.71635		

For those STPs which had both water quality and discharge data, the TP loads could be calculated. Table 4.4 shows the relevant data for this calculation: Discharges were taken from Table 4.3 and compared with the weather conditions of the sampling days. For this, the precipitation sums of the past days were calculated with the IDW-interpolated data of the upper catchment (upstream of Zarpen). As seen in Table 4.4, Q measurements could be considered as taken under dry conditions for the STPs of Heilshoop (HH) and Mönkhagen (MH). For Langniendorf (LN), the precipitation of the last 48 hours (P2) amounted to 6.14 mm, therefore the discharge was considered as measured under wet to dry conditions. For TP measurements, the weather conditions were considered in the same manner (see Table 4.4). When both TP and Q measurements were taken under dry conditions, the TP loads were calculated and amounted to 350.4 g/d and 201.7 g/d for HH and MH respectively. For LN, the conditions were not dry

and considering the rainfall of the past days they could not even be considered as fully wet either, therefore these measurements were of little representative value.

With the loads of HH and MH the specific loads could be calculated as load per capita, by using the population equivalent (PE) connected to the sewage systems in 2023. As Table 4.4 shows, these amounted to 0.6513 and 0.6264 g TP per capita and day, for HH and MH respectively. These specific loads could then be used for an estimation of loads under dry conditions for the other treatment plants, see below. It should be mentioned that these specific loads were in the same range as the one used by FZ Jülich for modelling private STPs, which was 0.7 g TP per capita and day (Tetzlaff et al., 2017).

Table 4.4: Calculation of specific TP loads for sampled STPs. ***Note:*** *Precipitation values P1, P2 and P10 refer to the sum of precipitation for the day of sampling, the last two days, and last 10 days before the sampling, respectively.*

ID	**HH (grab sample)**	**LN (24h mix)**	**MH (24h mix)**	**Unit**
Date of Q measurement	24/06/2024	19/06/2024	24/06/2024	
Q	94.188	22.544	48.716	[m^3/d]
State of Q (see Precip.)	dry	wet to dry	dry	
Date of TP measurement	24/06/2024	18/06/2024	24/06/2024	
TP	3.72	2.80	4.14	[mg/l]
State of TP (see Precip.)	dry	wet	dry	
Precip. at Q measurement:				
P1	0.00	0.05	0.00	[mm]
P2	0.00	6.14	0.00	[mm]
P10	19.6	39.2	19.6	[mm]
Precip. at TP measurement:				
P1	0.0	6.1	0.0	[mm]
P2	0.0	6.9	0.0	[mm]
P10	19.6	39.2	19.6	[mm]
Daily TP load	350.4	-	201.7	[g/d]
Annual TP load	127.9	-	73.6	[kg/a]
PE capacity	600	300	335	[PE]
PE use	538	284	322	[PE]
Percent use	90	95	96	[%]
Specific load	0.6513	-	0.6264	[g/(PE*d)]
Specific load	237.7104	-	228.6189	[g/(PE*y)]
Specific Q	175.1	-	151.3	[l/(PE*d)]

Table 4.5: Calculation of TP loads for STPs, using specific loads from Table 4.4. In red: estimated values based on available data.

ID	PE capacity	PE use [%]	PE use	Specific Load [g/(PE*d)]	Load [g/d]	Load [kg/a]
LN	300	95	284	0.62635	177.9	64.9
RB	525	80	418	0.62635	261.8	95.6
OW	104	90.155	94	0.62635	58.9	21.5
DI	650	90.155	586	0.62635	367.0	134.0
HH	600	90	538	0.65126	350.4	127.9
MH	335	96	322	0.62635	201.7	73.6

As shown in

Table 4.5, the specific load from Mönkhagen was used for estimating the loads of the remaining four STPs which could not be measured successfully. The reasoning for choosing MH as a reference was that firstly, in contrast to HH, the TP measurement of MH originated from a 24-h mixed sample, which improves the representativeness compared to a grab sample. Secondly, the type of treatment in HH differed from the others due to its aeration system, hence the conditions from MH were more likely to fit the remaining STPs.

As the PE connected to OW and DI were not available, they had to be estimated based on the average use of total capacity from the other STPs (90.155 %). The resulting PE were multiplied with the specific load and hence yielded the TP loads for each STP, as seen in

Table 4.5: Extrapolated to annual loads, these amounted to 21.5, 64.9, 73.6, 95.6, 127.9, and 134.0 kg/a for OW, LN, MH, RB, HH, and DI respectively.

It should be noted that these loads were calculated for dry conditions, yet wet conditions might result in different loads. Wet conditions, however, could not be successfully sampled regarding their discharges, and neither could retention times be estimated well without more detailed information about the geometry of the ponds. Thus, a quantitative analysis for wet conditions was limited. Nevertheless, the daily loads during dry conditions were seen as a good estimation for yearly loads, as wet conditions could both dilute the effluent while increasing the discharge, which in combination might only lead to small fluctuations of the total load.

4.4 TP Load: Temporal Variation within Main Channel

4.4.1 Annual Load according to FZ Jülich

With the provided results from the FZ Jülich model, a sum of all phosphorous pathways could be done for each subcatchment. For the catchment upstream of station GFV_23 at Heidekamp, the average load therefore amounted to 2423.41 kg/a. This included updated sewage loads from the calculations in the previous section. The data from FZ Jülich gave a first estimate based on modelled phosphorous flows, whereas the following sections show the loads calculated from measurements and modelled concentrations, allowing a more differentiated temporal variation.

4.4.2 Annual and Monthly Distribution of Loads

Figure 4.12 shows a monthly distribution of the results from both load calculation methods. As the quick-slow method could utilise every period with discharge data, the number of datapoints was larger than for the Q-weighted method, with 397 simulated months versus 78 observed months respectively. Nevertheless, a clear seasonal trend could be observed for both methods. Average and median loads were higher during winter than during summer, for example in the case of loads from the quick-slow method the median during winter months ranged from around 200 to 600 kg/month (Oct-Mar), whereas median values for summer months only ranged from around 55 to 120 kg/month (Apr-Sep). The same trend could be observed for extreme values, with 812 kg TP in July 2002, and 1517 kg in December 2023 (quick-slow method). For Q-weighted loads, the extreme maxima were even higher, with 2067 kg in December 2023 and 2508 kg in December 1993.

Figure 4.13, on the other hand, shows the yearly and monthly loads over time, in this example for the years 2019 to 2024 (the full period of 1991 to 2024 can be seen in the Appendix, Figure

8.6). Again, the seasonal variations of loads are visible. Additionally, it could be observed that the total annual loads varied significantly, too. In the example of Figure 4.13, the quick-slow results ranged from 1883 to 3783 kg/a within just four years. The Q-weighted results even ranged from 1216 to 4218 kg/a in the same years. The global maxima from 1991 to 2024 reached 7847 kg in 1993 for the Q-weighted method, and 6443 kg in 1994 for the quick-slow method (see Figure 8.6). Considering the precipitation data as shown in Figure 4.13 and Figure 8.6, the yearly loads generally covaried with the annual precipitation (and therefore discharges), although a clear covariation with medium to strong rain intensities could not always be observed, as the example of 2019 and 2020 show (Figure 4.13).

Regarding the difference between the two estimation methods, Table 4.6 shows a statistical analysis of the two estimation methods above, with an additional column for the FZ Jülich model results, for comparison. It was observed that the annual loads calculated with the Q-weighted method were generally more extreme than for the Quick-Slow method, with a lower minimum and maximum load of 1216 and 7847 kg/a respectively. Moreover, the Q-weighted method had a higher mean annual load and standard deviation (σ) of 3800.37 and 1906.67 kg/a respectively, whereas the Quick-Slow method had respective statistics of 3084.65 and 1070 kg/a. On average, the Q-weighted loads differed by ±18.3% compared to those of the Quick-Slow method, with one year being almost identical (0.1% difference, 1994) and one year more than double compared to Quick-Slow (108% difference, 1993).

When comparing the two estimation methods with the result from the FZ Jülich model, Table 4.6 reveals that the mean values for the last five years (2019-2023) were in a similar range as the mean annual load from FZ Jülich: 2754.19 kg/a for Quick-Slow, 2682.17 kg/a for Q-weighted, and 2423.41 kg/a for FZ Jülich. The reference period of five years was chosen due to the data which the FZ Jülich model was built with (also from 2019-2023).

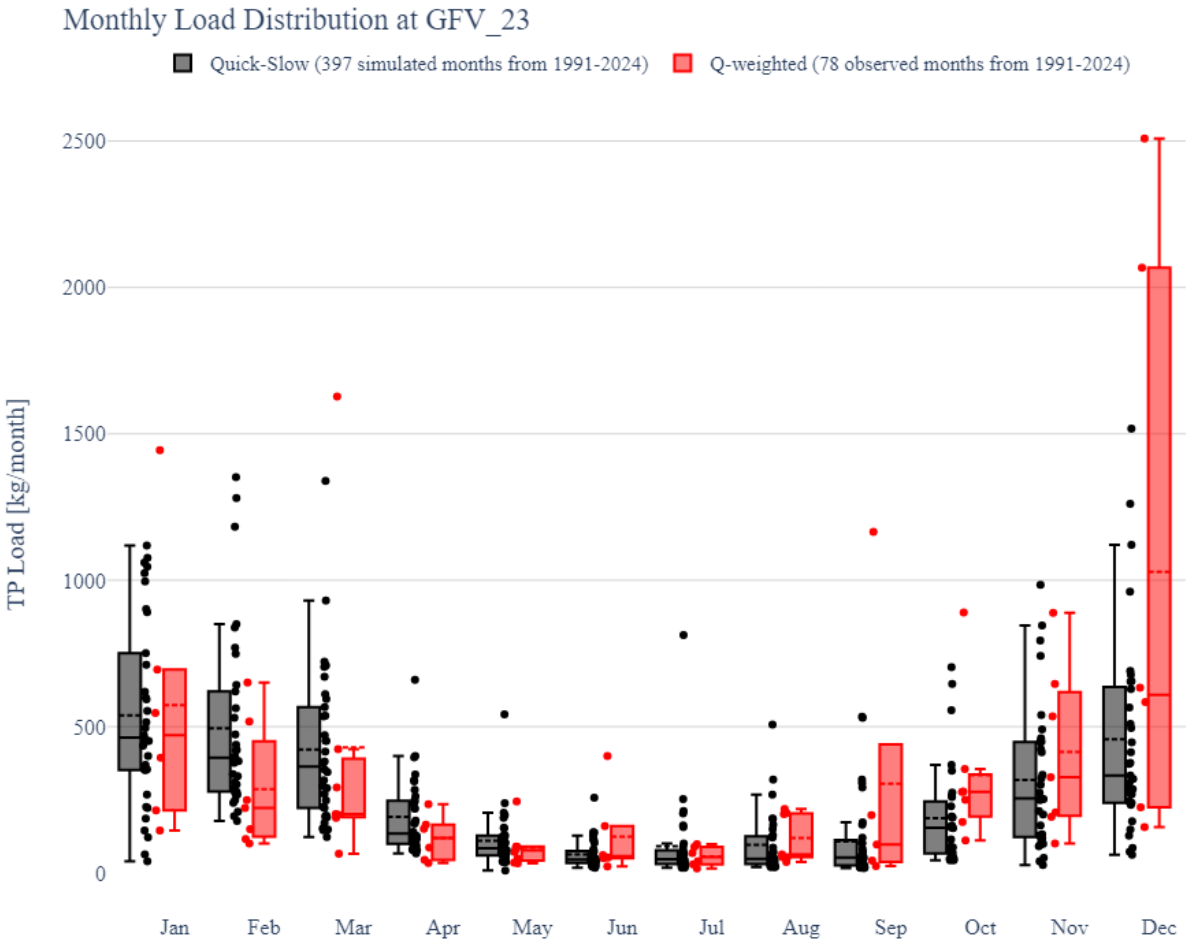

*Figure 4.12: Monthly TP load distribution for GFV_23 (Heidekamp), shown as point clouds and boxplots. The **black** plots show values calculated with the results from the C-$Q_{quick\text{-}slow}$ method, whereas the **red** plots were made with the loads from the Q-weighted method. Both methods used the estimated discharges for GFV_23.*

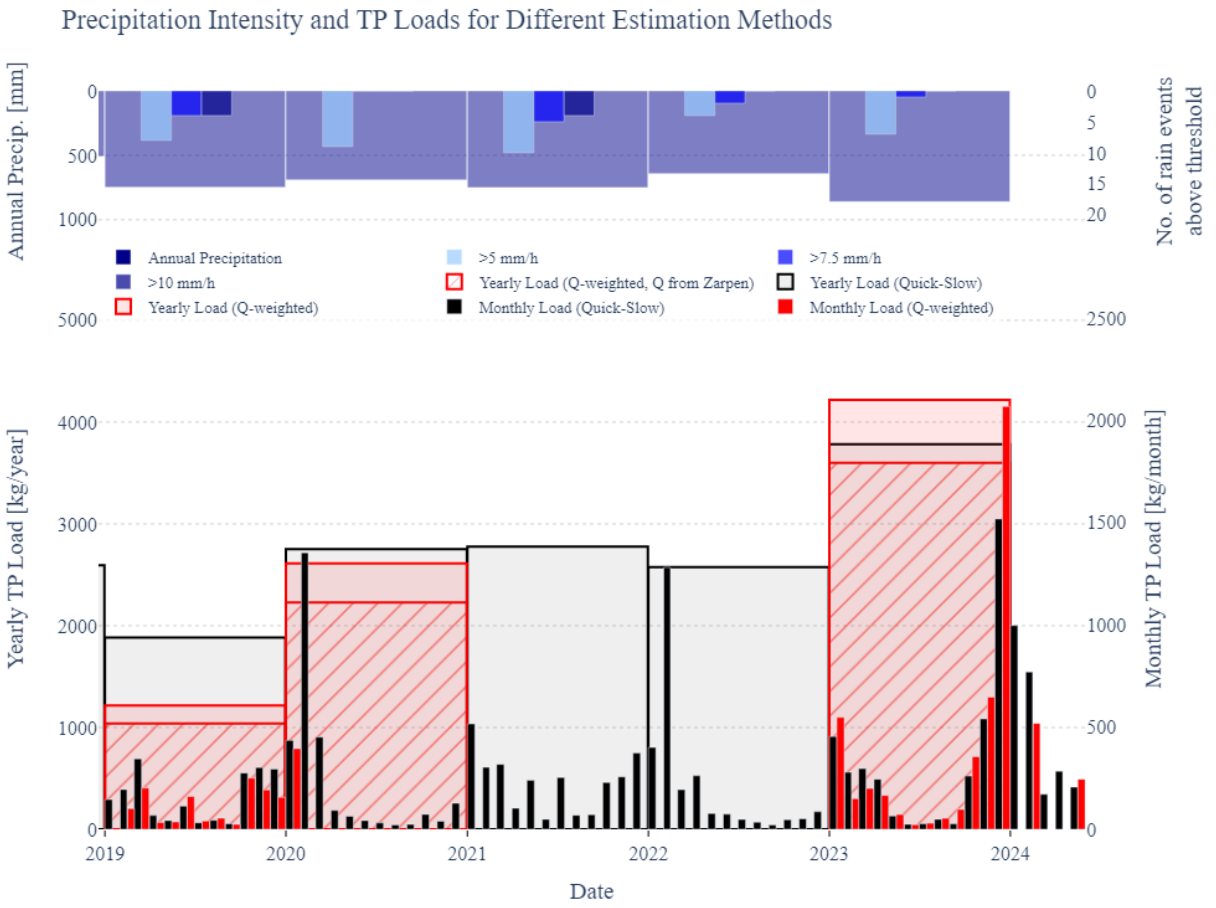

Figure 4.13: Yearly and monthly TP loads for the years 2019 to beginning of 2024 at station GFV_23. ***Top:*** *Precipitation data showing the annual precipitation in mm and the number of hourly records with rainfall intensities above the thresholds 5, 7.5, and 10 mm/h.* ***Bottom:*** *The red, diagonally striped bar plots are showing the yearly Q-weighted load with a different discharge input, from Zarpen instead of Heidekamp. This is shown as a potential lower boundary of loads. The other bars show the monthly and yearly TP loads as estimated through the Q-weighted and Quick-Slow approach.*

Table 4.6: Statistical analysis of annual TP loads for the three estimation methods. ***Note****: The "Difference" column was calculated for each year where Quick-Slow and Q-weighted loads were available. It refers to the whole dataset from 1991 to 2023 and not to the rows beside.*

	Quick-Slow [kg/a]	**Q-weighted [kg/a]**	**Absolute Difference [%]**	**FZ Jülich [kg/a]**
Min	1717.34	1216.37	0.1	
Median	2769.69	3035.14	6.3	
Mean	3084.65	3800.37	18.3	
Max	6443.24	7847.34	108.0	
σ	1070.00	1906.67	31.4	
Mean values for shorter reference periods:				
2019-2023:	2754.19	2682.17	17.3	2423.41
2014-2023:	2780.29	2682.17	17.3	

4.4.3 Short Timescale: Rainfall Event

Besides the monthly or weekly observations which could be used for monthly and yearly load estimations, the high frequency measurements from May 2024 at Zarpen were analysed regarding their loads. Figure 4.14 shows the calculated loads of TP and ortho-P in g/h, revealing a dynamic as indicated already by the concentration measurements: Along with the discharge the loads rose until the peak discharge, reaching a maximum of 1874.88 g TP per hour at 5 am on May 23rd. Later, the TP loads decreased along with the discharge to approximately 142 g/h on May 26. When linearly interpolating the loads for each hour in the sampling gaps, a total of 55,027 g (or ca. 55 kg) TP was transported during the time between May 22nd 09:00 and May 26th 00:00 (87 hours). For ortho-P, this total sum amounted to 29,804 g (or ca. 30 kg). On May 23rd alone, the total TP load amounted to 32.251 kg.

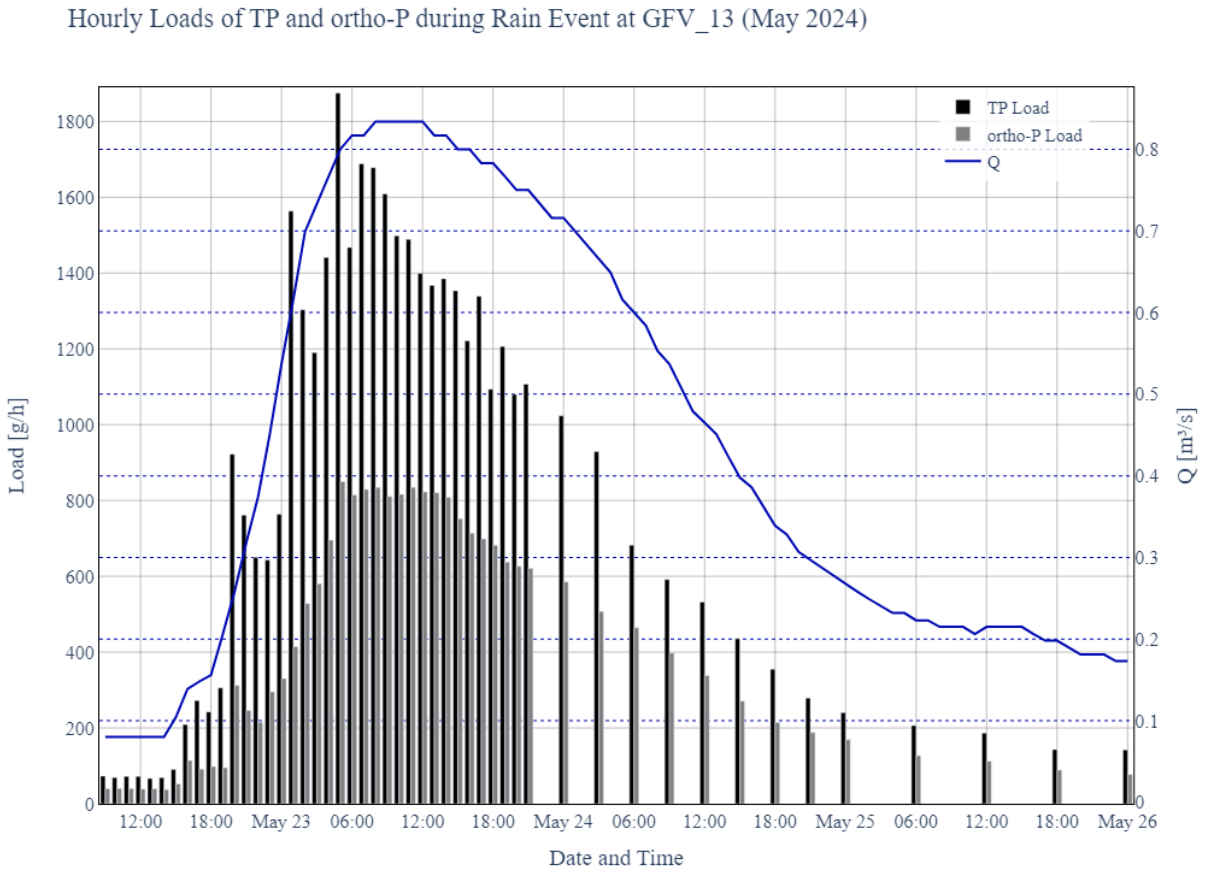

Figure 4.14: Hourly loads during rain event of May 2024. Hourly Q from gauge at Zarpen (LKN).

4.5 TP Load: Spatial Distribution and Apportionment

4.5.1 Apportionment according to FZ Jülich

Figure 4.15 shows the spatial distribution of TP loads on the subcatchment level, for all subcatchments draining towards GFV_23 at Heidekamp. The combined diffuse sources (including private STPs at this resolution) range from 0.686 to 167 kg TP per year, although the map shows total loads, not per area. When considering the draining area of each subcatchment, the TP loading rates ranged from 85.7 to 680.5 g/(ha*a). The loads from municipal STPs were the same as derived from the field campaign, all other loads were derived with data from FZ Jülich.

Regarding the total share of each pathway, a pie chart in Figure 4.15 shows the respective percentages for the station GFV_23. With 27.09%, the highest contribution of TP comes from erosion, followed by municipal STPs with 21.35% and drainage effluents with 19.41%. These top three contributors were followed by groundwater discharge (9.24%), rain canalisation (8.5%), private STPs (7.66%), washout (5.17%), atmospheric deposition (1.51%), and interflow (0.06%) at the lower end. A detailed spatial apportionment for each pathway can be seen in the Appendix, Figure 8.7. When categorising these pathways regarding urban or agricultural origin, agriculture amounts to 51.67% (erosion, washout, and drainage) and urban sources amount to 37.51% (STPs and rain canalisation). It should be noted that since these values are based on the FZ Jülich model results, the sum of all TP loads equals 2423.41 kg/a, which is lower than the loads derived through the Q-weighted and Quick-Slow methods (as shown in Section 4.4.2).

Regarding phosphorous hotspots, the analysis of Figure 4.15 in combination with Figure 8.7 (Appendix) revealed that the highest diffuse TP loads originate from subcatchments in the north and west of the upper catchment, largely caused by erosion and drainage. The most polluting point sources were the municipal STPs in Dissau and Heilshoop, followed by Reinsbek.

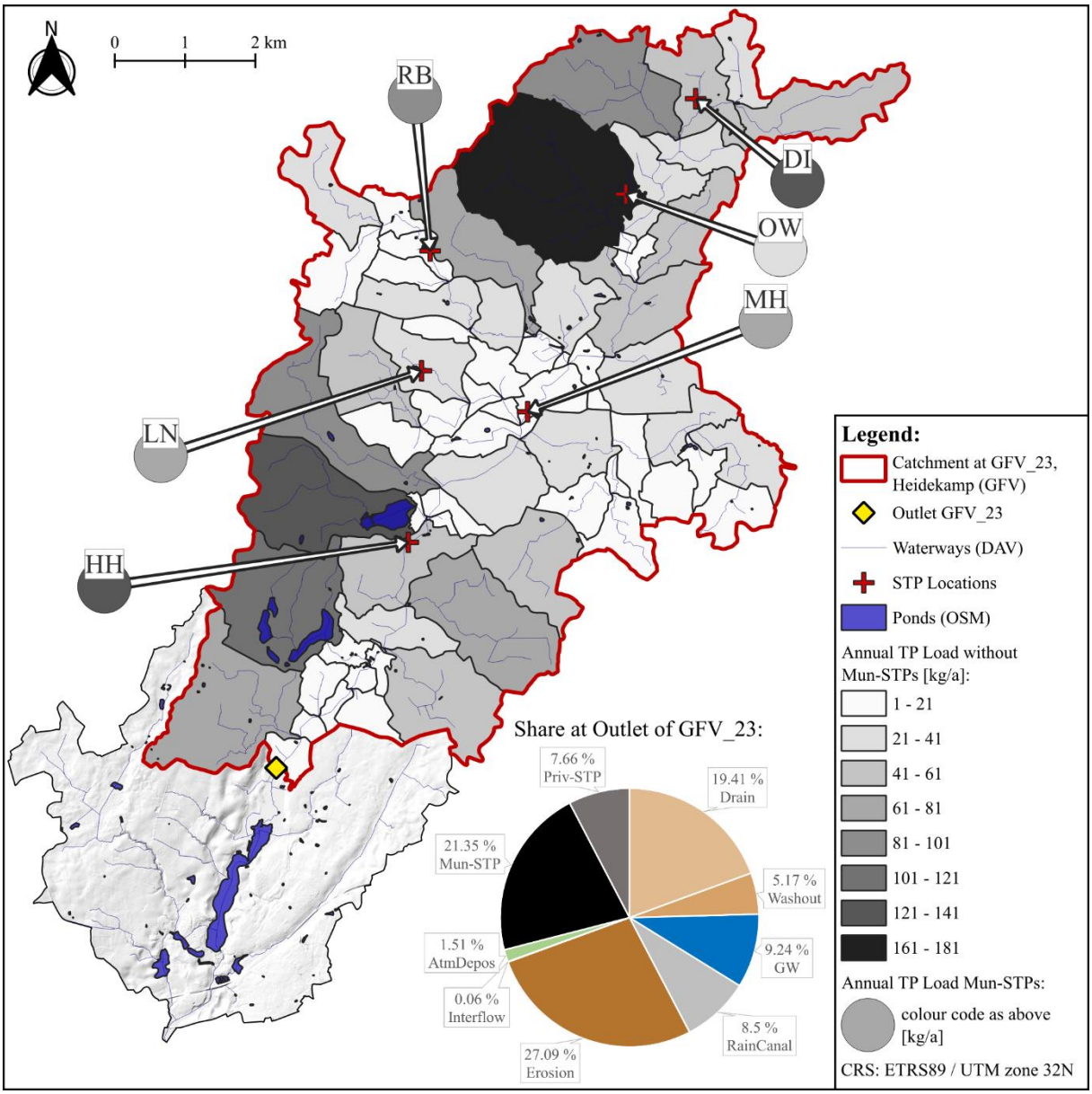

Figure 4.15: TP load apportionment upstream of GFV_23 (Heidekamp), based on data from FZ Jülich model and STP calculations. The subcatchments are shown with the load coming from all pathways except municipal STPs. The latter are shown separately. The pie chart shows the total share of TP sources at the outlet of GFV_23.

4.5.2 Load Apportionment from Field Campaign

The eight weeks of sampling selected GFV subcatchments allowed a differentiation of phosphorous loads between these catchments, when combined with the estimated discharges. Figure 4.16 shows the result for TP loads in each sampling day. As some dark grey areas indicate, the mass balance between upstream loads and outlet loads did not always result in additional loads but rather a loss, therefore functioning like a phosphorous sink. This was particularly observed for the most southern (downstream) subcatchment, which received more TP than what was calculated at its outlet in the 3rd, 4th, 5th, and 8th sampling day. For all other catchments and days, the loads ranged from 8 g/d to 10.1 kg/d. Overall, a covariation of TP

loads with precipitation and discharge could be observed: During the first four weeks, the P7 sums ranged from 0 to 12.36 mm, with moderate TP loads, as shown in the maps of Figure 4.16. The following weeks received higher precipitation with P7 sums ranging from 19.09 to 79.52 mm, and TP loads rose accordingly (see Figure 4.16). Regarding the role of municipal STPs, it was observed that for dryer conditions, the daily loads coming from these six STPs explain most of the TP loads within their respective subcatchment. An exception was the STP at Mönkhagen, contributing to GFV_85: On May 14th, the calculated daily load for the subcatchment was lower than what the STP should contribute each day.

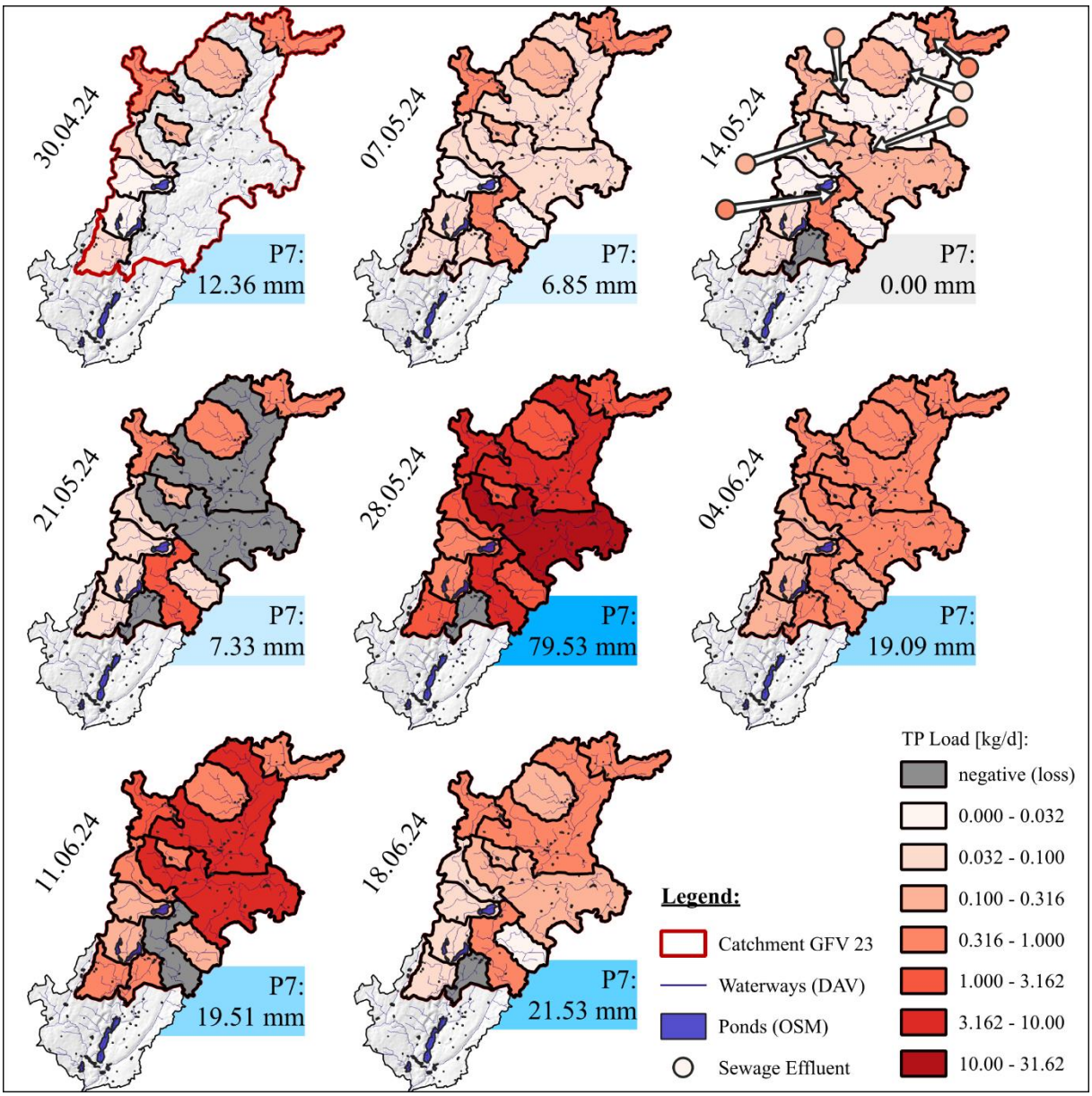

Figure 4.16: Origin of TP loads for each sampling day of the field campaign. Note that the colouring of each subcatchment follows a logarithmic scale, as seen in the legend. The daily sewage loads as calculated before are shown exemplary for May 14th but could be drawn for each day. Precipitation is indicated in blue, with P7 being the sum of precipitation for the last 7 days (including the day of sampling itself).

5 Discussion

The aim of this thesis was to carry out a phosphorous mass balance for the Heilsau catchment, with a particular focus on the area upstream of the Herrenteich. Of key interest were the yearly and seasonal variations of phosphorous loads reaching the Herrenteich through the Heilsau river. Another aspect was to determine the origin of the key nutrient within the catchment, in particular whether the loads were dominated by point sources or diffuse sources. This would then allow stakeholders to address the most relevant pathways first, in order to improve the water quality and ecological state of the catchment and the Herrenteich.

This chapter will first summarise the key findings from above and investigate potential causes for the observations. Additionally, the limitations of this study are presented and suggestions regarding future research will be proposed. Finally, the findings will be interpreted regarding their implications for an improved catchment management.

5.1 Summary and Discussion of Findings

Discharge:

The estimation method for other locations than the gauge at Zarpen fitted well for low and medium discharges, but higher flows need to be considered with care: The comparison of measured and calculated Q showed discrepancies for discharges above four times the multiannual mean discharge. Furthermore, the sources of observations (VerTe and gauge at Zarpen) might have higher uncertainties at these high flows, as a comparison between Heidekamp and Zarpen showed.

This uncertainty could be due to an underestimation of the VerTe measurements at higher flows or, alternatively, the discharge of the Heilsau on these dates was highly non-stationary, where an instantaneous measurement might vary greatly from the average flow of the day.

Concentrations in Heilsau Channel:

A seasonal trend was detected, with lower TP concentrations during winter and an increase during summer. This happened anticyclic to the discharge distribution, which showed higher flows during winter. The previously available concentration data was mostly of monthly frequency, whereas the field campaign included weekly and event measurements. The weekly campaign showed a trend of higher concentrations during

dry periods and lower concentrations during wet periods. However, high frequency event data showed increasing concentrations with discharges from the heavy rain event and a clockwise hysteresis could be observed regarding the C-Q relationship during that event.

A different pattern of dilution versus mobilisation of solutes at different time scales has been reported in several studies (Knapp et al., 2020; Minaudo et al., 2019; Rose et al., 2018). Knapp et al. (2020) for example observed that biologically active solutes like nitrate showed a mobilisation pattern during storm events while a general dilution pattern was observed over longer time scales (Knapp et al., 2020). Furthermore, Minaudo et al. (2019) reported that in 77% of 138 analysed catchments the total phosphorous concentrations showed a dilution pattern with seasonal discharge variations and a mobilisation pattern at the event scale (Minaudo et al., 2019). This behaviour matches with the observations in the Heilsau catchment and supported the consideration of baseflow and stormflow components for concentration estimation as done in the C-$Q_{quick\text{-}slow}$ model. An explanation for the opposite behaviour towards different time scales might lie in the potential cause of phosphorous mobilisation: For example, sediments of the riverbed or from floodplains could be re-mobilised during stormflow (Jarvie et al., 2012; Powers et al., 2016), whereas the seasonal pattern is likely to be shaped by the dilution of point sources during the wet period (Minaudo et al., 2019).

C-Q Analysis:

The C-$Q_{quick\text{-}slow}$ model showed a rather poor performance regarding its predictive accuracy, although low R-squared values are not uncommon in literature (Minaudo et al., 2019). The main cause for the low R^2 were the extreme observed concentrations which could not be simulated with the model. However, the p-values of the explaining variables $log(Q_{slow})$ and $log(Q_{quick})$ confirmed their significant impact on TP concentrations.

Regarding the general C-Q relationship, the analysis of available data showed that most samples were taken at conditions with dominant baseflow, only few datapoints represented conditions with a higher stormflow component. This might be a cause for the poor predictive power of the C-$Q_{quick\text{-}slow}$ model: if more data from event measurements would be available, the mobilising behaviour as observed during the rain

event in May 2024 would impact the development of the model towards a more event-sensitive prediction.

Both measured and modelled TP concentrations showed a negative C-Q slope in a log-log space, indicating dilution. However, the observations were scattered widely, which might be due to the opposing behaviour mentioned above: When the seasonal variation generally follows a negative slope (dilution), but the variation at the event scale experiences mobilisation (positive slope), the combination of both effects can lead to more scattered data within the log(C)-log(Q) space (see for example Knapp et al., 2020).

Point and Diffuse Sources:

Regarding drainage samplings, only few measurements were done: 20 samples in total for 13 locations. 12 out of the 20 analyses included discharge measurements, which ranged from ca. 18 l/d to a maximum of 42 m^3/d, most of them around 1 to 3 m^3/d. TP concentrations were generally low (more than half below detection limit), with some outliers from standing water or nearly dry drainage pipes. The FZ Jülich data was therefore preferred for the source apportionment, as it was for loads from rain canalisations, which were not sampled in the field campaign.

Regarding effluents from municipal STPs, dry loads could be determined for Heilshoop and Mönkhagen, whereas other STPs were estimated with a specific load of 0.62635 g TP per capita and day (derived from Mönkhagen). The highest contributors were Reinsbek, Heilshoop and Dissau. Although there was more concentration data available for Reinsbek, the lack of discharge data limited an analysis regarding potential seasonal fluctuations of TP loads.

For private STPs, no calculations were done, instead the data from FZ Jülich was used, which based on a specific loading rate of 0.7 g TP per capita and day. This value is similar to the specific loading rate of the municipal STPs, which is not surprising, given that the municipal treatment plants are waste stabilisation ponds (WSPs) and therefore have no conventional nutrient removal like precipitation of phosphorous. The removal efficiency therefore is likely to be similar for the WSPs and private STPs (which include for example oxidation ponds or septic tanks, according to the LfU).

Temporal Variation of TP loads:

Multiple methods were used to estimate the load of TP reaching the Herrenteich via the Heilsau, through station GFV_23 at Heidekamp. According to FZ Jülich data the annual load amounted to 2423.41 kg/a, but no distribution over the year was possible. The Q-weighted and Quick-Slow methods allowed monthly and annual distributions. Generally, the loads were higher during winter than during summer months, yet the annual loads varied significantly, e.g. with a range of 1717 to 6443 kg/a for the Quick-Slow method (1991-2023). The mean load for the past five years, however, was below the 30-year average, with 2754 kg/a (Quick-Slow) and 2682.17 kg/a (Q-weighted), a value similar to the one from FZ Jülich data. At the event scale, the analysis showed a mobilisation of TP during a heavy rain event, with a peak of 1875 g TP per hour and a maximum daily load of 32.251 kg/d for GFV_13 (gauge at Zarpen). This underlines the importance of understanding the role of heavy rain or flood events, as well as the need for more high frequency data to have a more accurate estimation of daily and weekly loads: The loads derived from the weekly sampling on May 21st and May 28th were 2.34 and 35.65 kg/d respectively. The event measurement in between, allowed an insight into what loads occurred in between, with 32.35 kg TP on May 23rd. A mere linear interpolation would have overseen such relevant peaks.

Regarding the role of precipitation, literature would suggest that the rainfall intensity should have a significant impact on erosion of all land uses (including forests), a process which in turn mobilises phosphorous attached to particles (Ramos et al., 2019). For annual precipitation, a positive covariation with annual TP loads could indeed be identified, however the analysis of medium to high rainfall intensities occurring each year could not clearly explain the variation. This indicates that at the annual scale, the TP load is mainly influenced by wet or dry years. This is not surprising given the load was calculated with the discharge, which in turn is depending on precipitation.

Spatial Distribution of Loads:

The analysis of the FZ Jülich model for the upper catchment showed that erosion, municipal STPs, and drainage make up the largest contribution of annual TP loads. The most polluting subcatchments could be found in the north and in the west. These are areas of high slopes and mostly agricultural cropland (see overviews in Section 3.1), thus leading to high modelled TP loads for erosion and drainage (Tetzlaff et al., 2017).

When categorising the TP pathways regarding urban or agricultural origin, agriculture amounted to 51.67% (erosion, washout, and drainage) and urban sources made up 37.51% (STPs and rain canalisation) of the total load reaching GFV_23 at Heidekamp. These drivers making up most of the TP load would also support the suggestion from the C-Q relationship analysis above: seasonal concentration and dilution patterns of TP could be influenced by point sources (municipal STPs), while events mobilise phosphorous attached to soil and sediments (erosion, washout, drainage).

Load estimations from own field measurements showed increased loads during wet periods in May and June, whereas rather dry weeks at the beginning of May transported lower amounts of TP. The mass balance between downstream and upstream catchments showed increasing loads for most catchments (as expected), yet a few days showed a negative balance for some subcatchments, especially the outlet catchment in the south, between Zarpen and Heidekamp. On the one hand, this result could be due to uncertainties in the data: firstly, the true discharge might differ significantly from the estimation for streams which are modified (such as piped underground or retained in ponds). Secondly, the samples were taken under varying stream flows, for example some stations of tributaries like GFV_71 had water levels of merely 1 cm during dry weeks, whereas samples from the main channel showed water levels of several dm to in the same period. This could have an impact on the sediment content in the sample, as sampling at a water level of just 1 cm creates turbulence and distortion of the stream bed (more sediments), whereas the sampling of the main channel can avoid such turbulence (less sediments).

However, if uncertainties in the data were not present, there could still be an explanation for the “loss” of phosphorous on the way: biological activity could change phosphorous concentrations and (temporary) sedimentation or sorption processes could explain the behaviour of a phosphorous sink during dry periods and low flow, even within merely a few km of a stream (Jarvie et al., 2012). On the other side of the spectrum, a highly dynamic (unsteady) flow condition can also cause the concentrations to vary within a short time. As the samples were taken from downstream to upstream, this dynamic can explain for example the “loss” in the southern subcatchment on May 28th (see Figure 4.4 and Figure 4.16): The samples were taken under increasing flows (rising limb), which, as seen in the high frequency data of Figure 4.5, can lead to a steep increase of concentrations. As the downstream station was sampled first, the concentration at that

time was most likely lower than at the time the upstream station was sampled. Indeed, on that day the TP concentration of GFV_23 (downstream) was 0.257 mg/l at 09:08, whereas the concentration at GFV_13 (upstream) was 0.403 mg/l at 13:22. As the load was calculated with the daily average discharge, this inevitably leads to a seemingly higher load upstream than downstream under dynamic conditions.

One last remark regarding the load analysis from the field campaign should be devoted to the sewage treatment effluents: It was observed that during dry periods of low flow, the daily loads calculated for the STPs explained most of the TP within their respective subcatchment. An exception was the STP at Mönkhagen, contributing to GFV_85: On May 14th (a sampling day of the driest conditions with a P7 of 0mm), the calculated daily load for the subcatchment was lower than what the STP should contribute each day. Here, the explanation most likely lies in an unfortunate sampling location: The outlet of the STP was less than 50 m upstream of the sampling point GFV_85, therefore the water might not have fully mixed by that point. This would result in a reading not representative for the upstream catchment, it would have been better to sample further downstream where fully mixed conditions could be assured. However, locations for sampling further downstream were not accessible.

5.2 Limitations and Recommendations

As indicated in the methodology and summary of findings, this study faced some limitations which will be presented in this section, along with recommendations of how to address these limitations in the future.

Firstly, the TP concentrations were subject to measurement uncertainties, as the example of varying flow conditions between tributaries and main channel showed, but also the laboratory analysis includes inherent uncertainties. Moreover, the uncertainty of discharge data: with few measurements in the catchment apart from the gauge, the true discharge might vary significantly from the estimations. In the future, particularly for the remaining time of the VerTe project, I would recommend more discharge measurements in the upper catchment, not limiting these to the immediate surrounding of Reinfeld. This would allow a better load estimation and source apportionment. Furthermore, information about the water level and discharge regulation of the Herrenteich and other ponds would be useful, as this could then be incorporated into discharge modelling of both downstream and upstream areas.

Secondly, this study focussed on total phosphorous only, but the actual bioavailability of the nutrient was not investigated. In general, the impact on aquatic ecology within the river and further downstream in the Herrenteich was not assessed. However, as more data of other parameters such as nitrogen compounds and pH were collected and measured, the database which was built during this thesis can be used to further assess the impact of the water quality on aquatic organisms.

Thirdly, regarding the C-Q relationship analysis, the effect of intense rainfall could only be analysed for one summer event after a 3-week period of almost no precipitation. For a better understanding of the C-Q dynamics, more high frequency data would be necessary. Especially the winter period would be of interest, but also more data on how storms affect C-Q relationships under previously wet conditions would allow a better understanding of the mobilising or retaining processes and drivers within the catchment.

Moreover, the C-Q relationship analysis was not able to exactly identify the sources responsible for the mobilisation or dilution of phosphorous. Due to the methodology and in line with common catchment understanding, the increase of TP with stormflow is often attributed to diffuse sources, e.g. erosion and washout. However, research has shown that phosphorous from point sources, in particular sewage effluents, can be temporarily retained by rivers at lower flows and then re-mobilised during storm events (Jarvie et al., 2012). A method to identify the contribution of sewage to the total phosphorous loads in rivers has been developed using chloride as a conservative tracer (Jarvie et al., 2012). This would require concentration data of the tracer, which was not available for this thesis, but future measurement campaigns could include that.

Concerning the C-$Q_{quick\text{-}slow}$ model, its performance could be improved if more concentration data was available at the sampling station GFV_13, at Zarpen, as the gauge would eliminate the uncertainty regarding discharges. Furthermore, to accommodate the hysteresis observed during the high frequency measurements, I would suggest to improve the model as follows: as the rising versus falling limb of the hydrograph came along with a rise and fall of the phosphorous concentrations at different rates, the slope of Q could be included as a factor for increasing or decreasing concentrations compared to the timestep before. Ideally, this timestep would be hourly like the discharge data available from the gauge, but maybe daily trends would suffice. Linking the concentrations between consecutive timesteps and adding a third explaining variable of "Q_{slope}" to the existing Q_{slow} and Q_{quick} would increase the complexity of the model to a manageable degree, while potentially improving the predictive power significantly.

Regarding sewage data, a potential variation of phosphorous removal efficiency was not included. Although data from the STP in Reinsbek was available for several years, the lack of discharge data made an analysis of varying loads challenging. Similarly for my own measurements at Heilshoop, Mönkhagen, and Langniendorf: critical parameters like the hydraulic retention time could not be calculated due to lacking data about the geometry and water levels in the ponds, as well as a lack of discharge measurements over multiple days and conditions (wet versus dry). A water balance for the STPs would improve the estimations significantly. In the future, deriving the sewage discharges should be included routinely in field campaigns from VerTe, as they did it for the surroundings of the ponds of Reinfeld.

Lastly, the phosphorous-emitting role of aquaculture in the catchment could not be included. Data regarding feeding and harvest of fish in the Herrenteich at Reinfeld and the Moorteich at Heilshoop was not available. This pathway was not included in the FZ Jülich model either, which might explain its lower annual load compared to the estimations from the Quick-Slow and Q-weighted method. To prove this hypothesis, however, data from the fish farmers would be necessary.

5.3 Implications for Catchment Management

Within the limitations and uncertainties, it can be said that the majority of phosphorous in the upper Heilsau catchment is coming from agricultural and urban sources, unsurprisingly. A differentiation with the FZ Jülich data enabled a more detailed image, by which about 27% of TP loads originate from erosion of agricultural surfaces, about 21% from municipal STPs, and ca. 19% from drainage systems in agriculture. This suggests to address these sources first, if the loads reaching the Herrenteich are to be reduced effectively.

5.3.1 Addressing Erosion

Regarding the magnitude of erosion, the findings underline the importance of sediment traps or retention zones along the streams. This is partly done already, for example at the Nachtkoppelbek, a tributary of the Gaffelbek north of Heidekamp (see Figure 5.1 a, b). Depending on the quality of the sediments which settle in such ponds or retention zones, these could then even be re-applied to the surrounding cropland or forest as fertilizer and to built up the ground which is lost to erosion. Kiani et al. (2021) for example excavated and reused sediments from a lake in Finland to improve nutrient-deficient sandy loam soils in the area (Kiani et al., 2021). However, to reduce potential N and P leaching from sediment-based fertilisers, the crop requirements for the nutrient should be considered when applying such

sediments (Kiani et al., 2023). Furthermore, it should be noted that even if the sediments are not to be used for agriculture, the dredging of such sediment traps should be considered in the maintenance plan of such measures, as otherwise phosphorous could re-enter the water cycle when desorbing from deposited sediments (Haddaway et al., 2018; Schwoerbel & Brendelberger, 2022).

The best effect of sediment retention would most likely be achieved in the western slopes of the Heilsau catchment, at tributaries like Gaffelbek, Wohldbek, Niendorferbek, Martelsbek, and Reinsbek (stream). These are all streams which run through narrow deep valleys (in German "Kerbtal"), where the valley slopes alone are prone to erosion due to their angle, but additionally they are draining catchments with mostly cropland upstream (Figure 3.2 and Figure 3.3 from the catchment description). Considering the modelled load from erosion according to FZ Jülich data, the subcatchment in the north draining towards the sampling point GFV_8 has the highest annual TP load among the subcatchments (see Figure 3.6 and Appendix, Figure 8.7). Therefore, this subcatchment located at Obernwohlde should be addressed with particular care. A reason for this area to be susceptible to erosion might be that it mainly consists of agricultural cropland (like corn) with slopes higher than 3%, therefore the retention of sediments at the outlet or with riparian buffers along the fields could reduce this pathway (Haddaway et al., 2018).

Furthermore, the temporal variation of loads should be considered, as the majority of TP loads reach the Heilsau during winter months. Since that season receives the highest precipitation while agricultural activity is presumably the lowest, bare cropland could be particularly prone to erosion. Some measures to counter the erosion during winter could be a combination of cover-crops with no-tillage practices, i.e. a conservative agricultural practice (Jacobs et al., 2022).

It should be noted that besides the steep tributaries in the upstream catchment, other tributaries further downstream should also include measures to reduce sediment transport, for example the streams Bergkoppelbach and Piepenbek, which flow into the Herrenteich and Schwarzer Teich.

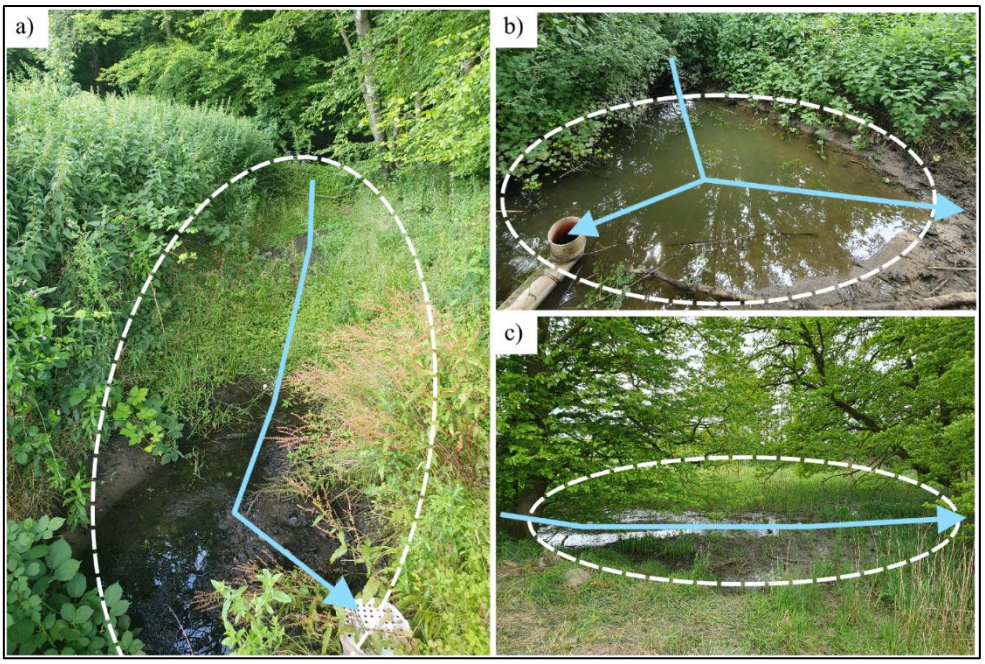

Figure 5.1: Retention zones implemented or naturally occurring in the upper Heilsau catchment, with blue arrows indicating flow direction. ***A:*** *Sequential retention ponds along the Nachtkoppelbek, retaining sediments from forest.* ***B:*** *Retention pond at Nachtkoppelbek, just before entering Gaffelbek. The stream follows the arrow on the right, the T-outlet on the left discharges overflow.* ***C:*** *Floodplain and wetland at Zarpenbek, upstream of GFV_46.*

5.3.2 Addressing Sewage Effluents

Regarding the effluents from municipal STPs, a straightforward solution to reduce P emissions would be to upgrade the waste stabilisation ponds in the catchment. This would include removal methods such as precipitation of phosphorous with chemicals, although this might involve pH control, which could have adverse effects on the biological treatment in the WSPs (Ohizumi et al., 1985; Reif et al., 2023; Rousseau, 2023). Another method could be an end-of-line phosphorous removal at the outlet of the existing WSPs via a geochemical barrier made of phosphorous sorbing materials, such as limestone, zeolite, apatite, or materials coated with P-sorbing biopolymers or fly ash (Jarosiewicz et al., 2022; Negussie et al., 2012; Rousseau, 2023; Szklarek et al., 2018).

5.3.3 Addressing Drainage

Concerning TP loads from drainage systems, the subcatchments in the north and to the west of the upper Heilsau catchment were the highest phosphorous emitters, a similar spatial distribution as erosion (see Appendix, Figure 8.7). Practices which could reduce these loads could involve the reduction of applied fertilisers or practices to improve the sorption of phosphorous to the soil. However, the main cause of P-losses from loamy soils (as found in most of the catchment, see Figure 3.2) is not a lack of sorption capacity but rather the loss through particle-bound phosphorous, which leaves the drainage systems with fine sediments

(Beauchemin et al., 1998). Similar to the measures for sewage effluent, the particle-bound and dissolved phosphorous from drainage pipes could be captured and potentially reused with P-sorbing materials at the end of the drainage system (collecting pipes). Furthermore, effective measures to improve P retention from drained agricultural fields include other "edge-of-field" technologies such as buffer zones or constructed wetlands (Dantas Mendes, 2020).

5.3.4 Catchment Restoration

As already mentioned in Section 2.2.3.2, the report by Hansen and Greuner-Pönicke (2002) suggested potential measures for improving the river morphology and quality. These measures focussed mostly on restoring the river towards a more natural state in order to improve biodiversity, yet their measures would have a positive impact on nutrient dynamics too (Hansen & Greuner-Pönicke, 2002). This includes the restoration of a more meandering Heilsau river to slow down the flow and allow natural regeneration of the river, but also reconnection of floodplains to accommodate flood water. These measures, if not already implemented, would be advisable from an ecologic perspective alone, and this thesis can support the additional potential benefits regarding nutrient and sediment retention with these measures (Hansen & Greuner-Pönicke, 2002). Moreover, a combination of nutrient management with restoration measures could qualify sustainable management practices for subsidisation, like the ones offered by the DVL (*DVL Naturschutzberatung-SH*). This could give an incentive to land managers (like farmers) for adopting to conserving practices without fearing economic loss.

6 Outlook and Conclusion

This thesis aimed to carry out a comprehensive phosphorous mass balance for the Heilsau catchment, with a focus on the area upstream of the Herrenteich. The results reveal that both point and diffuse sources contribute significantly to the phosphorous loads, with seasonal and event-based variations further adding complexity to the dynamics of nutrient input into the Herrenteich. The study highlighted that phosphorous concentrations increased during stormflow events, with diffuse sources such as erosion potentially playing a substantial role. At larger timescales, the concentrations showed an inverse relationship to seasonal flow patterns, possibly due to the varying contribution of point source loads to the total discharge.

The analysis of the spatial distribution and temporal variation of phosphorous loads allowed insights into the key contributors and pathways of nutrient pollution within the catchment. Erosion and drainage from agriculture, as well as sewage effluents, have been identified as critical sources of phosphorous, with agriculture contributing slightly more than urban sources. Moreover, the mobilisation of phosphorous during storm events underlines the importance of monitoring at a high-frequency, as low-frequency sampling campaigns may miss significant nutrient peaks.

However, this study also faced several limitations. Continuous discharge data was limited to the gauge at Zarpen, which is accompanied by uncertainties in the load calculations, particularly during unsteady flow conditions. Additionally, the focus was exclusively on total phosphorous, without considering its bioavailability or ecological impact on aquatic organisms, leaving gaps in understanding the broader ecological implications of phosphorous pollution. Future studies in the area would benefit from more extensive high-frequency data collection, especially during wet conditions, and the inclusion of other parameters like nitrogen compounds and bioavailable phosphorous. Furthermore, incorporating a tracer analysis, such as using chloride to distinguish the contribution of sewage sources, could significantly improve source apportionment.

Moreover, while the C-Q relationship analysis provided valuable insights into the relationship between flow conditions and phosphorous concentrations, the predictive accuracy of the C-$Q_{quick\text{-}slow}$ model could be improved with additional data from both storm events and baseflow conditions. Addressing these limitations would refine the accuracy of future mass balance assessments and improve the understanding of phosphorous dynamics in the catchment.

Looking ahead, the findings of this thesis provide a foundation for more targeted and effective catchment management strategies. Erosion control measures, particularly to the north and west of the catchment, could help reduce diffuse phosphorous inputs. Enhancing the treatment efficiency of STPs would also significantly contribute to lowering nutrient loads. Moreover, phosphorous retention from agricultural drainage water would be advisable.

In conclusion, the phosphorous mass balance developed in this thesis offers a crucial step towards understanding the nutrient dynamics in the Heilsau catchment. The insights gained can assist stakeholders in implementing more efficient and targeted measures to mitigate eutrophication in the ponds of Reinfeld, thereby enhancing both water quality and the overall ecosystem services provided by the catchment. Further research and continued monitoring will be essential to address the remaining knowledge gaps and to refine management practices over time.

7 Bibliography

Addy, K., & Green, L. (1996). *Phosphorus and Lake Aging* (Fact Sheet 96–2; Natural Resources Facts). University of Rhode Island. https://web.archive.org/web/20210728121848/https://web.uri.edu/watershedwatch/files/Phosphorus.pdf

Amtlicher Höhenbezug. (2021). schleswig-holstein.de. https://www.schleswig-holstein.de/DE/landesregierung/ministerien-behoerden/LVERMGEOSH/Themen/themaRaumbez/themaRaumDhhn2016

Baldwin, D. S., & Mitchell, A. M. (2000). The effects of drying and re-flooding on the sediment and soil nutrient dynamics of lowland river-floodplain systems: A synthesis. *Regulated Rivers: Research & Management*, *16*(5), 457–467. https://doi.org/10.1002/1099-1646(200009/10)16:5<457::AID-RRR597>3.0.CO;2-B

Baroto, R. (2023). *Improvement of ecosystem services in the Reinfeld ponds*.

Beauchemin, S., Simard, R. R., & Cluis, D. (1998). Forms and Concentration of Phosphorus in Drainage Water of Twenty-Seven Tile-Drained Soils. *Journal of Environmental Quality*, *27*(3), 721–728. https://doi.org/10.2134/jeq1998.00472425002700030033x

Biswas, J. K., Mondal, M., Kumar, V., Bhatnagar, A., Biswas, S., & Vithanage, M. (2022). Chapter 5—Nature-inspired ecotechnological approaches toward recycling and recovery of resources from wastewater. In V. Kumar & M. Kumar (Eds.), *Integrated Environmental Technologies for Wastewater Treatment and Sustainable Development* (pp. 101–145). Elsevier. https://doi.org/10.1016/B978-0-323-91180-1.00025-9

Borbor-Cordova, M. J., Boyer, E. W., McDowell, W. H., & Hall, C. A. (2006). Nitrogen and phosphorus budgets for a tropical watershed impacted by agricultural land use: Guayas, Ecuador. *Biogeochemistry*, *79*(1–2), Article 1–2. https://doi.org/10.1007/s10533-006-9009-7

Carpenter, S. R. (2005). Eutrophication of aquatic ecosystems: Bistability and soil phosphorus. *Proceedings of the National Academy of Sciences*, *102*(29), 10002–10005. https://doi.org/10.1073/pnas.0503959102

Carpenter, S. R., Caraco, N. F., Correll, D. L., Howarth, R. W., Sharpley, A. N., & Smith, V. H. (1998). Nonpoint Pollution of Surface Waters with Phosphorus and Nitrogen. *Ecological Applications*, *8*(3), 559–568. https://doi.org/10.1890/1051-0761(1998)008[0559:NPOSWW]2.0.CO;2

CDC Open Data. (n.d.). Retrieved 16 March 2024, from https://opendata.dwd.de/climate_environment/CDC/observations_germany/climate/

Chakrabarti, S. (2018). Eutrophication - A Global Aquatic Environmental Problem: A Review. *Research & Reviews: Journal of Ecology and Environmental Sciences*, *6*(2), 1–6.

Chislock, M. F., Doster, E., Zitomer, R., & Wilson, A. E. (2013). Eutrophication: Causes, consequences, and controls in aquatic ecosystems. *Nature Education Knowledge*, *4*, 10–12.

Contreras, E., Jurado-Ezqueta, M., Pimentel, R., Serrano, L., Hidalgo, C., Jiménez, A., & Polo, M. J. (2024). Assessment of seasonal and annual patterns in phosphorus content in a monitored catchment through a partitioning approach based on hydrometeorological data. *Environmental Research*, *242*, 117501. https://doi.org/10.1016/j.envres.2023.117501

Dantas Mendes, L. R. (2020). Edge-of-Field Technologies for Phosphorus Retention from Agricultural Drainage Discharge. *Applied Sciences*, *10*(2), 634. https://doi.org/10.3390/app10020634

Elser, J. J., Bracken, M. E. S., Cleland, E. E., Gruner, D. S., Harpole, W. S., Hillebrand, H., Ngai, J. T., Seabloom, E. W., Shurin, J. B., & Smith, J. E. (2007). Global analysis of

nitrogen and phosphorus limitation of primary producers in freshwater, marine and terrestrial ecosystems. *Ecology Letters*, *10*(12), 1135–1142. https://doi.org/10.1111/j.1461-0248.2007.01113.x

European Environment Agency (Ed.). (2005). *Source apportionment of nitrogen and phosphorus inputs into the aquatic environment*. Office for Official Publ. of the European Communities.

Evans, C., & Davies, T. D. (1998). Causes of concentration/discharge hysteresis and its potential as a tool for analysis of episode hydrochemistry. *Water Resources Research*, *34*(1), 129–137. https://doi.org/10.1029/97WR01881

Godsey, S. E., Hartmann, J., & Kirchner, J. W. (2019). Catchment chemostasis revisited: Water quality responds differently to variations in weather and climate. *Hydrological Processes*, *33*(24), 3056–3069. https://doi.org/10.1002/hyp.13554

Hackemann, P. (1994). *Nährstoffsituation und Wassergüte im Reinfelder Herrenteich unter Berücksichtigung seiner Zuflüsse und Einleitungen* [Diplomarbeit]. Fachhochschule Lübeck.

Haddaway, N. R., Brown, C., Eales, J., Eggers, S., Josefsson, J., Kronvang, B., Randall, N. P., & Uusi-Kämppä, J. (2018). The multifunctional roles of vegetated strips around and within agricultural fields. *Environmental Evidence*, *7*(1). https://doi.org/10.1186/s13750-018-0126-2

Hansen, P., & Greuner-Pönicke, S. (2002). *Gewässerpflegeverband Heilsau: Gesamtkonzept Heilsau—Erläuterungsbericht*. Gewässerpflegeverband Heilsau.

House, W. A., & Warwick, M. S. (1998). Hysteresis of the solute concentration/discharge relationship in rivers during storms. *Water Research*, *32*(8), 2279–2290. https://doi.org/10.1016/S0043-1354(97)00473-9

Jacobs, A. A., Evans, R. S., Allison, J. K., Garner, E. R., Kingery, W. L., & McCulley, R. L. (2022). Cover crops and no-tillage reduce crop production costs and soil loss, compensating for lack of short-term soil quality improvement in a maize and soybean production system. *Soil and Tillage Research*, *218*, 105310. https://doi.org/10.1016/j.still.2021.105310

Jarosiewicz, P., Fazi, S., & Zalewski, M. (2022). How to boost Ecohydrological Nature-Based Solutions in water quality management. *Ecohydrology & Hydrobiology*, *22*(2), Article 2. https://doi.org/10.1016/j.ecohyd.2021.11.005

Jarvie, H. P., Sharpley, A. N., Scott, J. T., Haggard, B. E., Bowes, M. J., & Massey, L. B. (2012). Within-River Phosphorus Retention: Accounting for a Missing Piece in the Watershed Phosphorus Puzzle. *Environmental Science & Technology*, *46*(24), 13284–13292. https://doi.org/10.1021/es303562y

Kiani, M., Raave, H., Simojoki, A., Tammeorg, O., & Tammeorg, P. (2021). Recycling lake sediment to agriculture: Effects on plant growth, nutrient availability, and leaching. *Science of The Total Environment*, *753*, 141984. https://doi.org/10.1016/j.scitotenv.2020.141984

Kiani, M., Zrim, J., Simojoki, A., Tammeorg, O., Penttinen, P., Markkanen, T., & Tammeorg, P. (2023). Recycling eutrophic lake sediments into grass production: A four-year field experiment on agronomical and environmental implications. *Science of The Total Environment*, *870*, 161881. https://doi.org/10.1016/j.scitotenv.2023.161881

Knapp, J. L. A., von Freyberg, J., Studer, B., Kiewiet, L., & Kirchner, J. W. (2020). Concentration–discharge relationships vary among hydrological events, reflecting differences in event characteristics. *Hydrology and Earth System Sciences*, *24*(5), 2561–2576. https://doi.org/10.5194/hess-24-2561-2020

Kurtzman, D., Navon, S., & Morin, E. (2009). Improving interpolation of daily precipitation for hydrologic modelling: Spatial patterns of preferred interpolators. *Hydrological Processes*, *23*(23), 3281–3291. https://doi.org/10.1002/hyp.7442

Leistungsfähigkeit von Maßnahmen zur Regenwasserbewirtschaftung im Trennsystem in Schleswig-Holstein (MaReT-SH) (MaReT-SH, Forschungsvorhaben der TH Lübeck im Auftrag das Landesamt für Umwelt (LfU) des Landes Schleswig-Holstein, Lübeck/ Kiel). (2024). [Dataset].

Li, J., & Heap, A. D. (2014). Spatial interpolation methods applied in the environmental sciences: A review. *Environmental Modelling & Software*, *53*, 173–189. https://doi.org/10.1016/j.envsoft.2013.12.008

Lyne, V., & Hollick, M. (1979). *Stochastic Time-Variable Rainfall-Runoff Modeling*. *79*.

Minaudo, C., Dupas, R., Gascuel-Odoux, C., Roubeix, V., Danis, P.-A., & Moatar, F. (2019). Seasonal and event-based concentration-discharge relationships to identify catchment controls on nutrient export regimes. *Advances in Water Resources*, *131*, 103379. https://doi.org/10.1016/j.advwatres.2019.103379

Moatar, F., Abbott, B. W., Minaudo, C., Curie, F., & Pinay, G. (2017). Elemental properties, hydrology, and biology interact to shape concentration-discharge curves for carbon, nutrients, sediment, and major ions. *Water Resources Research*, *53*(2), 1270–1287. https://doi.org/10.1002/2016WR019635

Mockler, E. M., Deakin, J., Archbold, M., Gill, L., Daly, D., & Bruen, M. (2017). Sources of nitrogen and phosphorus emissions to Irish rivers and coastal waters: Estimates from a nutrient load apportionment framework. *Science of The Total Environment*, *601–602*, 326–339. https://doi.org/10.1016/j.scitotenv.2017.05.186

Musolff, A., Schmidt, C., Selle, B., & Fleckenstein, J. H. (2015). Catchment controls on solute export. *Advances in Water Resources*, *86*, 133–146. https://doi.org/10.1016/j.advwatres.2015.09.026

Nathan, R. J., & McMahon, T. A. (1990). Evaluation of automated techniques for base flow and recession analyses. *Water Resources Research*, *26*(7), 1465–1473. https://doi.org/10.1029/WR026i007p01465

Negussie, Y., Urbaniak, M., Szklarek, S., Lont, K., Gągała, I., & Zalewski, M. (2012). Efficiency analysis of two sequential biofiltration systems in Poland and Ethiopia—The pilot study. *Ecohydrology & Hydrobiology*, *12*, 271–285. https://doi.org/10.2478/v10104-012-0028-9

NSG Oberer Herrenteich. (n.d.). NABU Schleswig-Holstein. Retrieved 6 May 2024, from https://schleswig-holstein.nabu.de/natur-und-landschaft/nabu-schutzgebiete/oberer-herrenteich/13684.html

Ohizumi, M., MASHIA, M., KOYANAGI, S., HARIGAI, T., TAGUCHI, Y., 学大泉, 聡小柳, 洋治田口, 美智雄真島, & 工針谷. (1985). Removal of phosphates from wastewater by titanium (IV) sulfate with precipitation method. 水質汚濁研究, *8*(10), 668. https://doi.org/10.2965/jswe1978.8.668

Osterhoff, L. (2020). *Stoffliche Anforderungen zum Umgang mit Regenwasser in Schleswig-Holstein*.

Pegel—Zarpen—Hauptwerte. (2024). [Dataset]. https://hsi-sh.de/pegel/pegel.html?mstnr=114151

Powers, S. M., Bruulsema, T. W., Burt, T. P., Chan, N. I., Elser, J. J., Haygarth, P. M., Howden, N. J. K., Jarvie, H. P., Lyu, Y., Peterson, H. M., Sharpley, A. N., Shen, J., Worrall, F., & Zhang, F. (2016). Long-term accumulation and transport of anthropogenic phosphorus in three river basins. *Nature Geoscience*, *9*(5), 353–356. https://doi.org/10.1038/ngeo2693

Ramos, M. C., Lizaga, I., Gaspar, L., Quijano, L., & Navas, A. (2019). Effects of rainfall intensity and slope on sediment, nitrogen and phosphorous losses in soils with different use and soil hydrological properties. *Agricultural Water Management*, *226*, 105789. https://doi.org/10.1016/j.agwat.2019.105789

Reif, D., Weisz, L., Kobsik, K., Schaar, H., Saracevic, E., Krampe, J., & Kreuzinger, N. (2023). Simultane Entfernung von organischen Spurenstoffen und Phosphor aus kommunalem Abwasser unter Einsatz einer Adsorptions-/Fällmittelsuspension. *Österreichische Wasser- und Abfallwirtschaft*, *75*(3–4), 152–160. https://doi.org/10.1007/s00506-022-00920-2

Reynolds, C. S., & Davies, P. S. (2001). Sources and bioavailability of phosphorus fractions in freshwaters: A British perspective. *Biological Reviews*, *76*(1), 27–64. https://doi.org/10.1111/j.1469-185X.2000.tb00058.x

Rose, L. A., Karwan, D. L., & Godsey, S. E. (2018). Concentration–discharge relationships describe solute and sediment mobilization, reaction, and transport at event and longer timescales. *Hydrological Processes*, *32*(18), 2829–2844. https://doi.org/10.1002/hyp.13235

Rousseau, D. (2023). *WATER TREATMENT TECHNOLOGY: PARTIM NATURE-BASED SOLUTIONS WASTE STABILIZATION PONDS* [Lecture at University of Antwerp].

Schindler, D. W. (2012). The dilemma of controlling cultural eutrophication of lakes. *Proceedings of the Royal Society B: Biological Sciences*, *279*(1746), 4322–4333. https://doi.org/10.1098/rspb.2012.1032

Schleswig-Holstein Downloadportal. (2024). https://geodaten.schleswig-holstein.de/gaialight-sh/_apps/dladownload/

Schwoerbel, J., & Brendelberger, H. (2022). *Einführung in die Limnologie: Stoffhaushalt - Lebensgemeinschaften - Technologie*. Springer Berlin Heidelberg. https://doi.org/10.1007/978-3-662-63334-2

Smith, V. H. (1983). Low Nitrogen to Phosphorus Ratios Favor Dominance by Blue-Green Algae in Lake Phytoplankton. *Science*, *221*(4611), 669–671. https://doi.org/10.1126/science.221.4611.669

Speir, S. L., Rose, L. A., Blaszczak, J. R., Kincaid, D. W., Fazekas, H. M., Webster, A. J., Wolford, M. A., Shogren, A. J., & Wymore, A. S. (2024). Catchment concentration–discharge relationships across temporal scales: A review. *WIREs Water*, *11*(2), e1702. https://doi.org/10.1002/wat2.1702

Stresius, I. (2006). *Eignung der Reinfelder Teiche für eine ökologische Teichwirtschaft* [Diplomarbeit]. Fachhochschule Lübeck.

Szklarek, S., Wagner, I., Jurczak, T., & Zalewski, M. (2018). Sequential Sedimentation-Biofiltration System for the purification of a small urban river (the Sokolowka, Lodz) supplied by stormwater. *Journal of Environmental Management*, *205*, 201–208. https://doi.org/10.1016/j.jenvman.2017.09.066

Tetzlaff, B., Keller, L., Kuhr, P., Kreins, P., Kunkel, R., & Wendland, F. (2017). *Endbericht zum Forschungsprojekt: Räumlich differenzierte Quantifizierung der Nährstoffeinträge ins Grundwasser und in die Oberflächengewässer Schleswig-Holsteins unter Anwendung der Modellkombination RAUMIS-GROWA-WEKU-MEPhos*. Forschungszentrum Jülich. https://www.schleswig-holstein.de/mm/downloads/Fachinhalte/Wasserrahmenrichtlinie/endberichtNaehrstoffmodellierung.pdf

Verbesserung der Ökosystemleistungen in den Reinfelder Teichen (VerTe) | BFN. (n.d.). Bundesamt für Naturschutz. Retrieved 9 May 2024, from https://www.bfn.de/projektsteckbriefe/verbesserung-der-oekosystemleistungen-den-reinfelder-teichen-verte

Wang, F., Maberly, S. C., Wang, B., & Liang, X. (2018). Effects of dams on riverine biogeochemical cycling and ecology. *Inland Waters*, *8*(2), 130–140. https://doi.org/10.1080/20442041.2018.1469335

White, P. J., & Hammond, J. P. (2006). *Updating the Estimate of the Sources of Phosphorus in UK Waters*. https://www.agindustries.org.uk/resource/updating-estimate-sources-of-phosphorus-uk-waters.html

Willems, W., & Stricker, K. (2017). *Regionalisierungsupdate 2017*. Landesamt für Landwirtschaft, Umwelt und ländliche Räume Schleswig-Holstein.

Yang, N., Zhang, J., Liu, J., Liu, G., Boyer, E. W., Guo, L., & Wang, G. (2020). Concentration–Discharge Relationships in Runoff Components during Rainfall Events at the Hydrohill Experimental Catchment in Chuzhou, China. *Water*, *12*(11), Article 11. https://doi.org/10.3390/w12113033

8 Appendix

8.1 Soil Classification

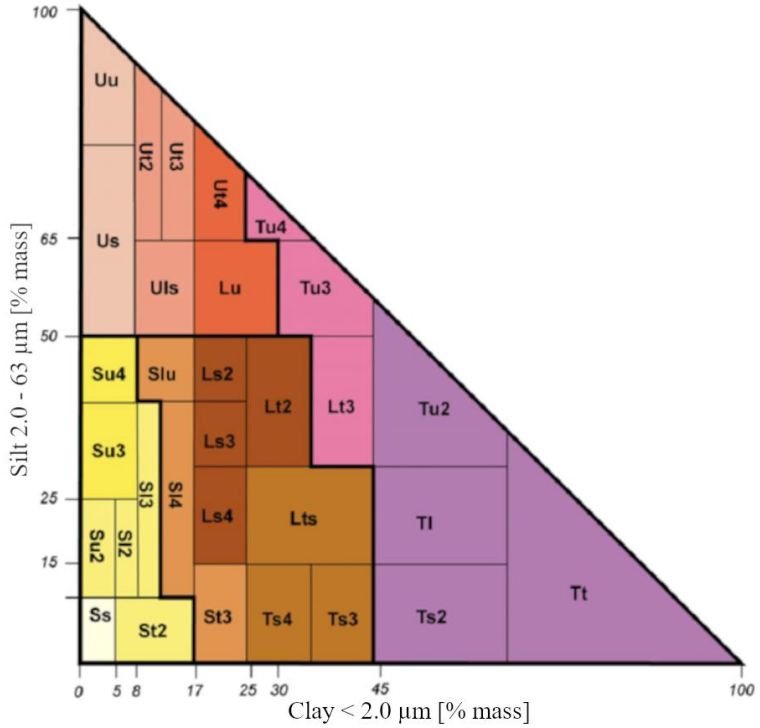

Figure 8.1: German soil texture classification diagram, adapted from (Burbaum et al., 2019). Translation into English soil texture classes was done following the comparison by the Bundesanstalt für Geowissenschaften und Rohstoffe - AG Boden (BodenspezifischenKennwerteKA5, p. 54)

8.2 General Sampling Procedure

The field sampling, including both stream and drainage water samples, was done following the protocol below:

1. **Preparation:**
   - Cleaning of sampling containers and measuring jugs in dishwasher, followed by rinsing/spraying with acetone.
   - Gassing out of acetone, closing of containers for transport.
   - Control of WTW MultiLine® 3620 IDS (multiparameter probe).
2. **Sampling:**
   - Washing out of sampling containers with sampling water (conditioning).
   - Grab samples of 1 litre taken in the middle of each stream/river (for drainage: pipe outlet), using a jug fixed to a pole.

- Measurement of field parameters pH, T, EC, and DO with WTW MultiLine® 3620 IDS.
- Documentation of field data such as date, time, weather, and field parameters in field survey app “merginmaps” (© 2024 Lutra Consulting Limited), synchronised with QGIS.

3. **Transport and Storage:**
   - After sampling, immediate transfer of water samples to car fridge (8°C).
   - Storage of samples in lab at 5°C.

8.3 General Lab Protocol

The procedure to process field samples in the laboratory of the TH Lübeck was as follows:

1. **Sample Preparation:**
   - The samples from the fridge were acclimatised to a room temperature of 18 to 22 °C.
   - Each sample was gently shaken to have a fully mixed water column.
   - For unfiltered analysis (TP, TNb, COD), the samples were transferred to 250 ml beakers.
   - For filtered analysis (ortho-P, NO3, NO2, NH4), 25 ml of each sample was filtered through membranes with 0.45 µm pore size and transferred to 50 ml beakers.
2. **Concentration Analysis:**

   All nutrient and COD concentrations were analysed following the instructions and best practice as documented by Hach © (see for example *Phosphate (Ortho/Total) cuvette test | Hach United Kingdom*). The test ranges were chosen according to the expected concentrations, for example drainage and water samples were tested at a low range, whereas sewage samples were tested at higher ranges.
   - TP: Hach © cuvette tests LCK 349 or LCK 350
   - Ortho-P: Hach © cuvette tests LCK 349 or LCK 350
   - TNb: Hach © cuvette tests LCK 138 or LCK 338
   - NO3: Hach © cuvette test LCK 339
   - NO2: Hach © cuvette test LCK 341
   - NH4: Hach © cuvette tests LCK 304, LCK 303, or LCK 302
   - COD: Hach © cuvette tests LCK 314 or LCK 514

8.4 Interpolation of Hourly Precipitation

Table 8.1: Exemplary interpolation of hourly precipitation for the catchment upstream of Zarpen, May 22nd 2024.

Date Time	P Wittenborn [mm/h]	P Groß Parin [mm/h]	P Lübeck-Blankensee [mm/h]	IDW Söhren [mm/h]	Share of Day [%]	IDW Söhren adjusted [mm/h]	IDW Zarpen centroid [mm/h]
22/05/2024 00:00	0	0	0	0	0.00%	0	0
01:00	0	0	0	0	0.00%	0	0
02:00	0	0	0	0	0.00%	0	0
03:00	0	0	0	0	0.00%	0	0
04:00	0	0	0	0	0.00%	0	0
05:00	0	0	0	0	0.00%	0	0
06:00	0	0	0.2	0.04057484	0.12%	0.056706242	0.059989034
07:00	0.1	0.1	0.1	0.1	0.29%	0.13975716	0.120889442
08:00	0	0.2	0	0.05791127	0.17%	0.080935152	0.107246139
09:00	0	0	0	0	0.00%	0	0
10:00	0	0	0	0	0.00%	0	0
11:00	0	0	0	0	0.00%	0	0
12:00	0	0	0	0	0.00%	0	0
13:00	0	0	0	0	0.00%	0	0
14:00	0	0	0	0	0.00%	0	0
15:00	0	0	2.4	0.48689806	1.40%	0.680474907	0.719868403
16:00	9.6	6	1.9	6.99546577	20.08%	9.776664273	7.365378159
17:00	8.6	4.4	3.2	6.28834259	18.05%	8.788409003	6.524619207
18:00	4	6.2	7.2	5.28622144	15.17%	7.387872946	6.975109755
19:00	2.1	4.2	3.7	3.03266709	8.70%	4.238369395	4.144675014
20:00	1.4	2.1	2.2	1.76498882	5.07%	2.46669824	2.307769812
21:00	1.8	12.1	1.6	4.7418558	13.61%	6.627082988	7.639197081
22:00	2	4	4	2.98486113	8.57%	4.171557144	4.09014057
23:00	1.5	7.4	0.8	3.06637066	8.80%	4.285472548	4.767141114
SUM:				**34.846157**	**100 %**	**48.7**	**44.822024**

Explanation for Table 8.1: First, the hourly distribution of precipitation was interpolated via IDW with hourly data from Wittenborn, Groß Parin, and Lübeck-Blankensee. Result: “IDW Söhren”. Then, this total distribution [mm/h] was used to determine the share of precipitation throughout the day [%]. Since the total daily sum for Söhren should amount to the registered amount from the observations (for this date: 48.7 mm), the percentage distribution was multiplied with the total daily sum, to receive a better approximation of the variation throughout each day [mm/h]. Finally, this interpolated and adjusted precipitation was used for estimating the rainfall in the catchment upstream of Zarpen via IDW. The distances from the centre of mass of this catchment (centroid) to Söhren, Lübeck-Blankensee, and Groß Parin were used respectively for IDW.

8.5 Validation of Q Estimation Method

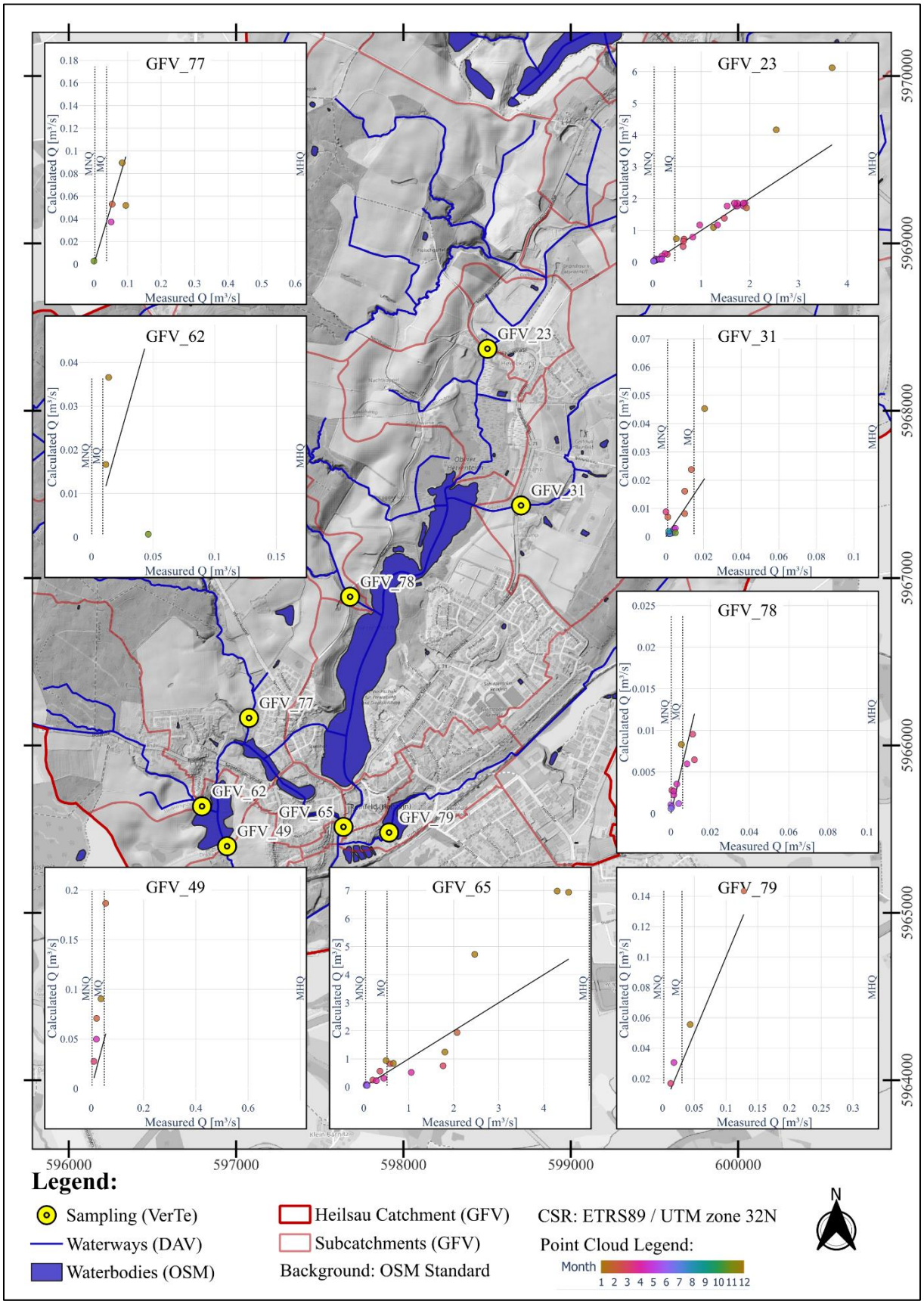

Figure 8.2: Validation of Q estimation method.

8.6 C-$Q_{quick\text{-}slow}$ Model

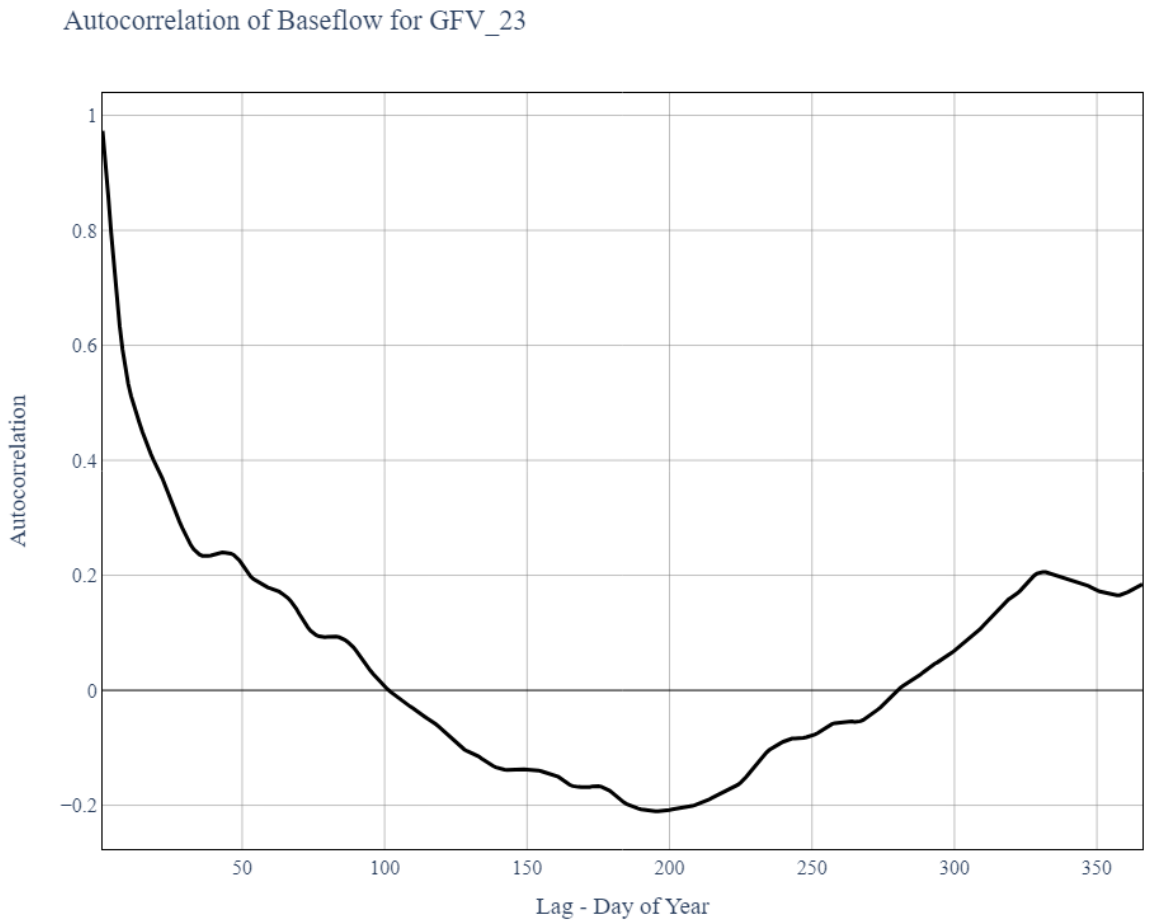

Figure 8.3: Autocorrelation result for baseflow from quick-slow separation method with recursive filter. A clear positive correlation could be observed for discharges of the same season (i.e. neighbouring days and days one year apart). Furthermore, a clear negative correlation can be observed between opposite seasons (Lag of around 150 days.

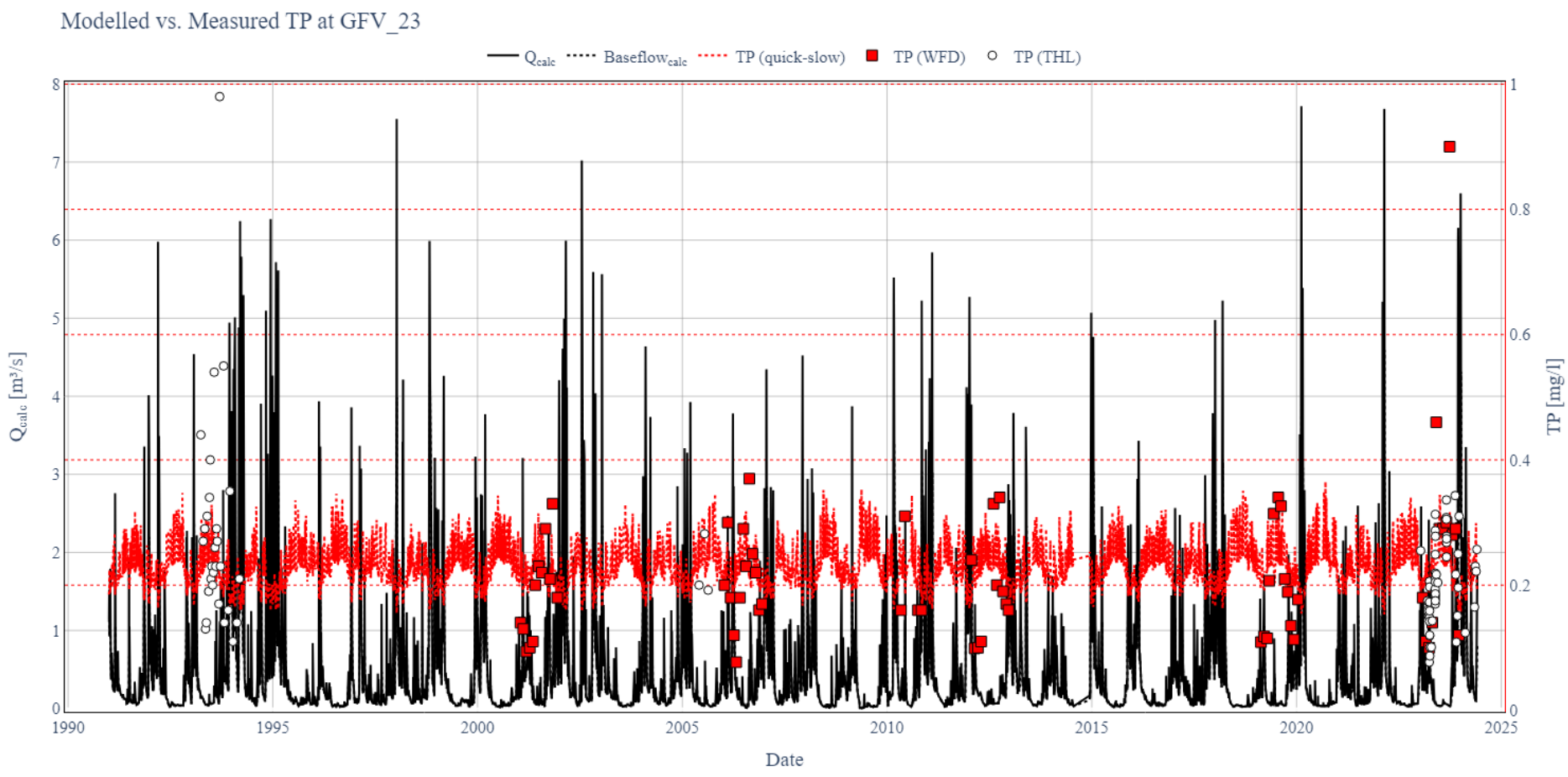

Figure 8.4: Modelled versus measured TP concentrations for GFV_23 at Heidekamp, 1991 to 2024

*Table 8.2: Measurements of sewage effluents from field campaign, ordered by date. **In red**: values outside of measuring range.*

ID	Date Time	T	pH	EC	COD	BOD5	TN	NH4-N	NO3-N	NO2-N	TP	ortho-P	Q	Sample type
	-	°C	-	µS/cm	mgO/l	mgO/l	mg/l	mg/l	mg/l	mg/l	mg/l	mg/l	l/s	
HH_out	28/05/2024 10:00	21.4	7.95	1005	139		41.9	30.4	0.272	0.143	5	3.12		Grab sample
LN_out	28/05/2024 10:30	21.4	7.74	666	78.5		8.99	6.81	0.205	0.039	2.92	2.42		Grab sample
MH_out	28/05/2024 11:00	21	7.99	913	45.7		15.7	15.8	0.145	0.008	4.84	4.65		Grab sample
HH_out	11/06/2024	15.1	8.06	800	99.8	30	24.4	18.3	0.416	0.267	3.09	2.17		**24 h mix**
LN_out	18/06/2024	17.3	7.58	623	71.4		14.8	11.2	0.26	0.004	2.8	2.53		**24 h mix**
LN_out	18/06/2024 15:30				89.1		15.2	10.9	0.309	0.001	2.85	2.4		1 h mix
LN_out	18/06/2024 19:30				108		14.6	11.2	0.269	0.003	2.93	2.5		1 h mix
LN_out	18/06/2024 23:30				175		14.3	11.2	0.233	0.003	2.75	2.49		1 h mix
LN_out	19/06/2024 03:30				86		14.7	11.4	0.223	0.004	2.82	2.52		1 h mix
LN_out	19/06/2024 07:30				65.9		14.3	11.5	0.24	0.004	2.7	2.57		1 h mix
LN_out	19/06/2024 11:30				65.5		15	11.4	0.236	0.004	2.74	2.57		1 h mix
LN_out	19/06/2024 15:00												0.26092	Q measurement
MH_out	24/06/2024	20.7	8.17	868	54.1		20.1	17.4	0.191	0.015	4.14	3.67		**24 h mix**
HH_out	24/06/2024 14:20												1.09014	Q measurement
HH_out	24/06/2024 14:20	21.3	7.68	860	143		23.8	17.6	0.317	0.205	3.72	2.15		Grab sample
MH_out	24/06/2024 15:45				85		19.7	17	0.194	0.026	5.07	3.54		1 h mix
MH_out	24/06/2024 16:00												0.56385	Q measurement
MH_out	24/06/2024 19:45				56		18.9	16.7	0.183	0.027	4.85	3.44		1 h mix
MH_out	24/06/2024 23:45				70.2		19.5	17.6	0.264	0.008	4.63	3.65		1 h mix
MH_out	25/06/2024 03:45				35.9		19.3	17	0.172	0.006	4.04	3.68		1 h mix
MH_out	25/06/2024 07:45				54.6		28.5	16.9	0.184	0.008	4.05	3.77		1 h mix
MH_out	25/06/2024 11:45				86.2		23.3	17.5	0.194	0.025	4.61	3.7		1 h mix
MH_out	25/06/2024 14:45				78.3		29.3	17.4	0.261	0.026	3.89	3.64		1 h mix

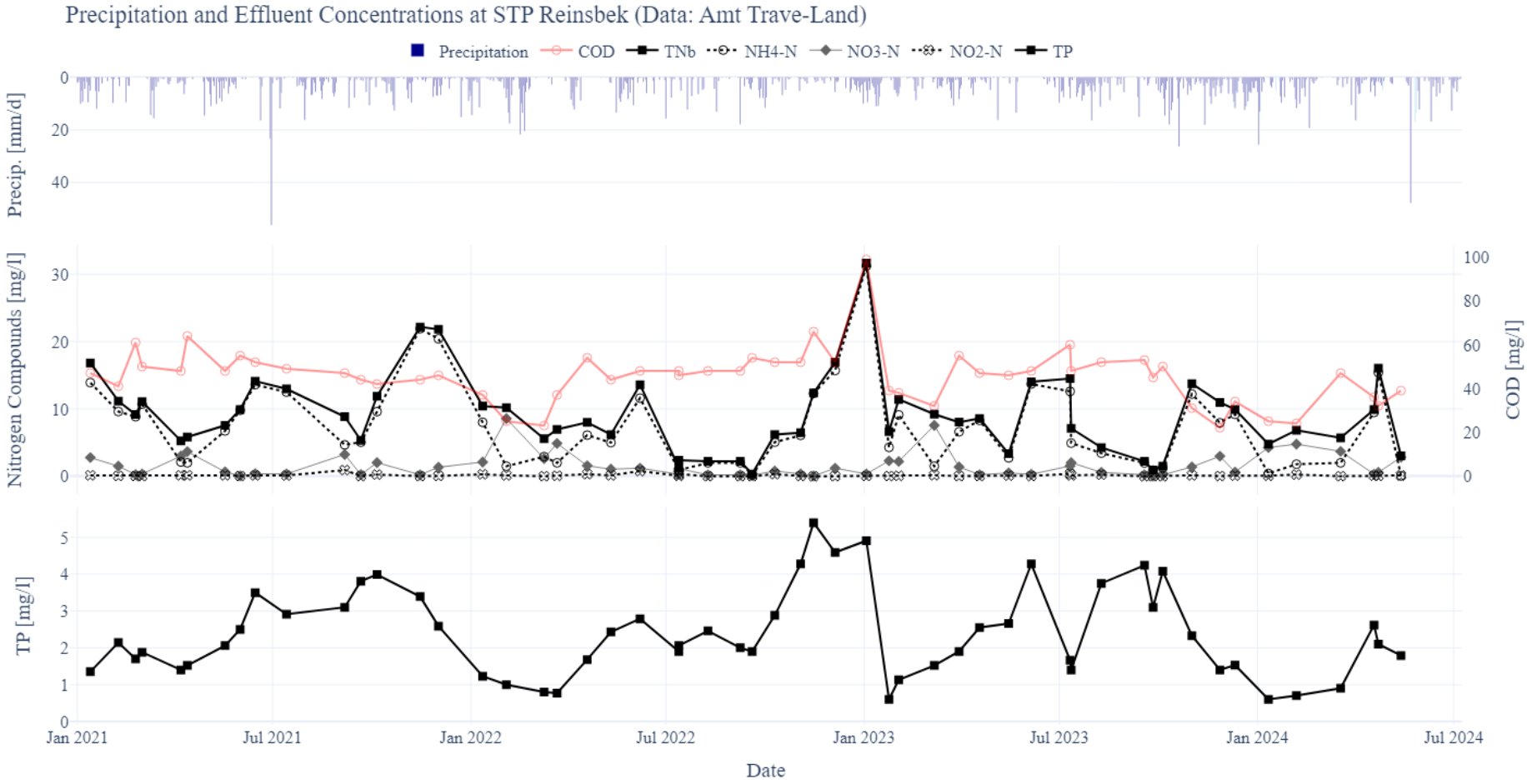

Figure 8.5: Effluent concentrations of STP at Reinsbek , along with interpolated daily precipitation data. Source for water quality data: Amt Trave-Land.

Comment: Reinsbek showed seasonal fluctuations, such as an increase of concentrations during spring months. However, a further analysis was limited due to missing discharge data for these readings, which would have allowed a load analysis over time.

8.8 Temporal Variation of TP Loads

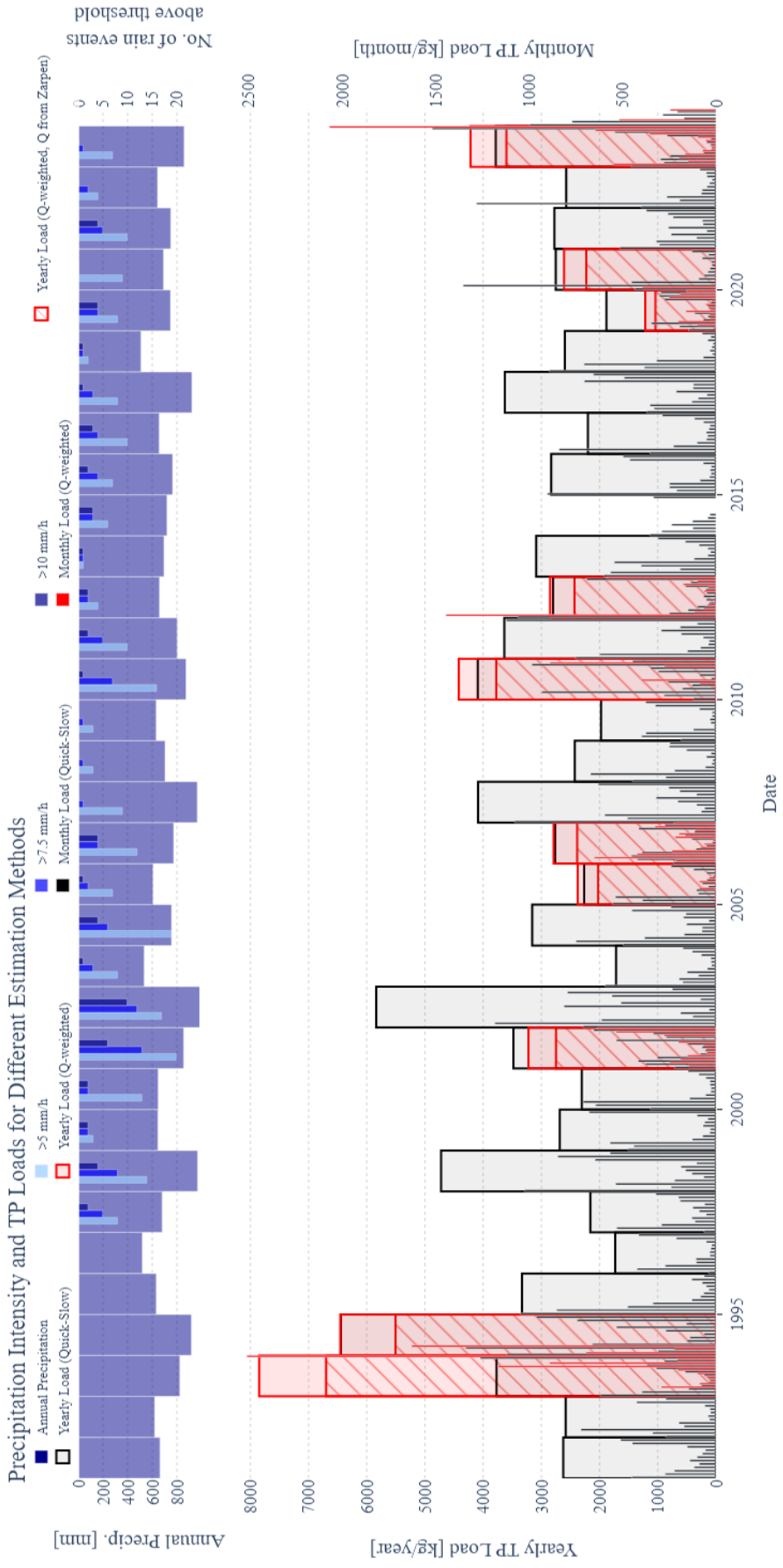

*Figure 8.6: Yearly and monthly TP loads for the years 1991 to beginning of 2024 at station GFV_23. **Top:** Precipitation data showing the annual precipitation in mm and the number of hourly records with rainfall intensities above the thresholds 5, 7.5, and 10 mm/h. **Bottom:** The red, diagonally striped bar plots are showing the yearly Q-weighted load with a different discharge input, from Zarpen instead of Heidekamp. This is shown as a potential lower boundary of loads. The other bars show the monthly and yearly TP loads as estimated through the Q-weighted and Quick-Slow approach.*

8.9 Spatial Distribution of Loads

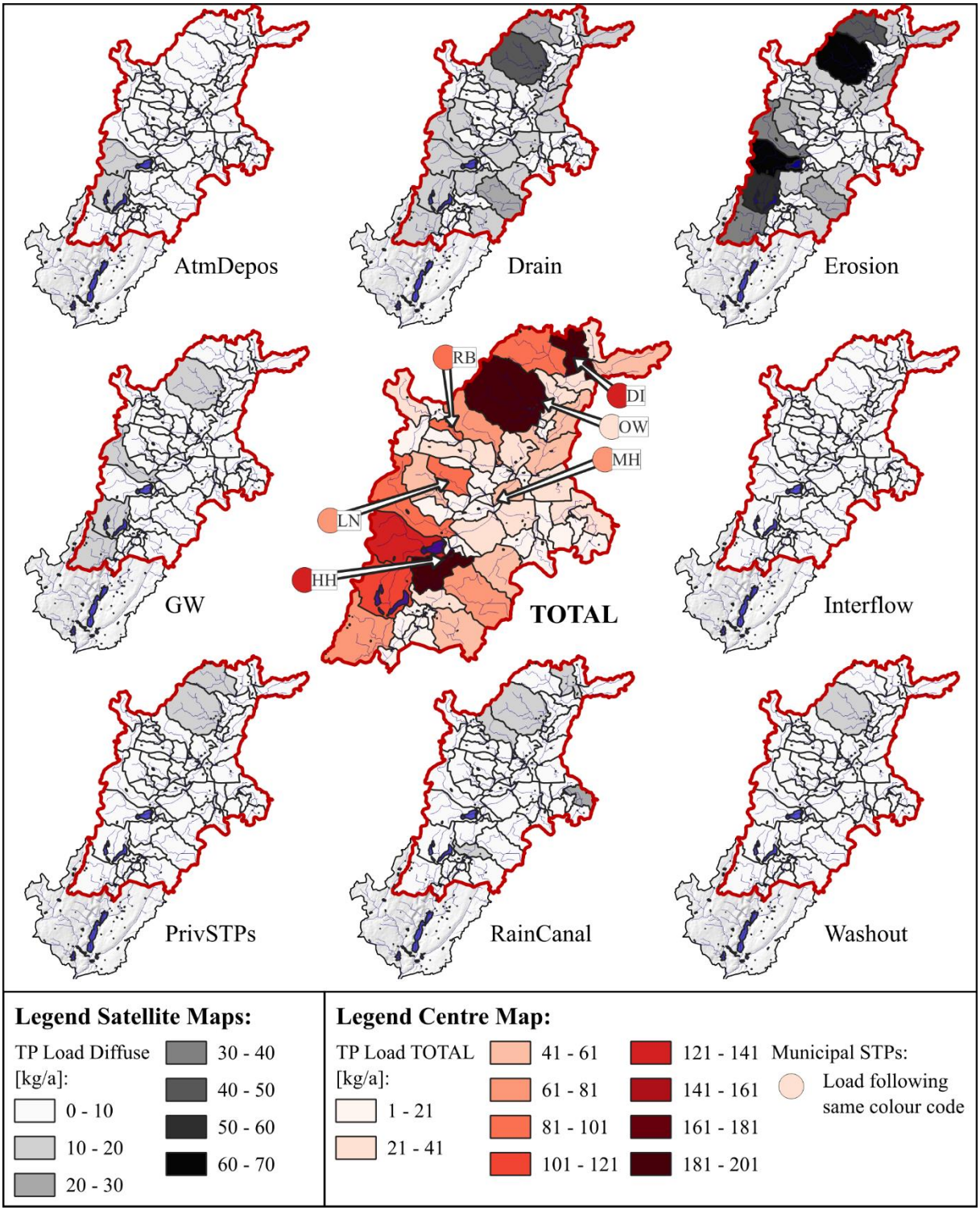

Figure 8.7: FZ Jülich model results for TP loads, separated by pathway within upper catchments. The "satellite" maps around the central one show the loads per diffuse pathway (legend on the left). The central map shows all diffuse sources combined with municipal STPs, following the colour scale of the right legend. The subcatchment shading already includes the loads from MunSTPs, the additional visualisation of STPs was only done for further information.

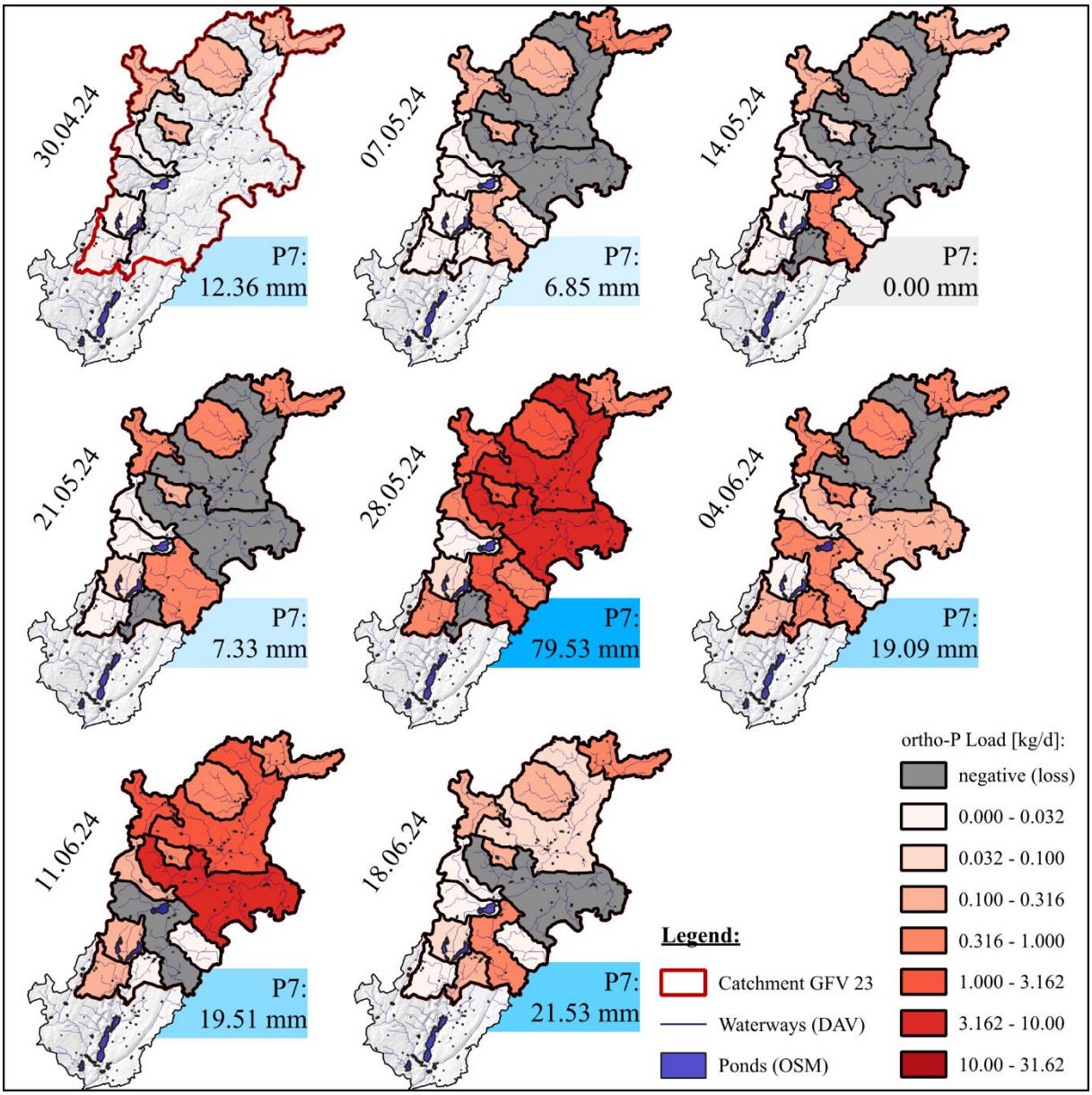

Figure 8.8: Origin of ortho-P loads for each sampling week of the field campaign. Note that the colouring of each subcatchment follows a logarithmic scale, as seen in the legend. Precipitation is indicated in blue, with P7 being the sum of daily precipitation of the last 7 days (including the day of sampling itself).